Identification of Novel Regulators of Adrenal Steroidogenesis



Doctoral thesis

for

the award of the doctoral degree
of the Faculty of Mathematics and Natural Sciences
of the University of Cologne

submitted by

Philipp Ferdinand Melchinger

accepted in the year 2025

Table of contents

List	of Figures and Tables	3
Index of Abbreviations		5
Zusammenfassung		7
Abs	stract	8
1	Introduction to Steroidogenesis	9
2	Scope of the Thesis	. 18
3	Results	. 19
5	Discussion	45
6	Materials and Methods	. 55
7	Supplemental Figures	65
8	References	. 74
9	Acknowledgements	. 82

List of Figures and Tables

Figure 1.1. Structure of pregnenolone.	9
Figure 1.2. The hypothalamus-pituitary-adrenal axis controls cortisol production.	10
Figure 1.3. Simplified schematic of intracellular signal transduction during steroidogenic stimulation.	
Figure 1.4. Schematic of StAR localization and interactors	11
	13
Figure 1.5. Cholesterol synthesis and its regulation.	15
Figure 1.6. Steroidogenesis in the adrenal cortex.	17
Figure 3.1. Dynamics of pregnenolone and cortisol production from cholesterol in NCI- H295R.	
Figure 3.2. Mitochondrial membrane potential and ATPase function but not mitochondrial	21
translation or mitochondrial fusion are required for steroidogenesis.	26
Figure 3.3. Lysosomal acidification is required for steroidogenesis independent of choleste homeostasis.	
Figure 3.4. Induction of protein misfolding at the ER by inhibition of N-glycosylation by tunicamycin partially inhibits corticoid synthesis.	30
Figure 4.1. Specific factors of LROs and ER increase at mitochondria during steroidogenes induction.	
Figure 4.2. Biogenesis of lysosome-related organelles complex 1 subunit 6 is required for steroidogenesis.	32
Figure 4.3. BLOC1S6 is found in the cytosolic fraction and with membrane-bound organell	
Figure 4.4. Membrane-permeable hydroxycholesterol rescues BLOC1S6 KO effect on steroidogenesis.	
Table 1. In vitro cell lines used in this thesis.	44
	55
Table 2. Primers used in this thesis.	56

Table 3. ssDNA oligos used for dsDNA oligo annealing into pLentiCRISPRv2.	
Table 4. Antibodies used in this thesis.	
Table 5. LC/MS charachteristics of steroids used.	
Supplemental Figure 3.1. Steroid production over time of forskolin stimulation in in NCI-H295R.	65
Supplemental Figure 3.2. Steroids produced during forskolin stimulation and mitochondrial inhibition.	
Supplemental Figure 3.3. Steroids produced during forskolin stimulation and mitochondrial inhibition.	66
Supplemental Figure 3.4. Steroids produced during forskolin stimulation and mitochondrial inhibition.	67
	68
Supplemental Figure 3.5. Lysosomal acidification is required for steroidogenesis independe of cholesterol homeostasis.	ent 69
Supplemental Figure 4.1. Specific factors of LROs and ER increase at mitochondria during steroidogenesis induction.	
Supplemental Figure 4.2. Biogenesis of lysosome-related organelles complex 1 subunit 6	
required for steroidogenesis.	71
Supplemental Figure 4.3. BLOC1S6 is found in the cytosolic fraction and with membrane-bound organelles.	
· · · · · · · · · · · · · · · · · · ·	72

Index of Abbreviations

ACTH adrenocorticotropic hormone

ATF4 Activating Transcription Factor 4

BiP Binding immunoglobulin Protein

BLOC1 Biogenesis of Lysosome-related Organelles Complex 1

BLOC1S6 Biogenesis of Lysosome-related Organelles Complex 1 Subunit 6

BORC5 BLOC1-Related Complex subunit 5

CCCP cyanide m-chlorophenyl hydrazone

COPII Coatomer II

CRN Calreticulin

CYPs Cytochrome P450 enzymes

DHEA dehydroepiandrosterone

DHT dihydrotestosterone

EMC10 ER Membrane protein Complex subunit 10

ER endoplasmic reticulum

F forskolin

GC/MS gas chromatography-mass spectrometry

GFP Green Fluorescent Protein

HA Human Agglutinin

HDL High-Density Lipoprotein

HMGCR 3-Hydroxy-3-methylglutaryl-CoA Reductase

IF immunofluorescence

IMM inner mitochondrial membrane

IMS intermembrane space (of mitochondria)

IP immunopurification

ISR integrated stress response

ISRIB ISR inhibitor

KO genetic knock-out

LAMP2 Lysosome-Associated Membrane Glycoprotein 2

LC/MS liquid chromatography-mass spectrometry

LC3B microtubule associated protein 1 Light Chain 3 Beta protein levels

LDL Low-Density Lipoprotein

LROs lysosome-related organelles

MAM mitochondria-associated membranes

OMM outer mitochondrial membrane

PKA cAMP-dependent Protein Kinase

Plin3 Perilipin 3

SCAP SREBP Cleavage-Activating Protein SDHA

Succinate Dehydrogenase Subunit A

SG steroidogenesis

SM Squalene Monooxygenase

SR-B1 Scavenger Receptor B1

SREBP Sterol Regulatory Element Binding Protein

SSR3 Signal Sequence Receptor subunit gamma

TMT tandem mass tag

UPR unfolded protein response

VDAC1/2 Voltage-Dependent Anion Channel 1 / 2

VLDL Very Low-Density Lipoprotein

WT wild-type

Zusammenfassung

Steroidhormone sind essenzielle Botenstoffe für die Entwicklung von Organismen und ihre metabolische Homöostase. Die zelluläre Synthese von Steroidhormonen wird durch die Bereitstellung von Cholesterin zu Mitochondrien reguliert, denn hier wird das erste Steroidhormon, Pregnenolon, synthetisiert. Alle weiteren Steroidhormone werden aus Pregnenolon über verschiedene Intermediate hergestellt, dies findet in dem Endoplasmatischen Retikulum (ER) und in Mitochondrien statt. Das Cholesterin das für Steroidhormonbiosynthese verwendet wird von extrazellulärem Cholesterin stammen, das über das Endolysosomale System aufgenommen wird, es kann von Zellen de novo im ER hergestellt werden, oder es kann in Lipid Droplets (zu Deutsch: Fetttröpfchen) oder der Zellmembran eingelagertes Choloesterin mobilisiert werden. Zusammengefasst bedeutet dies, dass eine Vielzahl von zellulären Organellen an der Produktion von Steroidhormonen beteiligt ist. Dies wirft die Frage auf ob und wie diese verschiedenen Organellen für die Steroidhormonbiosynthese kommunizieren um ihre jeweiligen Beteiligungen zu koordinieren.

Ich habe in der vorliegenden Dissertation untersucht, welche Funktionen der beteiligten Organellen für die Produktion von Steroidhormonen essentiell sind. Während mitochondriale Energieproduktion notwendig ist für Steroidproduktion, sind die Fusion von Mitochondrien und deren Biogenese nicht notwendig. Es zeigte sich, dass Lysosome und das ER möglicherweise mehr zur Steroidhormonbiosynthese beitragen als ihre bekannten Funktionen im Cholesterinstoffwechsel und, im Fall des ER, der Produktion von Zwischenstufen der Steroidhormonbiosynthese.

Des Weiteren habe ich untersucht wie sich die Zusammensetzung der Gesamtheit der Proteine (genannt das Proteom) in der Zelle oder spezifisch in Mitochondrien ändert, wenn Steroidhormonbiosynthese aktiviert wird. Dabei stachen drei Proteine hervor: eines ist bisher bekannt als einer der Regulatoren der Biogenese von Lysosom-ähnlichen Organellen; die beiden anderen sind beteiligt and der Insertion in oder der Translokation über die ER Membran von neu synthetisierten Proteinen. Ich produzierte Zelllinien mit genetischem Defekt jeweils spezifisch für eines dieser Proteine. Diese konnten Steroide nicht so effizient herstellen wie unveränderte Zellen. Von diesen drei Proteinen habe ich BLOC1S6 näher untersucht, und fand heraus, dass es insbesondere für die Synthese von Glucocorticoiden wie Cortisol notwendig ist. Dies stellt einen neuen Mechanismus der Regulation der Steroidproduktion dar, der spezifisch Glucocorticoid-Produktion reguliert.

Abstract

Steroid hormones are indispensable signaling molecules for organismal homeostasis. Steroid synthesis is known to be regulated by control of the supply of cholesterol to mitochondria where the first steroid in the pathway, pregnenolone, is produced. All other steroids are produced from pregnenolone in reactions taking place in mitochondria and the endoplasmic reticulum. Endolysosomal uptake, *de novo* synthesis in the endoplasmic reticulum, and mobilization from lipid droplets or plasma membrane can contribute cholesterol for steroidogenesis. How these different organelles coordinate their contributions to steroidogenesis is largely unknown.

Here, I aimed to identify novel mechanisms of steroidogenesis regulation in adrenocortical carcinoma cells. I characterized organellar functions required for steroidogenesis, finding that while mitochondrial energy production is essential, mitochondrial biogenesis and fusion are not required for steroidogenesis. Furthermore, lysosomes and endoplasmic reticulum may support steroidogenesis beyond their known contributions to cholesterol supply and intermediate steroid synthesis.

I also screened changes in the proteomes of mitochondria and the whole cell upon initiation of steroidogenesis for novel regulators of steroidogenesis. The candidates which emerged from this screen have known functions in biogenesis of lysosome-related organelles and insertion of newly translated proteins into the endoplasmic reticulum membrane and lumen, but they had no previously known role in steroidogenesis. Knock-out of these candidates was found to impair steroidogenesis. Specifically, I found the protein BLOC1S6 which is known to regulate biogenesis of lysosome-related organelles is required for production of glucocorticoids in adrenocortical carcinoma cells. This suggests that, in addition to the regulation of steroidogenesis at its initial step of cholesterol supply to mitochondria, the synthesis of downstream glucocorticoids is regulated in a BLOC1S6-dependent manner.

1 Introduction to Steroidogenesis

1.1 Classification of steroid hormones

Steroid hormones are a chemical class of hormones distinct from peptide hormones. Steroids are all derived from the major sterol in animals, cholesterol, thus sharing the characteristic four ring cyclopentanophenanthrene structure (Steiger & Reichstein, 1937), exemplified here by the structure of pregnenolone (Fig 1.1.). Physiologically, steroids regulate a broad variety of processes. These can be generally divided into two categories: 1) Homeostasis regulation by corticoids produced in the adrenal gland, and 2) regulation of development and reproduction by the sex steroids: androgens and estrogens. These distinct functions are reflected in the specialization of steroidogenic - that is steroid producing - organs, which mostly produce only one active steroid compound. Corticoids are even named after the site of their synthesis in the cortex of the adrenal gland. Androgens are mainly produced in the testes while estrogens are produced in the ovaries. Corticoids can be further divided into two subclasses, glucocorticoids and mineralocorticoids, each released by a specialized layer of tissue in the adrenal cortex zona fasciculata for glucocorticoids and zona glomerulosa for mineralocorticoids. Other sites of significant steroid release are the placenta, which produces progesterone during pregnancy, and the brain, where pregnenolone and some androgens are produced (Miller & Auchus, 2011). Mammals share these steroidogenic organs, yet the main physiologically active steroids released by these organs can vary between species (Vagnerová et al., 2023).

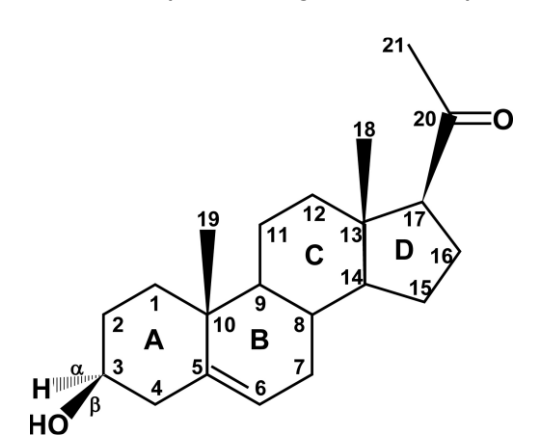


Figure 1.1. Structure of pregnenolone. Pregnenolone is the first steroid hormone synthesized from cholesterol. Numbers indicate carbons, letters denote rings, α or β indicate behind or front of the projected plane, respectively. Due to the double bond located between carbons 5 and 6, pregnenolone is a Δ^5 steroid. Adapted from (Miller & Auchus, 2011).

1.1.1 Roles of steroid hormones

Cortisol is the main active glucocorticoid in humans, it is released in response to stress but also to a lesser extent undergoes a pulsatile rhythm (Spiga & Lightman, 2015). In targeted tissues, it is immunosuppressive, anti-inflammatory, and affects metabolism and cognitive function (De Kloet, 2004). Aldosterone is the major mineralocorticoid in humans, it functions to

regulate blood pressure by modulation of sodium and potassium levels in vascular circulation (Condon et al., 2002).

Sex steroid production begins in the adrenal gland with the onset of adrenarche (the onset of steroidogenesis in the adrenal gland shortly before the begin of puberty) and subsequently starts in the gonads at the beginning of puberty and is required for development and function of the reproductive organs. Progesterone is released by the placenta during pregnancy and critical for its maintenance (Miller & Auchus, 2011).

A minor site of steroidogenesis is the brain, producing pregnenolone and related compounds as well as some androgens. These neurosteroids serve to balance mood, memory function and neuroprotective effects (Reddy, 2010).

1.1.2 Regulation of steroidogenesis in the whole organism

Steroids are not constantly produced; steroidogenesis is activated by tropic hormone stimulation or in reaction to environmental cues. Steroidogenic cells also do not store already synthesized steroids for release upon stimulation. Stimulating factors include adrenocorticotropic hormone (ACTH) which stimulates glucocorticoids in the adrenal and luteinizing hormone (LH) which mainly stimulates estrogen in ovarian granulosa cells as well as testicular testosterone production. These tropic hormones are released by the pituitary under the control of the hypothalamus, as exemplified for the hypothalamus-pituitary-adrenal axis in Fig. 1.2.

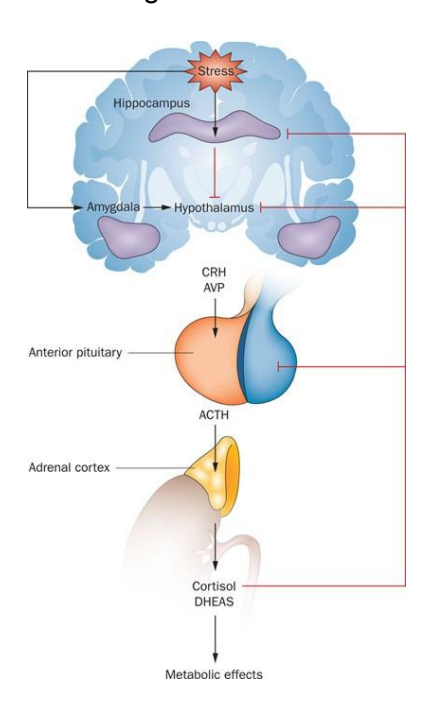


Figure 1.2. The hypothalamus-pituitaryadrenal axis controls cortisol production. CRH: corticotropin-releasing hormone, AVP: arginine vasopressin, ACTH: adrenocorticotropic hormone, DHEAS: dehydroepiandrosterone-slufate. Adapted from (Papadopoulos & Cleare, 2012)

Angiotensin II in concert with circulating potassium controls mineralocorticoid release (Helfenberger et al., 2019). It is produced from the precursor angiotensinogen that originates in the liver (Lu et al., 2016). Neurosteroid production is responsive to neurotransmitters and other hormones (Do-Rego et al., 2012).

1.1.3 Signal transduction of steroidogenic stimulation

The tropic hormones described above each bind to a specific receptor on steroidogenic cells, thereby inducing intracellular signal transduction. For ACTH and LH the main secondary messenger is cyclic adenosine-nucleotide monophosphate (cAMP), produced by adenylyl cyclase which is activated by G-protein coupled receptor binding. cAMP stimulates the activity of cAMP-dependent protein kinase (PKA). The signal is transduced from PKA to ERK (Gyles et al., 2001), which phosphorylates and thereby activates steroidogenic factor 1 (SF1), the main transcription factor activating the expression of steroidogenic genes (Fig. 1.3.A). During short term stimulation, the main gene transcribed encodes Steroidogenic Acute Regulator (StAR) protein (Jo et al., 2005), which will be described in detail in the next section. Long term steroidogenic stimulation will also increase the expression of steroidogenic enzymes, which are also addressed in a later section (Miller, 2013). In parallel, PKA also phosphorylates StAR increasing its activity (Arakane et al., 1997). Another target is cAMP response element binding protein (CREB), which binds to the corresponding transcription factor binding sites in genomic DNA activating the genes under their control (Sugawara et al., 2006).

Angiotensin II induced signal transduction in adrenal cells mainly involves calcium signaling through calmodulin, downstream activating protein kinase C, Ca2+/calmodulin dependent protein kinase, MEK, and ERK kinases (Condon et al., 2002). Calcium signaling may also stimulate adenylyl cyclase and thus cAMP signaling. In concert, these signal transduction pathways early on mainly result in StAR expression and activation, in the long-term they also stimulate expression of mineralocorticoid synthesis enzymes (Hattangady et al., 2012) (Fig. 1.3.B).

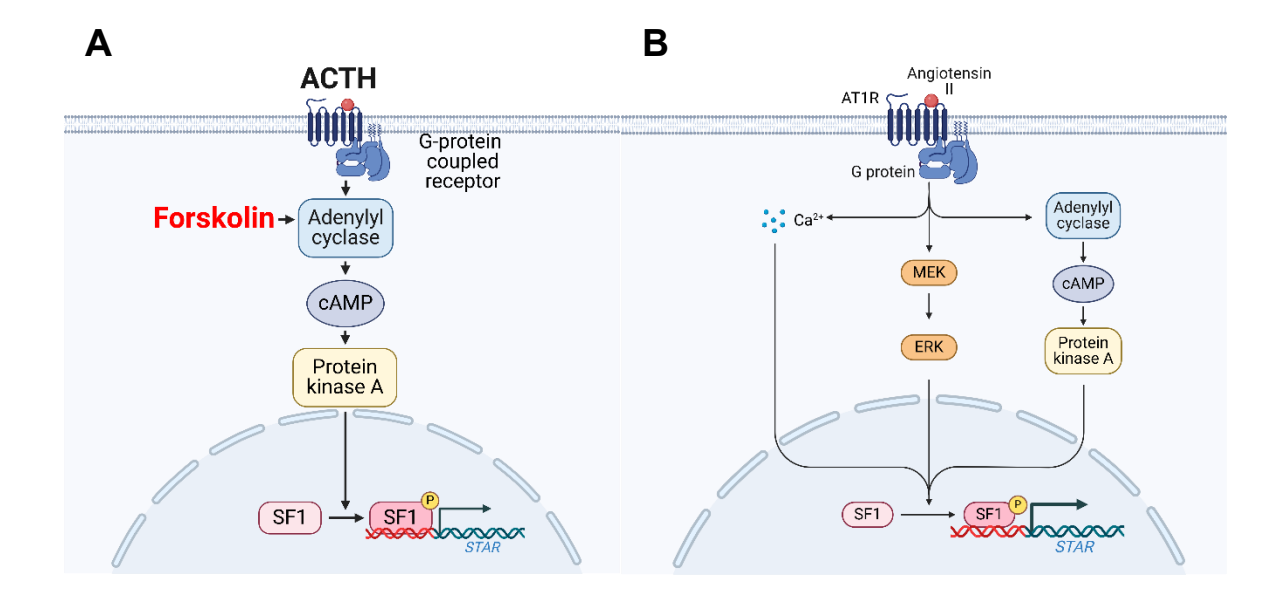


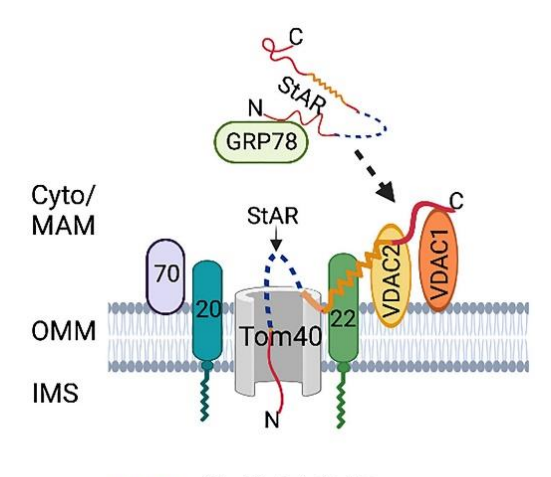
Figure 1.3. Simplified schematic of intracellular signal transduction during steroidogenic stimulation. A) ACTH and forskolin induced cAMP signaling, B) Angiotensin II induced signaling cascades.

1.1.4 Regulation of steroidogenesis by Steroidogenic Acute Regulator protein StAR

Induction of steroidogenesis rapidly induces expression of StAR, which has been found essential for steroidogenesis in most steroidogenic organs except placenta and brain. However, despite considerable focus on StAR as a regulator of steroidogenesis, its mechanism remains poorly understood. As will be described later, steroidogenesis requires the import of cholesterol into mitochondria, where the first steroidogenic reaction – synthesis of pregnenolone from cholesterol – takes place (Miller, 2025).

StAR localizes to mitochondria and possesses a mitochondrial targeting sequence allowing its import. StAR also has a binding site for cholesterol, allowing it to bind one molecule cholesterol per molecule StAR (Tsujishita & Hurley, 2000). This renders co-import of cholesterol with StAR insufficient to sustain the rate of cholesterol flow into mitochondria that is required for steroidogenesis (Artemenko et al., 2001). In addition, it has been determined that extramitochondrial StAR is stimulating mitochondrial cholesterol import, and StAR import renders it inactive (Arakane et al., 1996). Detailed study of the amino acid sequence of StAR revealed it contains a sequence that results in slowed mitochondrial import, next to its mitochondrial targeting sequence, and that this increases its facilitation of cholesterol import (Bose et al., 2023; Bose et al., 2002). Thus, StAR controls import of cholesterol into mitochondria at the OMM, which raises the question what the mechanism is.

It has been described that StAR is enriched in the cholesterol-rich mitochondria-associated membranes (MAM) of the endoplasmic reticulum (ER). These represent sites of contact between mitochondria and the ER. Several interaction partners of StAR have been found, which are also associated with the MAM. These include Voltage-Dependent Anion Channel (VDAC1/2), the σ-1 receptor (Marriott et al., 2012), GRP78 (Prasad et al., 2017), and Translocase of the Outer mitochondrial Membrane 40 (TOM40) (Bose et al., 2023), yet they are not essential for steroidogenesis, indicating redundant mechanisms exist (Fig. 1.4.). With the help of these interactors, StAR may facilitate cholesterol trafficking from MAM to the OMM. However, the precise mechanism of StAR and its regulation of cholesterol trafficking is still elusive. It is equally unclear how cholesterol is shuttled from the OMM to the IMM, where the first steroidogenic reaction occurs.



---- 31-62 AA StAR pause

Figure 1.4. Schematic of StAR localization and interactors. Cyto: cytosol, MAM: mitochondria-associated membranes, OMM: outer mitochondrial membrane, IMS: intermembrane space, StAR: steroidogenic acute regulator, VDAC: voltage-dependent anion channel; Tom: translocase of the outer mitochondrial membrane. Adapted from (Bose et al., 2023).

1.1.5 Homeostasis of cholesterol – the substrate for steroidogenesis

Cholesterol, the substrate for steroidogenesis, is a versatile metabolite. It is itself critical for membrane integrity, because the balance between non-polar cholesterol and polar lipids determines membrane rigidity and protein-membrane interactions as well as protein-protein interactions within membranes (Brown et al., 2021). This is reflected in membranes at different subcellular locations displaying different membrane lipid compositions, as well as the ability of single membranes to have a sub-structure of different lipid composition, termed lipid rafts which are also involved in membrane contact sites (Fujimoto et al., 2012; van Meer et al., 2008). Cholesterol is also a precursor, not only for steroids but also for bile acids, cholesterol esters and oxysterols (Brown et al., 2021). Cholesterol levels in the cell are tightly regulated since

they are not only required for these functions but excess can lead to membrane damage and ultimately organ damage (Brown et al., 2021).

Animals including humans satisfy their demand for cholesterol both from nutrition and by generating it themselves (Dietschy, 1984; Spady & Dietschy, 1983). Although most, if not all, tissues are able to synthetize cholesterol most of it is generated in the liver (Spady & Dietschy, 1983). On the cellular level, this is reflected in the importance of cholesterol import mechanisms as well as synthesis. Due to its hydrophobic nature cholesterol circulates in the vascular system bound to lipoproteins. Three cholesterol-binding lipoproteins are distinguished by their density: very low-density lipoprotein (VLDL), low-density lipoprotein (LDL) and highdensity lipoprotein (HDL). In cells requiring cholesterol uptake, LDL binds to its receptor LDLR and is internalized via endocytosis (Davis et al., 1986). The generated endosomes fuse with lysosomes, where LDL is thought to be degraded and the cholesterol is released and trafficked to storage, however, LDLR can be recycled to the plasma membrane (Clifford et al., 2023). VLDL uptake follows a similar mechanism (Go & Mani, 2012). Cholesterol bound to HDL is taken up upon binding to its receptor, scavenger receptor B1 (SR-B1) (Zanoni et al., 2016). Steroidogenesis mainly relies on cholesterol uptake rather than synthesis, however, the exact pathway utilized for uptake varies between organisms. In human SG, uptake of LDLcholesterol via LDLR is used, while rodents rely on HDL uptake by SR-B1 (Miller, 2013).

Cholesterol is synthesized *de novo* from acetyl-CoA via the mevalonate pathway (Fig. 1.5.A). Acetyl-CoA generation requires citrate that can be replenished from glucose via glycolysis and the tri-carboxylic acid cycle (TCA). Cholesterol synthesis is regulated through the negative feedback it induces by binding to sterol regulatory element binding protein (SREBP) cleavage-activating protein (SCAP) (Fig. 1.5.B). In cholesterol replete conditions SCAP and SREBP2 are anchored to the ER membrane in a complex with insulin induced gene (INSIG). Cholesterol depletion induces dissociation of INSIG and the trafficking of the SCAP-SREBP2 complex to the Golgi apparatus in coatomer II (COPII) vesicles. In the Golgi, SREBP2 is cleaved by site 1 protease (S1P) and site 2 protease (S2P) yielding a mature transcription factor that re-localizes to the nucleus where it activates transcription of the two enzymes that catalyze rate-limiting reactions of cholesterol synthesis, 3-hydroxy-3-methylglutaryl-CoA Reductase (HMGCR) and Squalene Monooxygenase (SM). Cleaved SREBP2 also induces transcription of LDLR for cholesterol uptake. (Brown & Goldstein, 1980; Gill et al., 2011; Sakai et al., 1996)

Cholesterol can be stored in lipid droplets as cholesterol esters when esterified by sterol-O-acetyltransferase (SOAT), this cholesterol can be released by de-esterification by Niemann Pick type C protein 1 (NPC1). Another major cholesterol store is the cholesterol contained in membranes themselves, especially the plasma membrane. Cholesterol may be exchanged between membranes of different organelles via membrane contact sites. Due to its

hydrophobicity, cholesterol cannot freely diffuse in the cytosol, where it can be transported by proteins containing cholesterol binding sites (Miller, 2013).

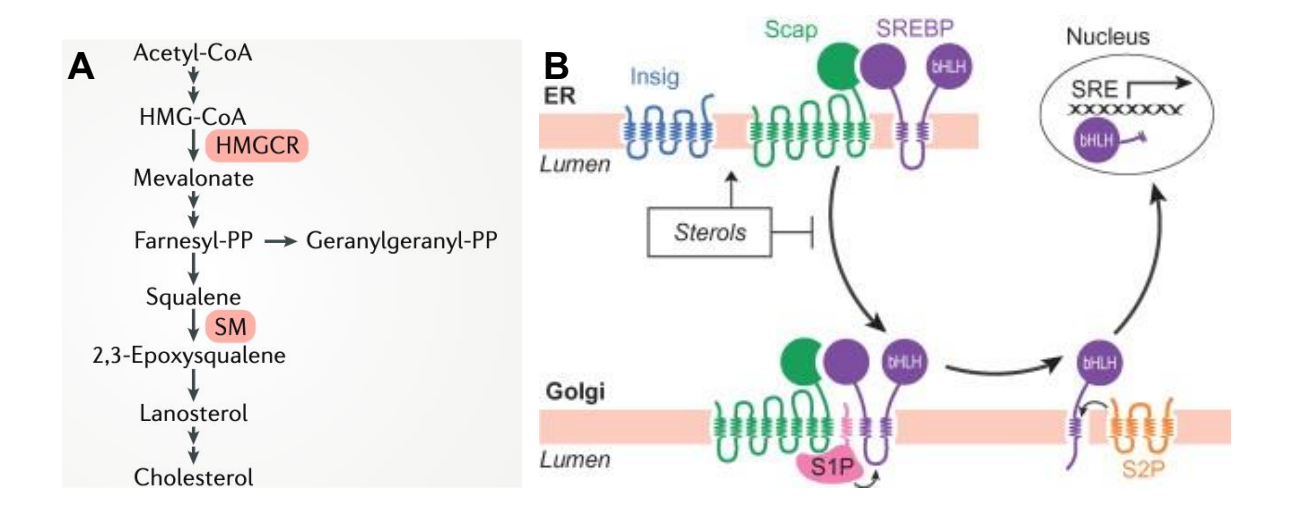


Figure 1.5. Cholesterol synthesis and its regulation. A) Simplified schematic of cholesterol synthesis from acetyl-CoA, highlighted are the enzymes 3-hydroxy-3-methylglutaryl-CoA Reductase (HMGCR) and Squalene Monooxygenase (SM) that catalyze the rate-limiting reactions in this pathway. Adapted from (Luo et al., 2020). **B)** Simplified schematic of cholesterol sensing for transcription regulation. Adapted from (Radhakrishnan et al., 2010).

1.1.6 Enzymatic mechanisms of steroidogenesis

Steroids are produced by two classes of enzymes: cytochrome P450 enzymes (CYPs) and hydroxysteroid dehydrogenases (HSDs) (Agarwal & Auchus, 2005; Miller, 2005). CYP enzymes are heme-containing oxidases that reduce oxygen to hydroxylate target residues. The electrons required for this reaction are donated by nicotinamide adenine dinucleotide phosphate (NADPH) via an intermediate flavoprotein. In mitochondria the electrons are transferred via the flavoprotein ferredoxin reductase (FDXR), also known as adrenodoxin reductase, and the iron-sulfur cluster protein ferredoxin (FDX), also known as adrenodoxin. In the endoplasmic reticulum (ER) CYPs receive electrons from NADPH via a membrane-bound flavoprotein called P450 oxidoreductase (POR). HSDs do not contain heme and rely on NADH/NAD+ or NADPH/NADP+ cofactors to reduce or oxidize steroids.

The first step in steroidogenesis is the cleavage of the side chain of cholesterol to yield pregnenolone catalyzed by CYP11A1, also known as P450 side chain cleavage enzyme (P450scc). This step is slow and therefore constitutes the rate-limiting step of steroidogenesis (Kuwada et al., 1991; Tuckey & Cameron, 1993a). It comprises three reactions catalyzed by a

single enzyme: sequential hydroxylation reactions at carbons C22 and C20 followed by oxidative scission of the bond between these carbons, producing pregnenolone and isocaproaldehyde (Tuckey & Cameron, 1993b). The CYP11A1 enzyme also accepts its intermediates, such as 22(R)-hydroxycholesterol (22R), as substrates which can be used in experiments to bypass cellular cholesterol transport and import into mitochondria, because hydroxycholesterols, unlike cholesterol, are soluble in water (Lin et al., 1995).

In the ER, pregnenolone can be converted into progesterone, the first steroid in the pathway with physiological activity, by 3bHSD in two steps: dehydrogenation of the hydroxyl group to a keto group and isomerization from D⁵ to D⁴ steroid. This enzyme catalyzes the same reactions for 17a-hydroxypregnenolone to 17a-hydroxyprogesterone, dehydroepiandrosterone (DHEA) to androstenedione, and androstenediol to testosterone (Lorence et al., 1990; Thomas et al., 1989).

Progesterone can be converted to 17a-hydroxyprogesterone by 17a-hydroxylase (CYP17A1), which is ER-membrane bound (Nakajin et al., 1984). The enzyme is capable of the same reaction on pregnenolone, but 3bHSD has higher affinity to pregnenolone, thus the pathway via progesterone is favored (Auchus et al., 1998). CYP17A1 also has 17,20-lyase activity which preferentially turns 17a-hydroxypregnenolone into DHEA and 17a-hydroxyprogesterone into androstenedione with low affinity (Zuber et al., 1986).

The ER-resident steroid 21-hydroxylase (CYP21A2) catalyzes hydroxylation at C21 of pregnenolone, resulting in deoxycorticosterone, the first mineralocorticoid. It also synthesizes the first glucocorticoid 11-deoxycortisol from 17a-hydroxyprogesterone (Chaplin et al., 1986; Parker et al., 1985).

In humans, the final steps in corticoid synthesis are performed by 11b-hydroxylase (CYP11B1) and aldosterone synthase (CYP11B2) in mitochondria (Fardella & Miller, 1996; White et al., 1994). CYP11B1 produces cortisol and aldosterone by 11b-hydroxylation of 11-deoxycortisol and deoxycorticosterone, respectively. CYP11B2 catalyzes 18-hydroxylation and 18-methyl oxidation of corticosterone to yield aldosterone.

The final steps in sex steroid synthesis are all performed by ER-localized enzymes. 17b-HSD, of which numerous isozymes exist, convert androstenedione to testosterone, estrone to estradiol, and DHEA to androstenediol, among other reactions (Labrie et al., 1997). Estrogens are produced from their androgen counterparts by aromatase (CYP19A1) (Simpson et al., 2002). Testosterone can be converted to the more active dihydrotestosterone (DHT) by 5a-reductase (SRD5A1) in target tissues (Bruchovsky & Wilson, 1968).

1.1.7 Adrenal steroidogenesis in vivo and in vitro

In this work I studied steroidogenesis in an *in vitro* model of adrenal origin. The mechanisms described so far summarize general principles of steroidogenesis. However, steroidogenic organs and tissues are specialized to produce only certain steroids, thus they selectively possess the required parts of the steroidogenic machinery (Miller & Auchus, 2011). The cortex of the adrenal gland is structured in three layers of tissue. The outermost zona glomerulosa expresses CYP11B2 but not CYP17A1 permitting only mineralocorticoid synthesis. The zona fasciculata does not express angiotensin II receptors but instead expresses the ACTH receptor (MC2R) and an isoform of CYP11B2 which cannot produce aldosterone (Mulatero et al., 1998). The lack of cytochrome b_5 in the zona fasciculata prevents androgen production (Suzuki et al., 2000). The zona reticularis bordering the adrenal medulla is also ACTH sensitive, but has minimal CYP21A2 or CYP11B2 such that corticoid synthesis is suppressed. Instead, high levels of CYP17A1 and cytochrome b_5 yield DHEA and DHEA sulfate (DHEAS) (Auchus et al., 1998; Auchus & Rainey, 2004; Suzuki et al., 2000).

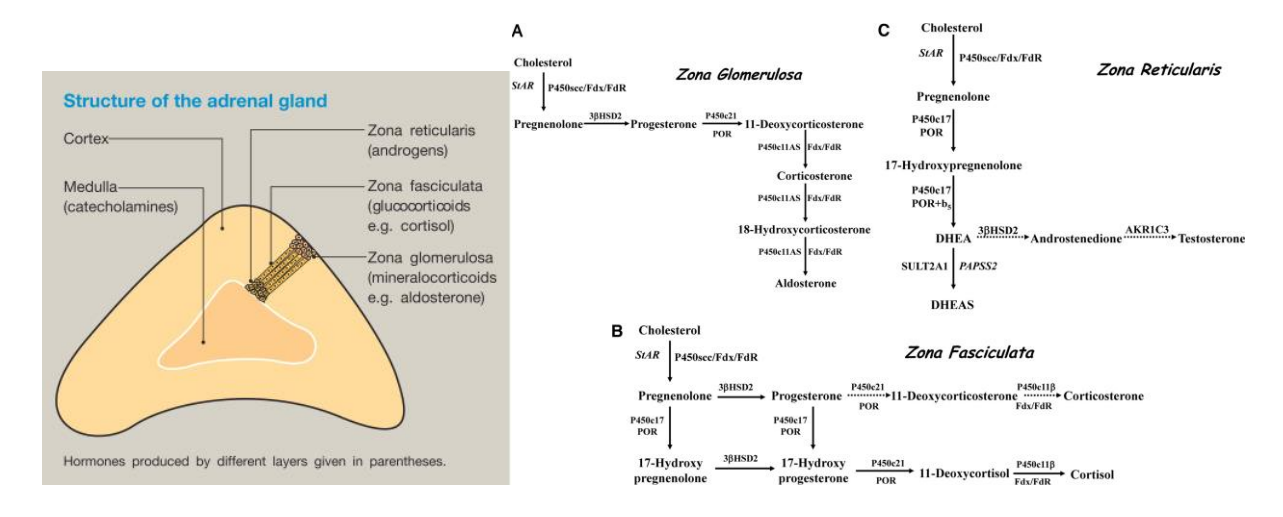


Figure 1.6. Steroidogenesis in the adrenal cortex. A) Simplified schematic of the main steroidogenic tissue layers of the adrenal cortex surrounding the medulla. Adapted from (Osman & Clayton, 2017). **B)** Schematic of specialized steroidogenic pathways in the tissues of the adrenal cortex. Adapted from (Miller & Auchus, 2011).

The adrenocortical carcinoma cell line NCI-H295R used here has been derived from the adrenal zona fasciculata (Gazdar et al., 1990). However, either due to carcinogenesis or adaptation in *in vitro* culture, it has lost MC2R expression and gained sensitivity to angiotensin II, resulting in the capacity to generate mineralocorticoids in addition to glucocorticoids (Mountjoy et al., 1994). Since ACTH sensitivity is lost without MC2R, stimulation of steroidogenesis through cAMP signaling can be achieved by treatment with cAMP directly or stimulation of adenylyl cyclase with the chemical forskolin (Rainey et al., 1994).

2 Scope of the Thesis

Organelles must remain interconnected and synchronized to perform specialized functions. One crucial mechanism that enables this coordination is the dynamic relocalization of proteins between organelles, which helps regulate essential cellular processes.

Steroid hormones are indispensable signaling molecules for organismal homeostasis, and their production – steroidogenesis (SG) – is a highly coordinated process involving multiple organelles. SG begins with the delivery of cholesterol to mitochondria, where the first and rate-limiting step occurs, before subsequent reactions take place in the endoplasmic reticulum (ER) and again in mitochondria (Miller & Auchus, 2011). Cholesterol for SG can originate from multiple sources, including endolysosomal uptake, de novo synthesis in the ER, and mobilization from lipid droplets or the plasma membrane (Miller, 2013). However, how these different organelles coordinate their contributions to SG remains largely unknown. Here, I aimed to uncover novel regulatory mechanisms of SG, with a particular focus on mitochondria, given their central role in the rate-limiting step of this process. Specifically, I investigate the contributions of other organelles, their potential communication with mitochondria through protein relocalization, and how such dynamic changes influence SG.

This thesis is structured around two major research aims:

- 1. Investigating the essential functions of mitochondria and other SG-related organelles in steroidogenesis.
 - How do mitochondria and associated organelles contribute to cholesterol mobilization and processing for SG?
 - What roles do mitochondria, lysosomes and the ER play in regulating SG?
- 2. Define the mobile mitochondrial proteome during steroidogenesis stimulation using a proteomic approach.
 - Do specific proteins or organelles relocalize to mitochondria to facilitate SG?
 And if so, how do novel candidate regulators change their localization and how do they contribute to SG?

By addressing these questions, this work seeks to expand our understanding of steroidogenesis regulation, uncover potential inter-organelle communication pathways, and identify novel factors involved in this critical cellular process.

3 Results

- 3.1 A model of Steroidogenesis of Adrenocortical Carcinoma Cells In Vitro
- 3.1.1 Characterizing in vitro steroidogenesis of adrenocortical carcinoma cell line NCI-H295R

To investigate the role of interorganellar communication in the regulation of SG, I utilized the well-established NCI-H295R cell line. The NCI-H295R cell line was derived from adrenocortical carcinoma and has been shown to be responsive to SG stimulation *in vitro* using forskolin, cAMP and angiotensin II. These stimuli result in release of glucocorticoids, mineralocorticoids, pregnenolone and progesterone and their hydroxylated forms, as well as DHEA and DHEA-S (Kurlbaum et al., 2020; Rainey et al., 1994).

At early stages of SG pregnenolones and progesterones are produced, at later stages glucocorticoids such as cortisol and mineralocorticoids such as aldosterone accumulate (Kurlbaum et al., 2020). However, to my knowledge a detailed time course of steroid production in NCI-H295R has not been published. To therefore characterize SG in NCI-H295R cells, I assessed steroids released during SG stimulation at several timepoints, spanning 10 minutes to 3 days. I used forskolin to induce the cAMP signal cascade that stimulates SG and is activated by ACTH *in vivo*.

Culture media were harvested and analyzed by liquid chromatography-coupled mass spectrometry (LC/MS) based profiling following induction with forskolin medium for the time course spanning 3 days. As expected, I found that the first steroid hormone produced during SG from cholesterol by CYP11A1, pregnenolone, was significantly increased 3- to 4.5-fold upon forskolin stimulation compared to untreated cells from 30 minutes to 24 hours (h), peaking at 2 h post induction (Fig. 3.1A). A similar pattern was observed for progesterone and 17hydroxyprogesterone which are derived from pregnenolone (Suppl. Fig 1.1A,B). Cortisol, the final product, was first increased 4-fold by forskolin compared to untreated condition at 24 h post induction. This effect became more pronounced over time, reaching an increase of 12fold at 48 h and finally 30-fold by 72 h (Fig. 3.1B). The two other glucocorticoids, 11deoxycortisol and cortisone, follow a similar trend over time but were less strongly induced compared to cortisol (Suppl. Fig. 3.1C,D). The accumulation of early pathway intermediates within minutes to hours after stimulation, and that of downstream glucocorticoids and mineralocorticoids at later stages of induction is consistent with previous reports (Kurlbaum et al., 2020). However, it is striking to see in detail here the inverse correlation between pregnenolone and cortisol from 8 h SG stimulation onwards.

Because steroid production is regulated by the expression of key pathway components, the expression levels of the main steroidogenic regulator StAR and the first enzyme in SG, CYP11A1, were analyzed for these timepoints by immunoblot (Fig. 3.1C). The induction of

StAR by forskolin was evident as early as 4 h, with maximal induction at 24 h. CYP11A1 was unchanged by forskolin for all early timepoints up to 24h, afterwards moderate induction was observed at 48 h, increasing at 72 h. Thus, the increase in production of pregnenolone (and progesterone) precedes the upregulation of key pathway regulators StAR and CYP11A1. Detectable glucocorticoid induction by forskolin at 24 h occurs later than StAR induction at 8 h but before CYP11A levels start to be increased at 48h. This observation, consistent with previous reports (Miller, 2013), suggests that other modes of steroidogenesis regulation are responsible for early steroidogenesis activation within hours of induction.

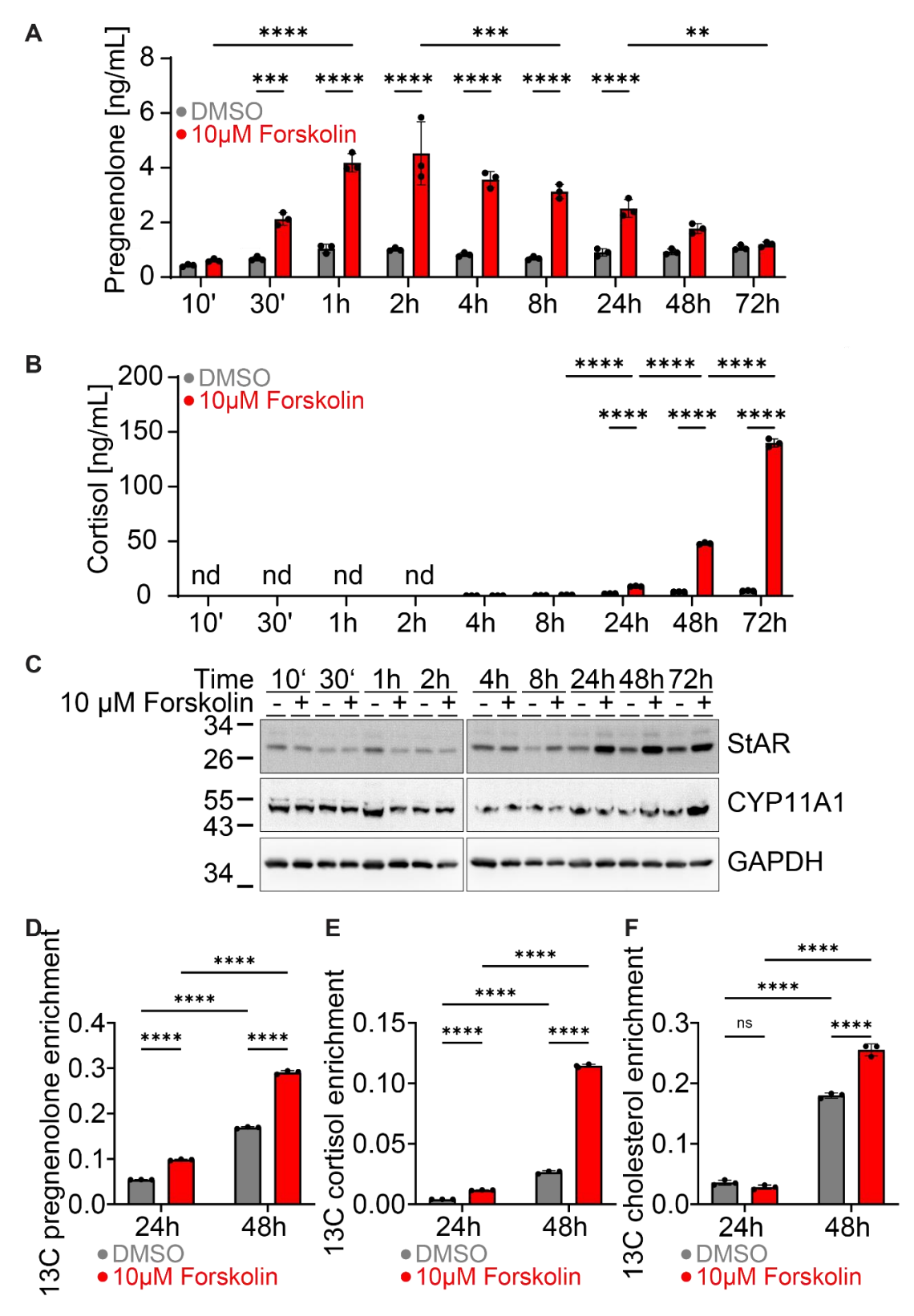


Figure 3.1. Dynamics of pregnenolone and cortisol production from cholesterol in NCI-H295R. A) Pregnenolone, and B) cortisol secreted by wt NCI-H295R into the cultured media for the indicated time analyzed by LC-MS. C) Immunoblot detection of StAR, CYP11A1 and GAPDH from the same cells. D) 13 C-containing pregnenolone and cortisol, and E) 13 C-cholesterol produced by wt NCI-H295R supplied with 13 C₆glucose in the medium during the experiment, as fraction of the total amount of each, analyzed by LC-MS. LC-MS data are mean \pm s.d. of n=3 replicates. '= minutes, h = hours, d = days, grey = vehicle DMSO, red = 10 μ M forskolin, nd = not detected, ns = not significant, ** = p<0.01, **** = p<0.001, **** = p<0.0001 (two-way ANOVA).

3.1.2 Contribution of *de novo* cholesterol synthesis to steroidogenesis of NCI-H295R

To assess whether *in vitro* steroidogenesis of adrenocortical carcinoma cells relies on endogenous *de novo* cholesterol synthesis or cholesterol uptake and mobilization of intracellular storage, metabolic isotopic label tracing was used. Glucose feeds *de novo* cholesterol synthesis via the TCA cycle and the mevalonate pathway (Bloch, 1965). Thus, I cultured NCI-H29R cells with ¹³C₆-glucose during forskolin induction of steroidogenesis, and examined the incorporation of ¹³C₆ into steroids by LC/MS analysis. This approach ensures that *de novo* synthetized cholesterol that is further processed into steroids during this time, would be ¹³C-labeled, while steroids derived from cholesterol produced, taken up or stored by the cells prior to forskolin induction and onset of ¹³C labeling will remain unlabeled.

Steroids accumulated in culture media were harvested at 24 and 48 hours after forskolin treatment, and analyzed for the fraction of the total amount of each steroid labeled by ¹³C (Fig. 3.1D,E). ¹³C isotope-labeled and total cholesterol was also measured by gas chromatographymass spectrometry (GC/MS) (Fig. 3.1F).

I found that although forskolin treatment did not increase cholesterol synthesis at 24 h post stimulation, a significant increase in ¹³C-labelled cholesterol from 18% to 25.5% was observed after 48 h forskolin treatment. At 24 h steroidogenic stimulation and ¹³C glucose feeding, the small fraction of 3 to 4% ¹³C-labeled cholesterol in unstimulated cells did not increase by forskolin stimulation. At 48 h ¹³C-labeled cholesterol was increased from 18% without stimulation to 25.5% with forskolin treatment (Fig. 3.1F). Remarkably, the total cholesterol pool of these cells was unchanged at 24 h and 10-fold increased at 48 h of forskolin stimulation (Suppl. Fig 3.2B). This possibly reflects significant depletion of cholesterol stores during prolonged SG stimulation. For the first steroid, ¹³C-incorporation into pregnenolone was observed at 5% and 17% under basal conditions at 24 and 48h, respectively. Forskolin stimulation significantly increased ¹³C-incorporation into pregnenolone to 10% and 30% at 24 and 48 h post treatment (Fig. 3.1D). Pregnenolone derivative 17αOH-pregnenolone behaved in a similar fashion as pregnenolone (Suppl. Fig. 3.2A). The ¹³C-labeled fraction of cortisol increased from 0.4% to 2.7% under basal condition and from 1.2% to 11% upon forskolin treatment, between 24 h and 48 h, respectively (Fig. 3.1E). The other glucocorticoids 11deoxycortisol and cortisone followed the same pattern as cortisol (Suppl. Fig. 3.2C,D). These results suggest a moderate contribution of de novo cholesterol synthesis to in vitro SG of adrenal cells, but an increasing role for cholesterol synthesis in prolonged SG stimulation.

In vitro cell culture media are supplemented with fetal bovine serum (FBS) to supply cells with lipids and growth factors. In steroidogenesis research this supplementation could introduce exogenous steroids that interfere with treatments and analysis of steroids. This is addressed in two ways; first experiments analyzing steroids released by SG stimulation are performed in serum-free media. Second, FBS is usually replaced with NuSerum® when working with NCI-H295R cells (Kurlbaum et al., 2020). NuSerum® is 75% defined amounts of nutrients, growth factors and trace elements, and contains 25% FBS (Wong & Tuan, 1993). It also contains the steroids progesterone, 17ß-estradiol, testosterone, hydrocortisone. This project was started by culturing NCI-H295R in DMEM/F12 with 5% NuSerum® and 1x ITS-X. At one point, the manufacturer of NuSerum® was unable to deliver it for more than one year. Thus, culture medium formulation was switched to 1% FBS in DMEM/F12 with 1x ITS-X. This represents a similar percentage of animal-origin serum as 5% NuSerum®. To confirm that steroidogenesis was comparable in cells cultured in 5% NuSerum versus 1% FBS NCI-H295R cells were cultured with either formulation separately for 10 days before the experiment. 24 hours after forskolin stimulation, steroids from conditioned cells were compared. No significant difference between FBS and NuSerum® was found for cortisol production, both with and without forskolin stimulation (Suppl. Fig. 3.2E). In both formulations, forskolin did not significantly induce pregnenolone secretion. However, in cells conditioned with FBS-containing medium forskolin treatment led to a small but significant decrease of pregnenolone by 35% compared to vehicle, which remained unchanged in FBS relative to NuSerum® (Suppl. Fig. 3.2F). Because pregnenolone induction is decreasing after 4 h or longer SG stimulation, it is possible that lack of induction at 24 h here is due to variability between experiments (Fig. 3.1.A). Despite the small decrease in pregnenolone the two culturing models of NCI-H295R cells were deemed comparable and later experiments were performed with cells cultured with 1% FBS.

3.1.4 Mitochondrial membrane potential and ATPase function are required for steroidogenesis

In my doctoral research project, I evaluated which key functions of organelles involved in SG are required for SG. The first committed biosynthetic reaction for steroidogenesis is catalyzed by CYP11A1 in the mitochondria (Miller, 2013). This step is regulated by steroidogenic regulator protein StAR, which controls cholesterol import into mitochondria (Lin et al., 1995). Therefore, I tested parameters of mitochondrial function that are required for steroidogenesis. Mitochondria produce metabolites and energy in the form of NADH and ATP through the TCA cycle and oxidative phosphorylation (OXPHOS). The chemical energy released by oxidation in the TCA is used by four large protein complexes (complexes I-IV) forming an electron transport chain (ETC) in the IMM to create a protein gradient, resulting in an electrochemical potential difference across the IMM called the mitochondrial membrane potential $\Delta\Psi_{\rm M}$. This

membrane potential allows ATP synthase (also called complex V) in the IMM to use the energy of protons following the gradient through ATP synthase to phosphorylate ADP to ATP, which is used across the cell for energy consuming reactions. Several pharmacological compounds have been found to interfere with the function of proteins involved in OXPHOS, these can be employed to probe whether OXPHOS function as a whole or functioning of individual OXPHOS complexes is required for SG. To this end NCI-H295R cells were co-treated with such inhibitors during SG induction and both steroid levels in culture media and the levels of the major SG regulators were analyzed.

Disruption of $\Delta \Psi_M$ by the protonophore CCCP and inhibition of mitochondrial ATP synthase by oligomycin decreased forskolin stimulated steroidogenesis across all steroids (Suppl. Fig. 3.3A-E), as exemplified by pregnenolone and cortisol (Fig. 3.2A,B). Remarkably, the latter and some other steroids were even reduced below the levels of basal steroidogenesis. Similarly, when the electron transport across the mitochondrial inner membrane was impaired by inhibition of ETC complex I using piericidin or rotenone or inhibition of complex III with antimycin A, both basal and stimulated steroidogenesis were ablated (Fig. 3.2D and Suppl. Fig. 3.4A-E). This dependence of forskolin stimulated SG on functional OXPHOS was not surprising, as it has been shown that these treatments ablate SG in these and other steroidogenic cells (Allen et al., 2006; Duarte et al., 2007; Mele et al., 2012). These treatments led to a concomitant abolition of StAR induction by forskolin, indicating that mitochondrial membrane potential and ATP synthesis are required to maintain StAR levels, and thus for the import of cholesterol into mitochondria (Fig. 1.2C), which has also been shown before (Allen et al., 2006; Duarte et al., 2007). On the other hand, mitochondrial translation inhibition by actinonin did not affect steroidogenesis or StAR levels upon forskolin stimulation (Fig. 3.2A,B). Although it has been shown that mitochondrial biogenesis – for which mitochondrial translation is required – is induced by SG stimulation, it was not previously tested whether it was also a requirement for SG (Medar et al., 2021). Lack of SG decrease by actinonin indicates mitochondrial biogenesis is not required for SG.

Thus, I have replicated that SG and StAR levels during SG stimulation are dependent on functional ETC, $\Delta\Psi_{M}$, and ATP generation. In addition, I find mitochondrial biogenesis is not required for SG.

3.1.5 Mitochondrial dynamics and steroidogenesis

Since previous studies have shown that steroidogenesis stimulation by angiotensin II lead to an hyperfused mitochondrial network essential for steroidogenesis in adrenal cells (Helfenberger et al., 2019), I wondered whether fusion also occurs during forskolin stimulation of steroidogenesis. To this end, mitochondrial dynamics (*i.e.* changes in the mitochondrial network) was visualized by confocal microscopy upon forskolin and angiotensin II treatment using NCI-H295R cells expressing OMM-localized GFP.

The images of the mitochondria were further analyzed using mitochondrial network analysis (MirNA) with Image J. While I found a moderate but significant increase in mean branch length of mitochondria during angiotensin II treatment, no such effect was observed during forskolin treatment (Fig. 3.2F). That mitochondrial hyperfusion is not induced by both forskolin and angiotensin II suggests it is not strictly required for steroid production in general.

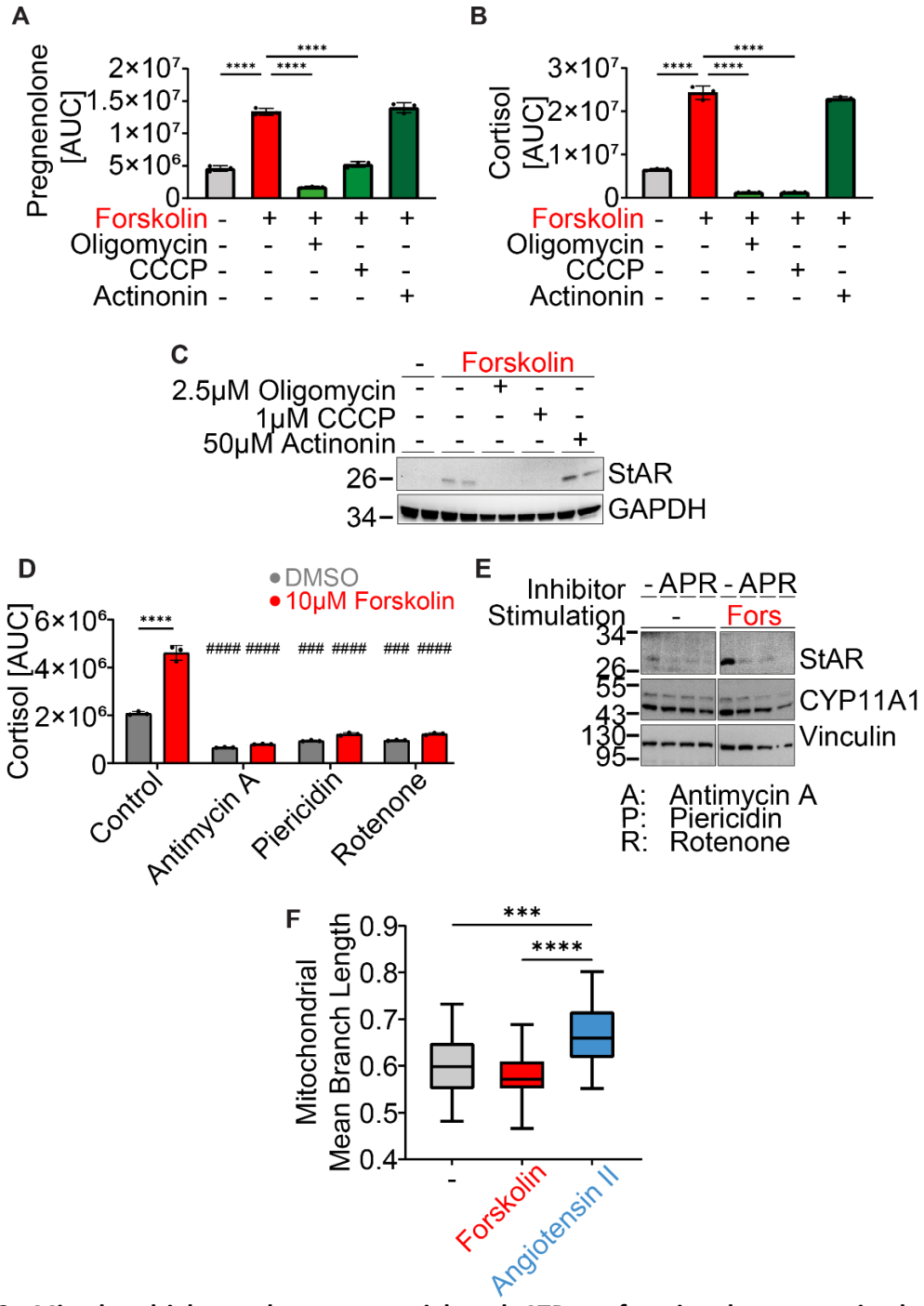


Figure 3.2. Mitochondrial membrane potential and ATPase function but not mitochondrial translation or mitochondrial fusion are required for steroidogenesis. A) Pregnenolone and cortisol secreted by wt NCI-H295R during 24 h treatment with 10 μ M forskolin, 2.5 μ M olicomycin, 1 μ M carbonyl cyanide m-chlorophenyl hydrazone (CCCP) or 50 μ M actinonin as indicated, analyzed by LC/MS. B) Corresponding mmunoblot detection of StAR and GAPDH. C) Cortisol secreted by WT NCI-H295R during 24 h treatment with 10 μ M forskolin, 2 μ M antimycin A, 3.7 μ M piericidin or 5 μ M rotenone as indicated, analyzed by LC/MS, and D) immunoblot detection of StAR, CYP11A1, pEIF2 α and vinculin. The blot is from a single membrane, samples not discussed here were cut out, the full membrane can be found in supplemental figure 1.4F. E) Mitochondria Network Analysis (MiNA) of live-cell confocal microscopy imaged NCI-H295R:HA-GFP-OMP25 treated with 10 μ M forskolin or 100nM angiotensin II as indicated. Data are mean \pm s.d. of n=3 replicates. AUC = area under curve. Grey = vehicle DMSO, red = 10 μ M forskolin, ns=not significant, */#=p<0.05, **/##=p<0.01, ***/###=p<0.001, ****/####=p<0.0001; asterisks refer to comparison indicated by line, hashtags compare to WT (AAVS1 KO) (in (A) one-way ANOVA, (D) two-way ANOVA, (F) t-test).

26

3.1.6 Lysosomal acidification is required for steroidogenesis

Lysosomes process LDL-cholesterol taken up from circulation via endocytosis by trafficking it to storage or releasing it (Go & Mani, 2012). This has been shown to be the major source of cholesterol during human adrenal SG *in vivo* (Miller, 2013). Therefore, I tested whether lysosomal acidification, a phenomenon essential to lysosomal functions such as proteolysis and other chemical reactions, is required for steroidogenesis in NCI-H295R cells *in vitro*. To this end, NCI-H295R cells were treated with bafilomycin, an inhibitor of the V-type ATPase that acidifies lysosomes (Bowman et al., 1988), with and without forskolin treatment. Bafilomycin treatment was confirmed by increased microtubule associated protein 1 Light Chain 3 Beta (LC3B) protein levels (Fig. 3.3C) (Fischer et al., 2020). I found that bafilomycin treatment significantly decreased the levels of the steroids pregnenolone and cortisol by 30 to 50% both during basal and forskolin-induced conditions (Fig. 3.3.A,B). Other steroids, especially pregnenolone-related compounds behaved analogous, with the exception of corticosterone (Suppl. Fig. 3.5.A-E). Bafilomycin treatment did not affect StAR levels, which was expected as there is no evidence suggesting StAR is associated to lysosomes or regulated by their acidification (Fig. 3.3.C,D).

One important step in steroid production is the delivery of cholesterol from intracellular stores to CYP11A1 in the mitochondrial matrix. To test whether lysosomal acidification is required to support cholesterol mobilization to mitochondria for steroidogenesis, cells were co-treated with membrane-permeable 22(R)-hydroxycholesterol (22R), which can reach CYP11A1 and be processed into steroids independent of the cell's machineries for cholesterol uptake, storage, supply to and import into mitochondria (Toaff et al., 1982). Supplementation with 22R did not rescue steroidogenesis upon bafilomycin treatment (Fig. 3.3.A,B, Suppl. Fig. 3.5A-E), though the intracellular presence of 22R was not analyzed in these samples, thus the treatment cannot be verified. Of note, StAR protein levels were unaffected by 22R (Fig. 3.3.C,D). Thus, if 22R treatment can be confirmed this would suggest lysosome function is required for steroidogenesis beyond cholesterol release from endolysosomes.

Cholesterol can be released from lysosomes via the NPC1 transporter (Infante et al., 2008). Inhibition of NPC1 with the inhibitor U18666A (Lange et al., 2000) did not decrease steroidogenesis, upon either basal or forskolin stimulated conditions (Fig. 3.3A,B, Suppl. Fig. 3.5.A-E). Moreover, co-treatment of hydroxycholesterol during NPC1 inhibition treatment had no effect on steroid production (Fig. 3.3.A,B, Suppl. Fig. 3.5.A-E). Concurrently, NPC1 inhibition alone or with supplementation of hydroxycholesterol did also not affect StAR levels (Fig. 3.3C.,D). A limitation of this experiment is that no control for successful NPC1 inhibition was included. Nevertheless, the data is in agreement with previous research on ovarian

granulosa cells that shows NPC1 function is required for SG to utilize cholesterol from LDL but it is not required for SG in general (Watari et al., 2000).

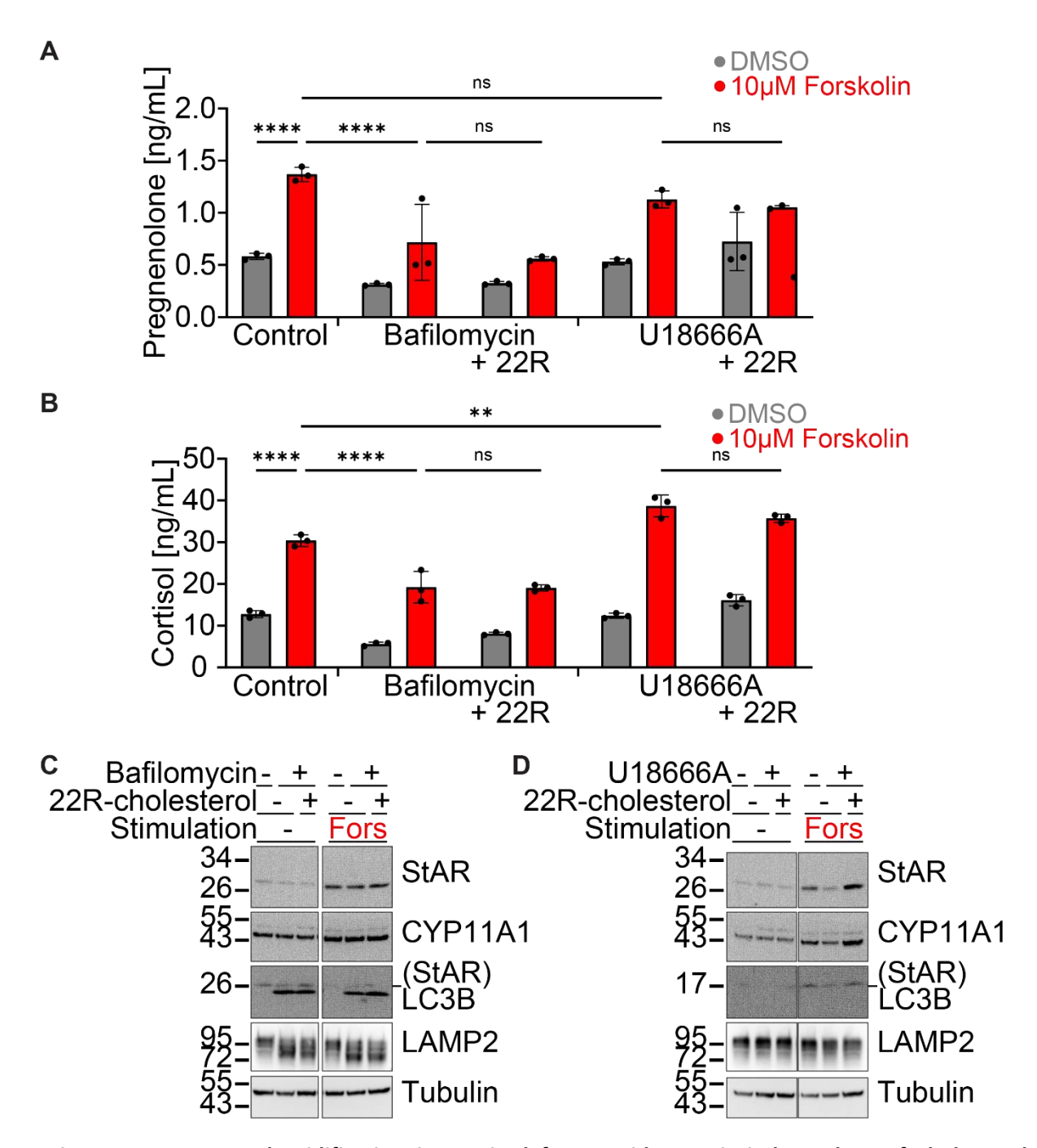


Figure 3.3. Lysosomal acidification is required for steroidogenesis independent of cholesterol homeostasis. A) Pregnenolone, and B) cortisol secreted by wt NCI-H295R during 24 h treatment with 10 μ M forskolin, 100 nM bafilomycin, 10 μ M μ M 22R-hydroxycholesterol or 100 nM u1666A as indicated, analyzed by LC-MS. C) Immunoblot detection of StAR, CYP11A1, LC3B, LAMP2 and GAPDH for bafilomycin and untreated samples. D) Immunoblot detection of StAR, CYP11A1, LC3B, LAMP2 and GAPDH for U1666A and untreated samples. Both blots are from a single membrane, samples not discussed here were cut out, the full membrane can be found in supplemental figure 1.5F,G. Data are mean \pm s.d. of n=3 replicates. Grey = vehicle DMSO, red = 10 μ M forskolin, ns = not significant, ** = p<0.01, **** = p<0.001, ***** = p<0.0001 (two-way ANOVA).

3.1.7 Induction of protein misfolding at the ER partially inhibits corticoid synthesis

Since *de novo* cholesterol synthesis as well as steroidogenic reactions downstream of pregnenolone take place in the ER, and as it is a hub of protein translation, I asked whether inhibiting ER function would affect steroidogenesis. To do so, I used the inhibitor tunicamycin which impairs N-glycosylation of proteins synthetized at the ER, leading to protein misfolding that induces the cellular stress responses unfolded protein response (UPR) and ISR (Friedlander et al., 2000).

Tunicamycin treatment of NCI-H295R cells led to an increase in the levels of the ER stress-induced chaperone Binding immunoglobulin Protein (BiP) (Bull & Thiede, 2012), as confirmed by immunoblot (Fig. 3.4.C). Additionally, tunicamycin not only reduced basal cortisol levels but also suppressed forskolin-induced cortisol production by 50% (Fig. 3.4.A). A similar effect was observed for 11-deoxycortisol (Suppl. Fig. 1.6A) but not for other glucocorticoids, mineralocorticoids, pregnenolones or progesterones (Fig. 3.4.B and Suppl. Fig. 3.6.B-E). Tunicamycin did not affect StAR induction by forskolin, suggesting its effects on SG are independent of StAR (Fig. 3.4C).

To assess whether tunicamycin disruption of steroidogenesis is dependent on ISR activation, the small molecule integrated stress response inhibitor (ISRIB) was applied during tunicamycin treatment and steroidogenic induction (Anand & Walter, 2020; Sidrauski et al., 2013). NCI-H295R cell treatment with ISRIB was unable to rescue BiP protein levels (Fig. 3.4C), consistent with BiP being induced by the unfolded protein response independent of ISR activation (Brewer et al., 1997; Peñaranda-Fajardo et al., 2019; Rabouw et al., 2019). I tested the ISR-induced activating transcription factor 4 (ATF4) as well (Rabouw et al., 2019), but it was unresponsive in these cells (Fig. 3.4C). ISRIB application also failed to restore basal or forskolin-induced cortisol or 11-deoxycortisol levels upon tunicamycin treatment (Fig. 3.4A, Suppl. Fig. 3.6A). Unfortunately, these results are inconclusive regarding whether tunicamycin induced stress affects glucocorticoid synthesis by a direct effect of protein misfolding or via the ISR. In fact, I could not confirm the activation of the ISR in response to tunicamycin-induced protein misfolding at the ER.

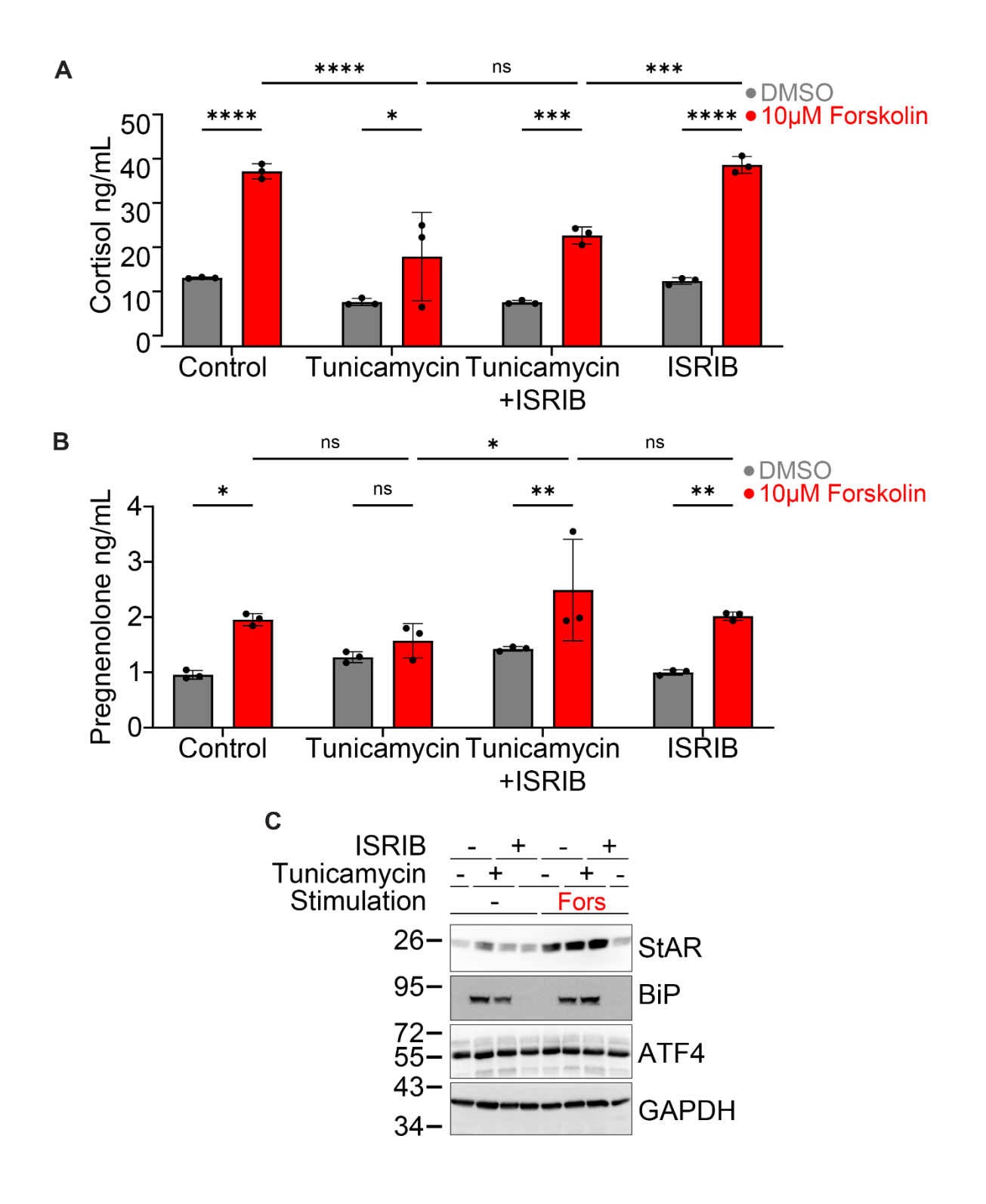


Figure 3.4. Induction of protein misfolding at the ER by inhibition of N-glycosylation by tunicamycin partially inhibits corticoid synthesis. A) Cortisol, and B) pregnenolone secreted by wt NCI-H295R during 24 h treatment with 10 μ M forskolin, 10 μ M tunicamycin, or 1 μ M ISRIB as indicated, analyzed by LC/MS. C) Immunoblot detection of StAR, BiP, ATF4 and GAPDH for the same experiment. Data are mean \pm s.d. of n=3 replicates. Grey = vehicle DMSO, red = 10 μ M forskolin, * = p<0.05, ** = p<0.01, *** = p<0.001 (two-way ANOVA).

- 4 Identifying novel regulators of steroidogenesis
- 4.1 An Unbiased Proteomics Screen for Mitochondrial Regulators of Steroidogenesis
- 4.1.1 Isolation of Intact Mitochondria by Immunopurification

To capture changes in steroidogenic mitochondria such as novel mitochondrial localized regulators of steroidogenesis or proteins with mitochondria specific enrichment by steroidogenesis induction, a method for the isolation of intact mitochondria by immunopurification (mitoIP) was adapted (Chen et al., 2016). I used NCI-H295R:NCI-H295R:3xHA-GFP-OMP25 cells stably expressing OMM localized triple HA-tag by which intact mitochondria can rapidly be immunopurified (IP) using anti-HA antibody coated magnetic beads.

Mitochondria were isolated from organellar suspension derived from NCI-H295R:3xHA-GFP-OMP25 by trituration. The integrity of isolated mitochondria was assessed by immunoblot analysis of established marker proteins for mitochondrial subcompartments (Fig. 4.1A). The marker proteins used were voltage-dependent anion channel 1 and 2 (VDAC1/2) for OMM, succinate dehydrogenase subunit A (SDHA) for IMM and citrate synthase (CS) for the mitochondrial matrix. Similar enrichment of all three subcompartment markers in the mitoIP compared to the whole cell fraction indicates the mitochondria isolated were intact. StAR enrichment by forskolin confirms induction of steroidogenesis and its enrichment at mitochondria indicates it remains associated during mitoIP. The purity of isolated mitochondria was tested based on co-enrichment of potential contamination by organelles such as ER, by the marker protein Calreticulin (CRT). Residual signal of ER was observed in isolated mitochondria, but it was de-enriched in mitoIP compared to whole cell as opposed to the enriched mitochondrial markers.

To determine whether the expression of GFP-targeted to the OMM affected steroidogenesis, steroids in culture media of NCI-H295R:3xHA-GFP-OMP25 were analyzed by LC/MS. Levels of steroids 24 h after forskolin induction were similar between WT and OMM-GFP-expressing NCI-H295R cells. For example, forskolin induced a 5-fold increase in cortisol (glucocorticoid) and a 4-fold increase in corticosterone (mineralocorticoid) in both cell lines (Suppl. Fig. 4.1.A). Thus, expression of OMM-localized GFP did not impair the ability of these cells to produce steroids in response to SG stimulation.

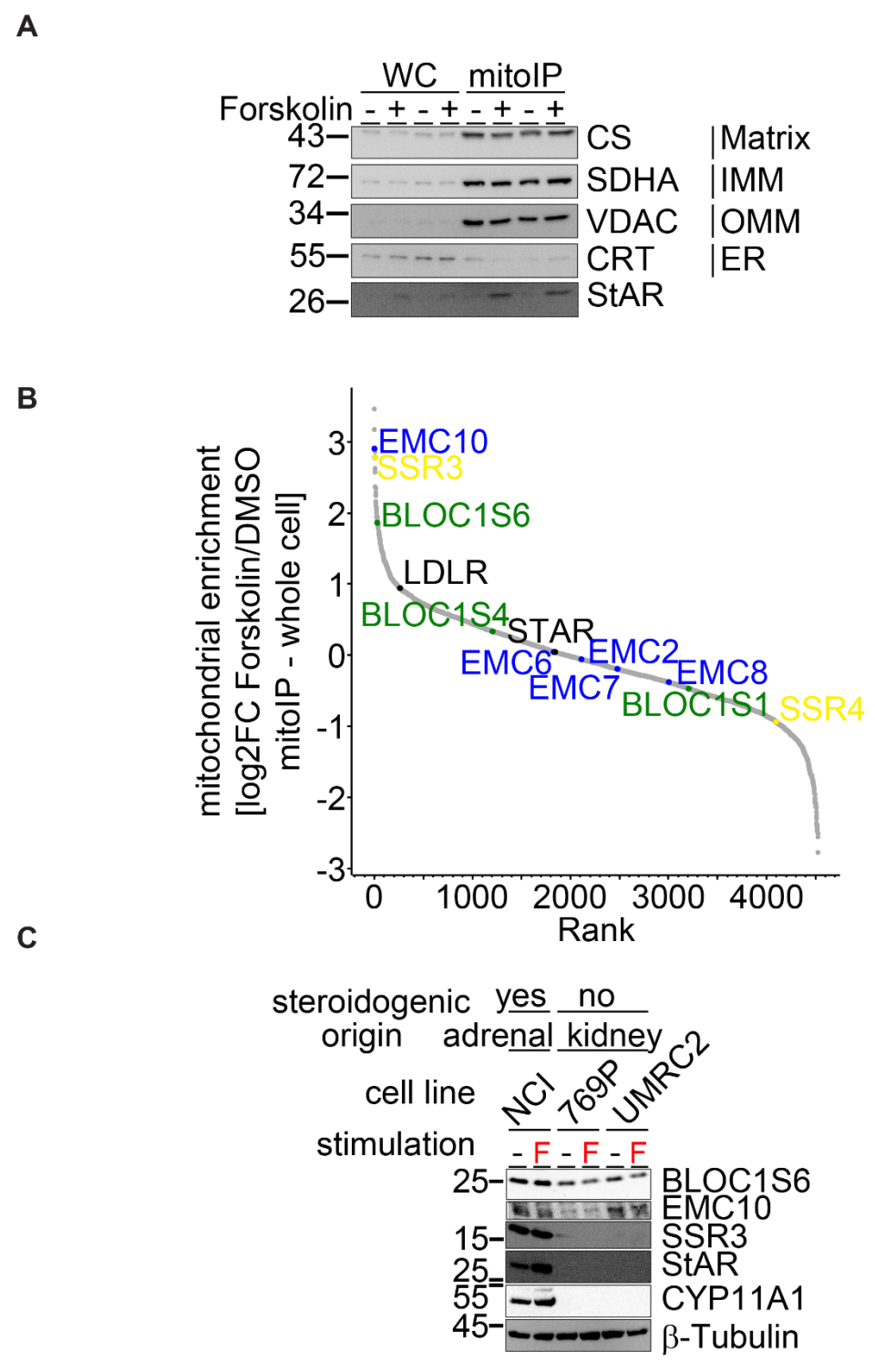


Figure 4.1. Specific factors of LROs and ER increase at mitochondria during steroidogenesis induction. A) Immunoblot of whole cell lysate (WC) and mitochondria isolated by IP (mitoIP) from organellar suspension of NCI-H295R:HA-GFP-OMP25 treated with 10 μ M forskolin or vehicle DMSO for 24 h. Analyzed for Citrate Synthase (CS), SDHA, VDAC1/2, Calreticulin (CRT) and StAR. B) Mitochondrial enrichment, calculated as the difference between mitoIP and whole cell in the log₂ fold change induced by forskolin compared to vehicle, detected in TMT-based quantitative proteomics by LC/MS. Ranked from the largest (positive) to the smallest (negative) enrichment. C) Immunoblot detection of BLOC1S6, EMC10, SSR3, StAR, CYP11A1, and beta-Tubulin in WT NCI-H295R (NCI), WT 769P and WT UMRC-2 cells.

4.1.2 Changes in the Whole Cell Proteome and Mitochondrial Proteome during Steroidogenesis Induction

Whole-cell and mitochondria isolated by IP from NCI-H295R cells stimulated for 24 hours with forskolin or vehicle were processed and analyzed using tandem mass tag (TMT)-based quantitative proteomics by LC/MS. In the adjusted analysis, 6663 and 4541 proteins were identified in the whole cell and mitochondrial proteomes, respectively. This corresponds to 32.3% and 22% coverage of the human reference proteome, respectively. Of these, in the whole cell proteome 1597 proteins were significantly upregulated and 1470 were significantly downregulated upon forskolin stimulation of steroidogenesis. For the mitochondrial proteome 546 were upregulated while 511 were downregulated.

KEGG pathway analysis of proteins significantly increased more than 3-fold upon forskolin treatment in the mitoIP fraction identified upregulation of steroidogenic and cholesterol metabolism pathways (Kanehisa et al., 2016). However, this enrichment was driven solely by the upregulation of StAR and LDLR. Pathway analysis of downregulated proteins revealed bile acid secretion; however, both of these analyses did not find either of these pathways to be changed with statistical significance (data not shown). GO term enrichment analysis, another method for pathway analysis, yielded similar results (Gaudet et al., 2011).

Remarkably, I found StAR upregulated by almost exactly the same 4-fold change in both the whole cell and mitoIP fractions upon forskolin treatment (Suppl. Fig. 4.1.C). This finding aligns with the well-established understanding that StAR regulation primarily occurs at the transcriptional level (Miller, 2013). Surprisingly, LDLR, known as a plasma membrane-localized import receptor for cholesterol, was identified in the mitoIP fraction. It exhibits a 4-fold enrichment upon forskolin treatment compared to only 2-fold induction in the whole cell proteome (Fig. 4.1B, Suppl. Fig. 4.1.C). LDLR mitochondrial localization and its role in SG has recently been described by others (Zhou et al., 2023). Next, I examined known mitochondrial proteins, based on MitoCarta3.0 classification (Rath et al., 2020), to see whether specific factors are distinctively regulated by forskolin stimulation of steroidogenesis. Most mitochondrial proteins were upregulated (381) or unchanged (484), less proteins were downregulated (47), at the whole cell level. In contrast, most mitochondrial proteins remained unchanged (678) or were downregulated (162), with fewer proteins being upregulated (41), in the mitoIP (Suppl. Fig. 4.1.C). Specific outliers from these patterns, such as mitochondrial proteins behaving like StAR, were not observed.

Since other organelles, especially ER and lysosomes, play important roles in cholesterol homeostasis and steroidogenesis (Miller, 2013), I examined whether factors from other organelles are identified in the mitochondrial fraction and enriched by forskolin treatment. The proteins signal sequence receptor subunit gamma (SSR3) and (ER membrane protein

complex subunit 10 (EMC10) of the ER and biogenesis of lysosome-related organelles complex 1 subunit 6 (BLOC1S6) were enriched at mitochondria in forskolin treated cells. This means that these proteins were upregulated by forskolin in the mitoIP fraction, but present at levels similar to unstimulated at the whole cell level (Fig. 4.1.B). For example, SSR was 9.4-fold increased in the mitoIP but only 1.4-fold in the whole cell. EMC10 was 9.1-fold increased in mitoIP and not significantly changed at the whole cell level. BLOC1S6 was 2.9-fold increased in mitoIP and unchanged across the whole cell. In contrast, other components of the EMC complex that were also identified in the mitoIP fraction were not induced by forskolin in either fraction (Fig. 4.1.B). For another SSR complex component, SSR4, the behavior in the fractions was inverse to SSR3, *i.e.* whole cell levels increased and mitochondrial levels decreased (Fig. 4.1.B). Interestingly, the three BLOC1 subunits identified all exhibited different behavior with subunit 4 being unchanged and subunit 1 being decreased in both fractions (Fig. 4.1.B). BLOC1S1 has been previously identified as localized to mitochondria (Rath et al., 2020).

SSR3 is part of a protein complex also known as the translocon-associated protein complex (TRAP), which is required for the initiation of translocation of specific proteins across the ER membrane during their translation (Gemmer & Förster, 2020). It may also be involved in glycosylation of these proteins (Phoomak et al., 2021). The ER membrane protein complex (EMC) serves to insert newly translated proteins into the ER membrane (Guna et al., 2018). Their enrichment may indicate that translation and correct localization of certain proteins at the ER is supports steroidogenesis. The biogenesis of lysosome-related organelles complex 1 (BLOC1) is involved in the generation of cell type-specific organelles from early endosomes by sorting the proteins from various endosomal compartments. It may also be involved in trafficking of these lysosome-related organelles (LROs) and their association to the cytoskeleton. The most prominent example of a LRO are melanosomes in melanocytes. They also include dense and lytic granules in cells of the immune system and lamellar bodies in lung epithelial cells (Banushi & Simpson, 2022; Huizing et al., 2008). An LRO relating to steroidogenesis is so far unknown, but since they are related to lysosomes, they may be involved in cholesterol supply for SG. None of these proteins have previously been connected to SG regulation. Together, these results suggest that forskolin-induced steroidogenesis induces increase of specific factors from other organelles at mitochondria. Therefore, I investigated these candidates further to determine whether they play a role in SG.

4.1.3 Candidate regulators of steroidogenesis – BLOC1S6, EMC10 and SSR3 – are upregulated in adrenal cells

Conventional steroidogenic proteins such as StAR and CYP11A1 are highly expressed in steroidogenic tissues (Miller, 2013). Novel regulators of steroidogenesis may exhibit a similar tissue-specific expression pattern. To therefore address whether BLOC1S6, EMC10 and SSR3 followed a similar expression profile, the levels of these proteins were compared between steroidogenic adrenocortical carcinoma NCI-H295R cells and non-steroidogenic kidney epithelial cell lines 769P and UMRC-2 by immunoblot analysis. Remarkably, each of these candidates showed elevated expression in steroidogenic adrenal cells compared to non-steroidogenic kidney cell lines. Of note, SSR3 exhibited an expression profile very similar to that of StAR or CYP11A1, showing almost exclusive expression in steroidogenic cells (Fig. 4.1C).

- 4.2 BLOC1S6, EMC10 and SSR3 are novel regulators of steroidogenesis
- 4.2.1 Loss of BLOC1S6, EMC10 and SSR3 lead to defects in steroid production

If the candidates found enriched by forskolin in mitoIP proteomics and highly expressed in adrenal cells compared to kidney cells are involved in regulation of steroidogenesis, cells deficient in these proteins would be expected to have decreased steroid production. To this end genetic knockouts of these candidates were produced by population-level, *i.e.* non-clonal, CRISPR/Cas9 delivered to NCI-H295R cells. Clonal knockout cell lines cannot be produced from NCI-H295R cells because these cells don't survive when seeded as single cells. As a control for a known regulator that ablates SG upon deletion, a StAR deficient cell line was also generated. To control for the effects of generating these cell lines, a control cell line was generated using a CRISPR/Cas9 vector targeting the pseudogene AAVS1, which is expected to have no effect on steroidogenesis beyond any stress and adaptation to the lentiviral transduction and antibiotic selection processes, this cell line will hereto after be referred to as wild-type (WT). The ablation of target proteins in these cell lines was verified by immunoblot analysis (Fig. 4.2.C,D).

Steroids secreted from the candidate CRISPR/Cas9 cell lines during forskolin stimulation for 24 h were measured by LC/MS. The intermediate steroids pregnenolone and progesterone and their derivatives were modestly but significantly decreased for all three candidate knockouts compared to WT, with the exception of no decrease in 17OH-progersterone in BLOC1S6 KO upon forskolin stimulation (Suppl. Fig. 4.2.C). Specifically, 17α OH-pregnenolone, representative for this group of steroids, was decreased 17% in BLOC1S6 KO, 15% for EMC10 KO and 27% for SSR3 KO (Fig. 4.2.A). For technical reasons, the quantification standard for pregnenolone could not be accurately detected in this experiment,

therefore for this compound only relative comparison values are shown (Suppl. Fig. 4.2.A). Cortisol and 11-deoxycortisol were 38% and 34% reduced in BLOC1S6 KO, 24% and 23% reduced in EMC10 KO and 9% and 18% reduced in SSR3 KO, respectively (Fig. 4.2.B and Suppl. Fig. 4.2.D). Notably, all three candidates knockouts show already a small decrease in pregnenolone, cortisol and many other steroids at basal levels (Fig. 4.2.A,B and Suppl. Fig. 4.2.B-D). These reductions were not statistically significant, likely because non-forskolin stimulated levels of steroids are very low. In summary, all three tested candidates, BLOC1S6, EMC10 and SSR3, are required for proper functioning of SG.

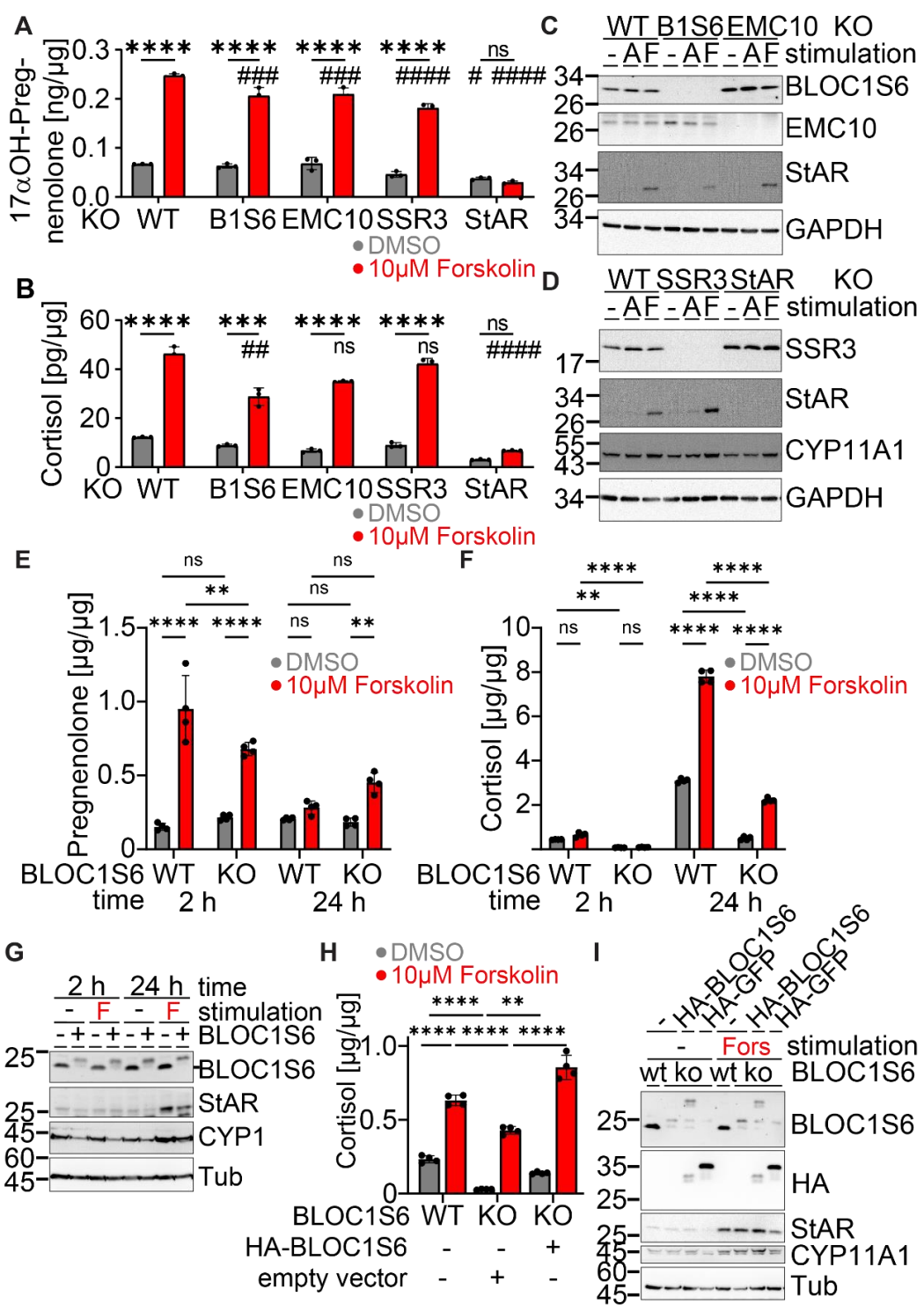


Figure 4.2. Biogenesis of lysosome-related organelles complex 1 subunit 6 is required for steroidogenesis. A) 17α OH-Pregnenolone, B) cortisol secreted by NCI-H295R CRISPR/Cas9 knockouts of indicated proteins after 24 h of 10 μ M forskolin (F) analyzed by LC/MS. Data are mean \pm s.d. of n=3 replicates. C, D) Immunoblot analyses corresponding to (A) and (B). E) Pregnenolone and F) cortisol secreted by NCI-H295R WT (AAVS1 KO) or BLOC1S6 KO following stimulation with 10 μ M Forskolin for indicated time. G) Immunoblot of lysates from the same experiment as (E) and (F). H) Cortisol secreted by NCI-H295R CRISPR/Cas9 AAVS1 (WT) or BLOC1S6 expressing HA-GFP (e.v.) or HA-BLOC1S6 during 48 h treatment with 10 μ M forskolin analyzed by LC/MS. I) Immunoblot detection for (H). Antibodies: BLOC1S6, EMC10, SSR3, HA-tag, StAR, CYP11A1 and beta-Tubulin (Tub). Data are mean \pm s.d. of n=4 replicates. Grey = vehicle DMSO, red=10 μ M forskolin, ns=not significant, */#=p<0.05, **/##=p<0.01, ***/###=p<0.001, ****/###=p<0.001 asterisks refer to comparison indicated by line, hashtags compare to WT (AAVS1) (two-way ANOVA).

4.2.2 Biogenesis of Lysosome-related Organelles Complex 1 Subunit 6 is Required for Steroidogenesis

Of the three potential candidates identified previously, the deletion of BLOC1S6 had the most pronounced effect on cortisol production. Cortisol is the most important glucocorticoid produced by adrenal cells (Miller, 2013). For this reason, I decided to further investigate the role of BLOC1S6 in SG. Due to the small effect observed on pregnenolone and related steroids, I tested a shorter period of SG stimulation in BLOC1S6 KO, as pregnenolone induction peaks hours post induction (Fig. 3.1.A). This allows a better assessment of BLOC1S6 KO effects on pregnenolone synthesis.

There was no effect of BLOC1S6 KO compared to WT (Fig. 4.2.G) in pregnenolone induction by forskolin, at neither 2 h or 24 h (Fig. 4.2.E). Although cortisol is not significantly induced by forskolin at 2 h a significant decrease by BLOC1S6 KO was already detectable at 2 h. This cortisol decrease by BLOC1S6 KO in both stimulated and unstimulated conditions persisted at 24 h (Fig. 4.2.F). Therefore, BLOC1S6 is required for glucocorticoid production, but not steroidogenesis in general.

Next, in order to substantiate that deficient SG in BLOC1S6 KO cells is due to the absence of BLOC1S6 and not a side-effect of cell line generation, I asked whether reconstitution of BLOC1S6 expression could rescue the defect on SG. To do so, BLOC1S6 with an N-terminal triple HA-tag (3xHA-BLOC1S6) and the same vector expressing 3xHA-GFP as an empty vector control (e.v.) were introduced in the NCI-H295R BLOC1S6 KO cells (Fig. 4.2.I).

After, both cell lines and WT cells were stimulated with forskolin for 48 h. This timepoint was chosen as cortisol accumulates over time, and effects on it become more prominent at later time. Loss of BLOC1S6 led to a significant 45% decrease in forskolin-induced cortisol accumulation. Basal cortisol production was also ablated by BLOC1S6KO. Re-expression of BLOC1S6 increased basal cortisol levels, though not to WT levels. But expression of 3xHA-BLOC1S6 in BLOC1S6 KO was able to restore cortisol production to levels comparable to WT upon steroid stimulating conditions (Fig. 4.2.H). Thus, BLOC1S6 is a novel regulator of steroidogenesis.

4.3 Assessment of the localization of BLOC1S6

4.3.1 BLOC1S6 is found in the cytosolic fraction and with membrane-bound organelles Because the established role of BLOC1S6 is as part of the BLOC1 complex in the generation of LROs and it is therefore localized to LROs, its identification as enriched in proteomics of mitochondria raises the question whether it truly localizes to mitochondria and how. Does the individual protein localize to mitochondria or is an LRO in proximity to mitochondria? To this

end, I first tested whether BLOC1S6 localizes exclusively to membrane-bound organelles or whether it is also found in a soluble form, dissociated from membrane-bound organelles such as LROs.

In order to assess whether BLOC1S6 is a soluble factor or a membrane-associated or organellar protein, a simple organellar fractionation of unstimulated NCI-H295R cells was performed. Organelles can be partially separated by differential centrifugation of cell lysates containing intact organelles (Itzhak et al., 2017). Such organellar suspension is achieved by trituration. In the separated fractions, the distribution of known marker proteins is used to assess the identity of the fractions and the quality of separation of organelles. Marker proteins for lysosomes (LAMP2) and mitochondria (CYP11A1) show enrichment of these organelles in the membrane fraction and de-enrichment in the soluble fraction in immunoblot. Inversely, the markers GAPDH for cytosolic proteins and Perilipin 3 (Plin3) for LD, which due to their lipid content have lower density than other organelles, were enriched in the soluble but not the membrane-bound organelles fraction (Fig. 4.3.A).

The fractionation results show endogenous BLOC1S6 is present both in the cytosol and the membrane-bound organelles fraction. The identity of the endogenous BLOC1S6 signal can be deduced from its absence in BLOC1S6 KO. Similarly, overexpressed 3xHA-BLOC1S6 is detected both by antibodies against BLOC1S6 and HA-tag in both fractions. The construct separately expresses GFP as a marker of transduction, which localizes to the cytosol. Moreover, SSR3 as well as LDLR were also identified in both fractions, but knock-out verification was not performed for these proteins (Fig. 4.3.A). This data allows two interpretations: either BLOC1S6, SSR3 and LDLR are partially present in soluble form in the cytosol, or partially associated with LDs. For BLOC1S6 as a membrane-associated but not membrane-anchored complex component cytosolic localization is plausible (Lee et al., 2012). SSR3 and LDLR, which contain transmembrane domains, are less likely to be truly cytosolic (Gemmer & Förster, 2020; Jeon & Blacklow, 2005).

4.3.2 Isolation of the BLOC1S complex by BLOC1S6-purification to screen for interactors

Protein-protein interactions can give insight into the function but also the localization of a protein. I asked whether the interactors of BLOC1S6 include mitochondrial proteins, which could support contact with or localization to mitochondria. Therefore, isolation of the BLOC1 complex by IP of 3xHA-BLOC1S6 was analyzed by proteomics comparing 3xHA-BLOC1S6 with 3xHA-GFP expressed in NCI-H295R cells.

In 3xHA-BLOC1S6 IP compared to 3xHA-GFP control IP, I found strong enrichment of BLOC1 subunits 1 through 6, as well as SNAPIN (also known as BLOC1S7) and DTNBP1 (also known as BLOC1S8). Thus, the entire BLOC1 was isolated intact. In addition, BLOC1-related complex subunit 5 (BORC5) and subunit 7 (BORC7) were enriched. These proteins belong to a complex that also contains BLOC1S1 and BLOC1S2, indicating these two complexes may form a single supercomplex (Fig. 4.3.B) (Ge et al., 2025; Tunganuntarat et al., 2023). 3xHA-GFP was strongly de-enriched in this comparison, as expected. Sixteen other proteins were significantly co-enriched with 3xHA-BLOC1S6 and the other BLOC1 components. Three enriched proteins were classified as mitochondrial by MitoCarta3.0 (Rath et al., 2020), including Grp E-like protein 1 (GrpEL1) which is a nucleotide exchange factor (NEF) for mitochondrial heat-shock protein 70 (mtHsp70), associated with presequence-associated motor complex (PAM) (Morizono et al., 2024). In summary, the co-enrichment of few mitochondrial proteins may indicate some form of interaction between BLOC1S6 and mitochondria. However, none of the co-enriched proteins have been described to function in steroidogenesis.

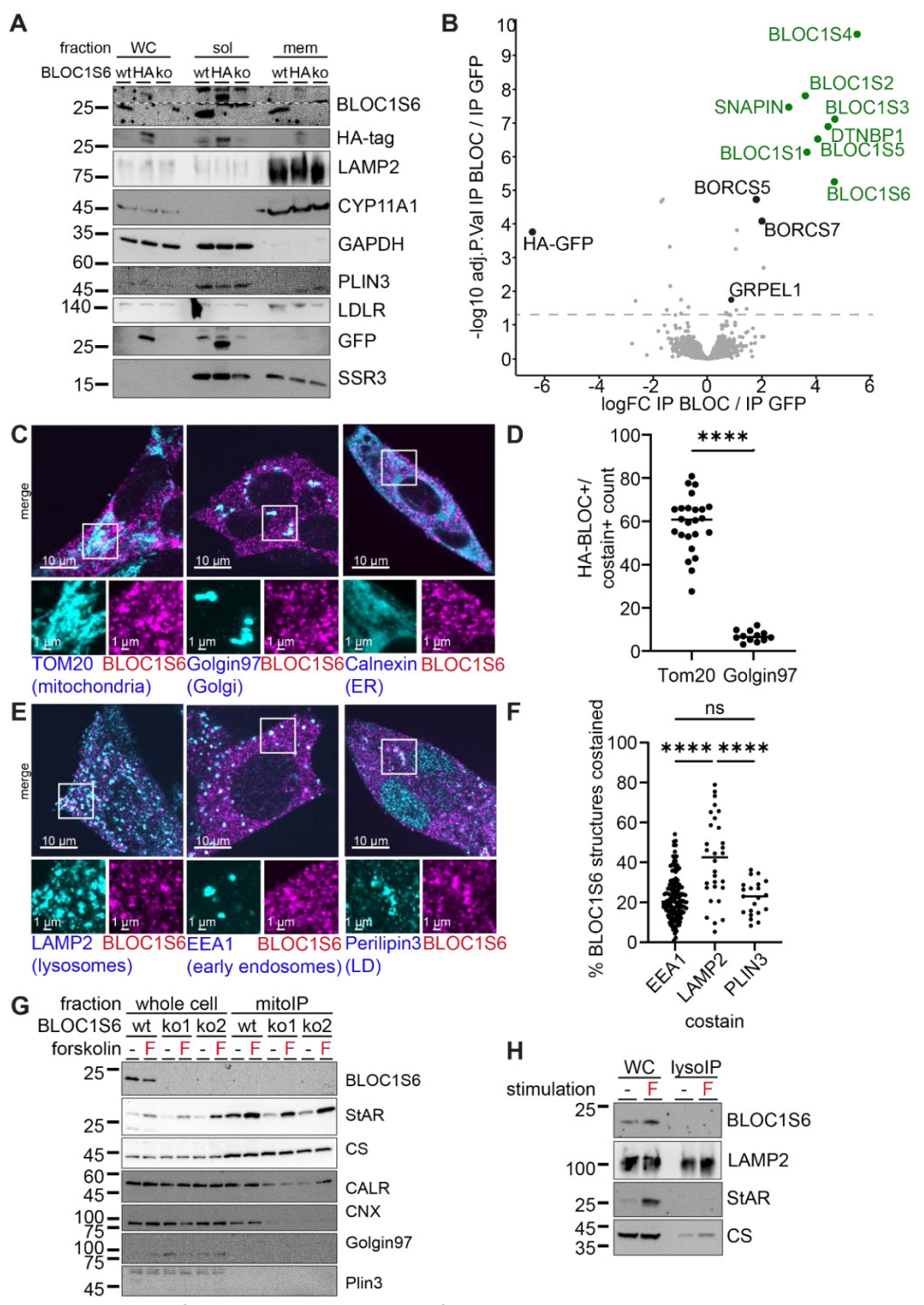


Figure 4.3. BLOC1S6 is found in the cytosolic fraction and with membrane-bound organelles.

A) Immunoblot of whole cells (WC), cytosolic/low density (sol), and membrane-bound organelle (mem) fractions from organellar suspension of NCI-H295R wild-type (wt, AAVS1), BLOC1S6 KO, and BLOC1S6 KO expressing 3xHA-BLOC1S6. Analyzed for BLOC1S6, HA-tag, LAMP2, CYP11A1, GAPDH, PLIN3, LDLR, GFP, and SSR3. Non-specific bands detected by anti-BLOC1S6 were cut out, the full membrane is shown in Suppl. Fig. 2.3. B) Enrichment of proteins by IP anti-HA of NCI-H295R:HA-BLOC1S6 vs. HA-GFP detected by label-free DIA LC-MS proteomics. C, E) Confocal microscopy on immunofluorescence-strained fixed NCI-H295R:3xHA-BLOC1S6 using antibodies against HA-tag in separate combinations with TOM20, Calnexin, Golgin97, LAMP2, EEA1, and Plin3. D, F) Quantification of of overlap events >100nm of these images. G) MitoIP of NCI-H295R AAVS1 (wt) vs. BLOC1S6 KO, and H) lysoIP of wt NCI-H295R immunoblots probed for BLOC1S6, CS, LAMP2 StAR, CALR, CNX, Golgin97 and Plin3.

4.3.3 Localization of BLOC1S6 in steroidogenic cells

Because BLOC1S6 was found enriched at mitochondria in proteomics (Fig. 3.1B), I attempted to characterize the subcellular localization of BLOC1S6, in order to elucidate whether it localizes to mitochondria or is in proximity to mitochondria or other cellular organelles. To this end, I compared the localization of 3xHA-BLOC1S6 relative to established marker proteins for other organelles by immunofluorescence (IF) using confocal microscopy. I found that BLOC1S6 did not co-localize with markers for mitochondria (TOM20), Golgi (Golgin97), ER (CNX), lysosomes (LAMP2), early endosomes (EEA1), or LD (Plin3) (Fig. 4.3.C,E). However, frequently points of contact or overlap of BLOC1S6 staining with organellar markers were observed. Quantification shows more frequent overlap with mitochondria (Tom20) than ER (CNX) and Golgi (Golgin97) and more frequent overlap with lysosomes (LAMP2) than early endosomes (EEA1) or LD (Plin3) (Fig. 4.3.D,F). Taken together, BLOC1S6 appears to label an organelle distinct from the organelles tested here. This organelle may be in contact with other organelles such as mitochondria, but this requires further investigation.

4.3.4 Isolation of mitochondria or lysosomes does not co-purify BLOC1S6

The question whether BLOC1S6 localizes to mitochondria or lysosomes was also approached biochemically by mitochondria and lysosome immunopurification. The results show that BLOC1S6 does not co-IP with either the mitochondria fraction (mitoIP) or the lysosome fraction (lysoIP) (Fig. 4.3.G,H). Importantly, steroidogenesis induction with forskolin did not alter this outcome. Of note, specific enrichment or de-enrichment of expected organellar proteins (CS for mitochondria, LAMP2 for lysosomes) was observed in both fractions, confirming the successful isolation of mitochondria and lysosomes. The lack of BLOC1S6 in mitoIP analyzed by immunoblot is in contrast to its identification as enriched in the mitoIP fraction by proteomics. A weak interaction of BLOC1S6 with mitochondria, or only a miniscule fraction of the total BLOC1S6 in the cell interacting with mitochondria, could explain that proteomics but not immunoblot identifies BLOC1S6 with isolated mitochondria. The existing data is not sufficient define BLOC1S6 localization in relation to mitochondria, requiring further study.

4.3.5 Membrane-permeable hydroxycholesterol rescues impaired steroidogenesis in BLOC1S6KO cells

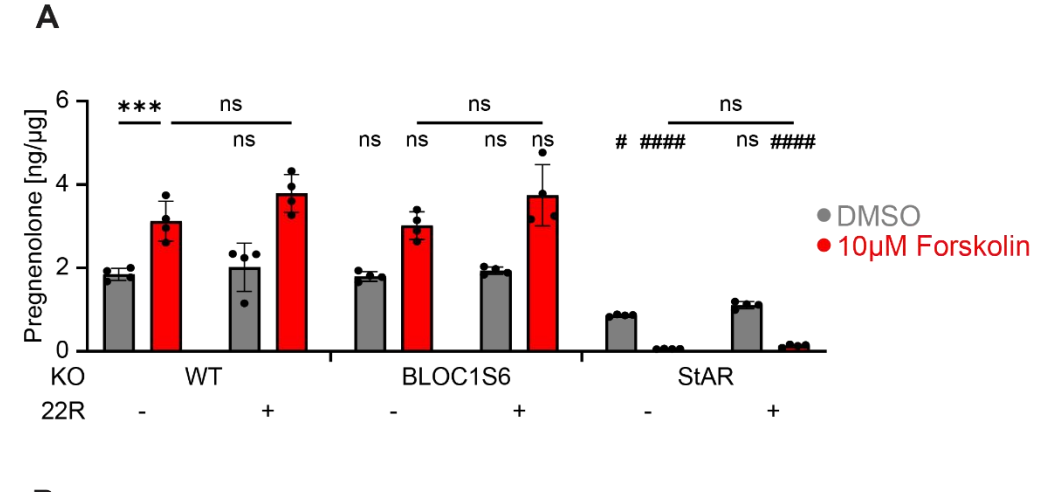
That BLOC1S6 is required for steroidogenesis (Fig. 4.2.) raises the question how such an effect is mediated. As the major regulator of steroidogenesis, StAR, is controlling cholesterol import into mitochondria, involvement in control of cellular cholesterol homeostasis is a likely mechanism of steroidogenesis regulation. When membrane-permeable 22(R)-

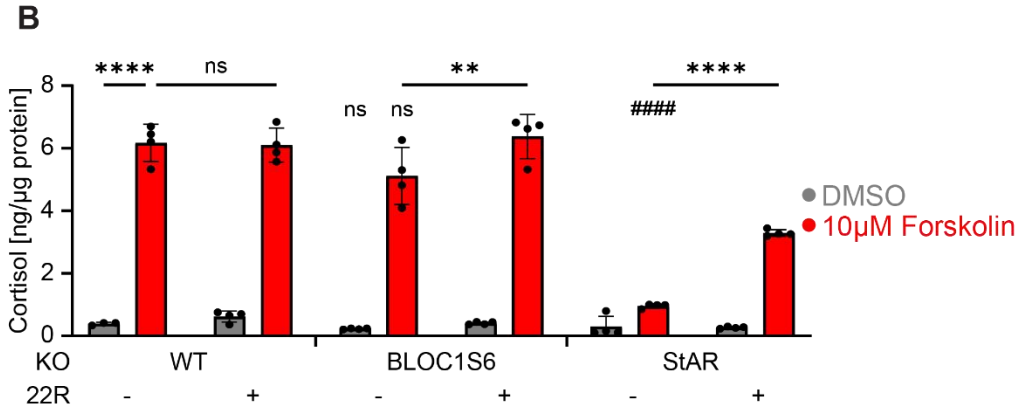
hydroxycholesterol (22R) is added to cell cultures, it can reach the IMM where CYP11A1 is located independent of the cellular cholesterol import, transport and storage machineries, including StAR. Regulation of steroidogenesis via regulation of cholesterol transfer to mitochondria and import to the IMM can therefore be indicated if the effect of regulator ablation is diminished by 22R treatment. I then asked whether BLOC1S6 affects steroid production in a similar fashion. To do so, I examined steroid levels in BLOC1S6 KO supplemented with 22R with and without forskolin treatment. I found no change of pregnenolone in BLOC1S6 KO in either unstimulated or forskolin conditions (Fig. 4.4.A), suggesting perhaps a metabolic adaptation of the cells in cell culture or that small pregnenolone decreases detected in other experiments were due to metabolic variation. StARKO drastically reduces pregnenolone levels in all conditions.

However, loss of BLOC1S6 led to a decrease in cortisol levels by 41% and 17%, in basal conditions and upon forskolin treatment, respectively. Remarkably, 22R supplementation was sufficient to rescue cortisol levels in BLOC1S6KO (Fig. 4.4.B). Taken together, these results appear contradictory since rescue by 22R is generally used to infer an effect on cholesterol import into mitochondria, yet pregnenolone appears unaffected (Lin et al., 1995). This suggests BLOC1S6KO does not affect cholesterol supply to mitochondria but impairs downstream corticoid synthesis, and that 22R is able to rescue that effect.

Importantly, 22R supplementation was able to rescue the levels of cortisol but not pregnenolone in StAR KO upon steroid-stimulating conditions, consistent with previous reports for cortisol but not pregnenolone (Lin et al., 1995; Miller & Auchus, 2011) (Fig. 4.4.B). Due to pregnenolone being depleted at 48 h (Fig. 2.1.A), it is likely more rapidly processed into further steroids than produced from 22R here. In a preliminary experiment, treatment with higher levels of 22R did not improve production of steroids by StAR KO cells further (data not shown). Furthermore, neither BLOC1S6 KO nor 22R treatment affected StAR or CYP11A1 expression levels (Fig. 4.4C).

In summary, I first identified BLOC1S6 through its enrichment at mitochondria by steroidogenesis induction. I found it is required for full functioning of SG as its ablation reduced glucocorticoid production. Whether it truly interacts with mitochondria and how it supports steroidogenesis remains to be elucidated.





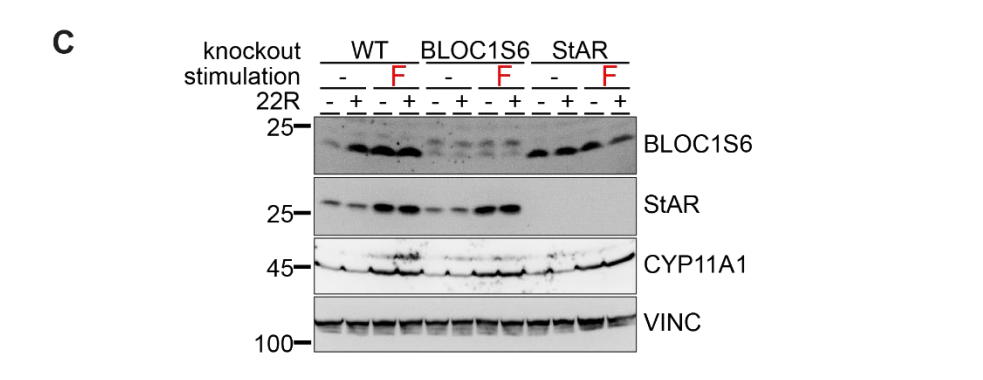


Figure 4.4. Membrane-permeable hydroxycholesterol rescues BLOC1S6 KO effect on steroidogenesis. A) Pregnenolone, and B) cortisol secreted by NCI-H295R CRISPR/Cas9 population knockouts with sgRNAs against indicated genes in 48 h of 10 μ M forskolin with 20 μ M 22R-hydroxycholesterol where indicated analyzed by LC-MS. C) Corresponding immunoblot of BLOC1S6, StAR, CYP11A1 and Vinculin. Data are mean \pm s.d. of n=4 replicates. Grey = vehicle DMSO, red = 10 μ M forskolin, ns = not significant, */# = p<0.05, **/## = p<0.01, ***/### = p<0.001, ***/### = p<0.0001; asterisks refer to comparison indicated by line, hashtags compare to WT (AAVS1) (two-way ANOVA).

5 Discussion

- 5.1 Steroidogenesis in adrenocortical carcinoma cells
- 5.1.1 Human adrenocortical carcinoma cells are a tool to study steroidogenesis in vitro

Here, I used the patient-derived NCI-H295R adrenocortical carcinoma cells as an *in vitro* cell culture model to study steroidogenesis (Gazdar et al., 1990). I confirmed that forskolin induces steroidogenesis in the synthesis NCI-H295Rs; at early time points following induction pregnenolone and other early intermediates are detected, while by 24 h and later time points cortisol accumulates (Fig. 3.1.A,B) (Kurlbaum et al., 2020). Therefore, steroidogenesis was mostly assessed at 24 hours following forskolin stimulation.

Cholesterol is key to the production of steroids, but also essential for membrane integrity and a multitude of cellular functions, and is thus required for cellular replication (van Meer et al., 2008). The main sources of cholesterol are the liver and dietary uptake (Spady & Dietschy, 1983). Circulating lipoprotein-bound cholesterol levels are controlled by the liver. But steroidogenic cells may need to adapt to very sudden dramatic increase in cholesterol demand when induced to produce steroids by tropic hormones. Adrenocortical and other steroidogenic cells can produce cholesterol de novo (Miller, 2013). I sought to discern how quickly previously produced or taken up cholesterol is used up by adrenal cells during steroidogenesis and how big the contribution of de novo synthesis is. I expected endogenous synthesis to contribute most cholesterol, as the cells are cultured without serum during steroidogenesis experiments, as is standard in the field (Kurlbaum et al., 2020). Surprisingly, using isotope-labeled glucose, I found that the fraction of cholesterol generated by de novo synthesis was minimal at 24 h (Fig. 3.1.F). Similarly, only small fractions of pregnenolone and cortisol were isotope-labeled (Fig. 3.1.D,E). However, stimulation of SG by forskolin increased labeled steroids, indicating newly synthetized cholesterol contributes to SG in this system. After 48 h SG in isotopic labeled glucose fed cells, the fraction of labelled cholesterol and steroids rises dramatically (Fig. 3.1.D-F). At this time the fraction of labeled pregnenolone (about 30%) was comparable to the fraction of labeled cholesterol, therefore synthetized cholesterol is efficiently trafficked to mitochondria for SG. Remarkably, the fraction of cortisol labeled remained low (about 12%), despite increasing with SG stimulation and over time. This shows that the SG pathway from pregnenolone to cortisol is quite slow.

These findings, indicate two key insights: first *in vitro* adrenal cells rely primally on stored cholesterol for the production of steroid hormones; second, they exhibit a remarkable ability to sustain steroidogenesis using stored cholesterol up to 48 h, highlighting the dynamic turnover of cholesterol in this process. Since SG *in vivo* mostly depends on cholesterol uptake, it is not surprising that SG cells have significant cholesterol storage capacity (Miller, 2013). This may

allow these cells to rapidly respond to SG stimulation because the uptake pathway(s) may be too slow to satisfy the sudden increase in cholesterol demand upon SG stimulation.

It is well established that the supply of cholesterol into mitochondria is the most important point of regulation of steroidogenesis. This step is regulated by StAR (Miller, 2013). My finding that the cholesterol utilized for SG is coming from mostly already present cholesterol in this adrenal model suggests that these cells need to coordinate its mobilization from storage or through the redirection of cholesterol still within the endolysosomal uptake pathway to mitochondria. This raises the question of how this mobilization is regulated.

5.1.2 Functional mitochondria are required for steroidogenesis

Mitochondria are essential to cellular metabolism, they are the site of production for several important metabolites, and they produce energy used throughout the cell. Since cholesterol production and its conversion into steroids is highly energy consuming, it may be unsurprising that inhibition of ATP synthase, ablation of the mitochondrial membrane potential and inhibition of ETC complexes abolishes steroidogenic function (Fig. 3.2.A,B,D). Notably, all treatments used to impair mitochondrial function also reduced or eliminated induction of StAR by forskolin (Fig. 3.2.C,E). This indicates that these mitochondrial mechanisms are directly required for StAR function. The alternative that CYP11A1 and other mitochondrial or ER-resident steroidogenic enzymes are not receiving enough reductive equivalents to support their function has been ruled out by others (Allen et al., 2006; Duarte et al., 2007).

An increase of mitochondrial mass could theoretically support enhanced steroidogenic capacity. However, the fact that mitochondrial genome translation was not required for steroidogenesis suggests that its induction does not stimulate or correlate with mitochondrial biogenesis. Another way mitochondrial function can be modulated during steroidogenesis is regulation of mitochondrial fission and fusion, termed mitochondrial dynamics. Mitochondrial fusion has been shown to be both induced and essential for angiotensin II-stimulated SG in adrenal cells (Helfenberger et al., 2019). Therefore, I investigated whether this phenomenon also occurs during forskolin stimulation. My findings show, that mitochondria in adrenal cells stimulated by forskolin did not display hyperfused mitochondria, which indicates this fusion is not required for steroid hormones synthesis (Fig. 3.2.F). Angiotensin-stimulated mineralocorticoid production occurs more rapidly compared to forskolin-stimulated glucocorticoid synthesis, so I speculate that the rate of steroid synthesis rather than the overall SG capability is enhanced by mitochondrial fusion during angiotensin II-stimulated steroidogenesis.

5.1.3 Lysosomes contribute more than cholesterol mobilization for steroidogenesis

Cholesterol that is internalized while bound to circulating LDL is endocytosed and processed by the endolysosomal pathway (Miller & Auchus, 2011). The release of this cholesterol requires functional lysosomes. Therefore, I investigated the contribution of lysosomal function during steroidogenesis. When I inhibited lysosomal acidification, which is essential to lysosomal function, steroidogenesis was dampened (Fig. 3.3.A,B). However, addition of membrane-permeable 22R did not rescue this phenotype, suggesting that lysosomes provide more than just cholesterol for steroidogenesis. Similarly, inhibition of NPC1 which mobilizes cholesterol did not impair steroidogenesis (Infante et al., 2008). For both 22R treatment and NPC1 inhibition, controls showing they achieved the desired effect were not included in the experiment. If the observed effects can be reproduced with proper controls, these results would suggest lysosomes support steroidogenesis in other ways.

Hypothetically, lysosomes may support the uptake and processing of nutrients for the iron-sulfur cluster cofactor biosynthesis that is required for the redox pathway that fuels cytochrome P450 enzymes which make up many steroidogenic enzymes. But these enzymes are relatively stably expressed in steroidogenic cells, including adrenal cells, such that biosynthesis is not induced and should not be required for acute steroidogenic stimulation (Miller, 2013). This renders this pathway unlikely to be the reason why functional lysosomes are required. Another pathway that might be involved is the central regulation of metabolism by mechanistic Target Of Rapamycin (mTOR). Signaling through mTOR is dependent on lysosomal acidification and could affect regulation of steroidogenesis (Goul et al., 2023). To this end, phosphorylation of key mTOR signaling factors could be analyzed during SG induction in combination with inhibition of lysosomal acidification.

5.1.4 ER stress impairs glucocorticoid synthesis

The ER plays a crucial role in steroidogenesis. For instance, it is the site of cholesterol synthesis and sensing, as well as the production of intermediate steroids. Furthermore, the ER is a major hub of protein translation. Although StAR is produced in the cytosol and translation of steroidogenic enzymes is not induced during acute steroidogenesis other regulators of steroidogenesis may depend on ER translation (Tugaeva & Sluchanko, 2019). I therefore sought to address the role of ER function during steroidogenesis. Impairing ER translation by inducing protein misfolding through inhibition of N-glycosylation at the ER inhibited synthesis of glucocorticoids such as cortisol but not overall steroidogenesis, as intermediate steroids like pregnenolone were unaffected (Fig. 3.4.A,B and Suppl. Fig. 3.6.A-C). StAR protein levels were not affected as expected due to its translation in the cytosol. ER stress activated the integrated

stress response (ISR), a pathway that promotes cellular survival under various stress conditions (Pakos-Zebrucka et al., 2016). The inhibition of the ISR during tunicamycin treatment, though it could not be confirmed, did not rescue glucocorticoid levels, suggesting a direct effect of the stress itself, rather than downregulation of SG by the stress response. Other methods of induction of ER stress, such as clogging the complexes for ER protein import, could be used to substantiate this hypothesis.

These results are curious, since the final steps of glucocorticoid synthesis take place in mitochondria, utilizing intermediate steroids synthetized in the ER as substrates. How ER stress influences this process is not clear. I speculate that stress at the ER affects the translocation of intermediate steroids from the ER to mitochondria. On the other hand, in this experiment pregnenolone production was lower than observed in other 24 h experiments, at 2-fold as opposed to 3-fold (Fig. 3.4.B and Fig. 3.1.A) Potentially, the pregnenolone induction was for unknown reasons already decreased to such extents that effects on it, and related steroids, were no longer observable. The experiment would have to be repeated, ideally with an earlier timepoint included, to learn more about this phenotype. If pregnenolone produced during shorter time of SG stimulation is also not affected by ER stress, the effect is specific to glucocorticoids. It would then be interesting to isolate mitochondria from stressed and control cells to see if the intermediate steroid 11-deoxycortisol, which is produced in the ER and was here unaffected, is specifically decreased in mitochondria. This result could attribute the decreased glucocorticoid production during ER stress to transport of the intermediate to mitochondria.

5.2 Identification of novel regulators of steroidogenesis

5.2.1 Proteomics of mitochondria isolated by IP captures steroidogenic regulators

In this study I have developed an unbiased approached to identify novel regulator of steroidogenesis. The method for rapid isolation of mitochondria was successfully adapted to adrenal cells, providing a novel tool for studying compartment specific regulators of steroidogenesis. With this approach I was able to prominently capture StAR, the key regulator of steroidogenesis (Fig. 4.1.B). The identical enrichment of StAR in the whole cell and mitochondria aligns with the current understanding that the cAMP signaling induced by forskolin or ACTH is controlling transcription of StAR, which is then rapidly translated and localized to mitochondria. Thus, the relative behavior in the two proteomic datasets can be used to identify potential novel regulators. If mitochondrial enrichment matches whole cell enrichment, then the candidate's translation is likely stimulated, or its degradation may be inhibited. If a protein is strongly enriched in mitochondria, without a corresponding increase at

the whole cell level, it may have been relocalized to mitochondria rather than newly synthesized. Mitochondria-specific de-enrichment could indicate either protein degradation or relocalization from mitochondria to other cellular compartments.

Remarkably, I found that the low-density lipoprotein (LDL) receptor (LDLR) that imports cholesterol required for steroidogenesis enriched at mitochondria. This is surprising as its localization had previously been thought to be limited to the plasma membrane and the endocytotic pathway. If the upregulation was equal in the whole cell, upregulation at mitochondria could have been interpreted as contamination of the mitoIP. Despite this result I decided not to further pursue LDLR, as its role supporting steroidogenesis is well established. Additionally, I did not expect import of LDL bound cholesterol to play a significant role in this in vitro model given that steroidogenesis was induced in the absence of LDL or cholesterol in the culture medium. However, recently other researchers also observed LDLR at mitochondria (Zhou et al., 2023). LDL with cholesterol that binds to LDLR and is endocytosed was shown to be trafficked in vesicles to mitochondria and imported to fuel steroidogenesis. Previously it was thought that LDL is being degraded in endolysosomes and other cholesterol transport mechanisms are being activated to supply cholesterol to mitochondria for SG (Miller, 2013). The multiple known pathways for intracellular cholesterol trafficking are likely to be active in parallel and may be able to compensate for defects in one of them. The confirmation of LDLR trafficking to mitochondria by others supports the interpretation that mitochondria-specific enrichment in my proteomics data reflects protein re-localization to mitochondria.

To find novel regulators of steroidogenesis, I evaluated proteins well established to localize to mitochondria by MitoCarta (Rath et al., 2020). I expected individual outliers from the overall behavior of mitochondrial proteins, or proteins behaving similar to StAR. Surprisingly, mitochondrial proteins clustered together, differently from StAR, with no obvious outliers. For that reason, no candidates were picked from this group to be further investigated. Overall, mitochondrial proteins identified at the whole cell level were stable or increasing, while those found in the isolated mitochondria were mostly stable with a slight trend to be decreased. I speculate this pattern could reflect a slight delay in mitochondrial protein import that could be due to increased steroidogenesis or increased import of steroidogenic proteins. Indeed, the delayed import of StAR itself into mitochondria is established and may cause import of other mitochondrial proteins to be delayed (Miller, 2025). This could be confirmed in StARKO or cells capable of StAR-independent SG such as those from the placenta or the brain.

5.2.2 BLOC1S6 is a novel regulator of steroidogenesis

Since I did not observe unique changes in mitochondrial proteins following steroidogenesis induction, I instead turned to candidates that were most enriched in mitochondria while distinctively less enriched across the whole cell. I focused on proteins known to localize to other organelles contributing to SG, specifically the ER, lysosomes and endosomes, and lipid droplets. Among these, three subunits of different protein complexes stood out due to their behavior being remarkably different to the other components of each complex (Fig. 4.1.B). These include BLOC1S6, associated with lysosome-related organelles (LROs), as well as EMC10 and SSR3, which belong to two different ER membrane protein complexes involved in insertion of newly translated proteins into the ER membrane or lumen.

Given that steroidogenesis takes place in specialized organs it is unsurprising that the expression of steroidogenic regulators and enzymes, such as StAR and CYP11A1, is strongly elevated in steroidogenic tissues compared to non-steroidogenic tissues (Miller & Auchus, 2011). By comparison of adrenal carcinoma cells to renal cell carcinoma lines I could replicate this phenomenon for StAR and CYP11A1. The candidates found in mitoIP proteomics displayed similar patterns of strong adrenal expression, which is especially surprising for components of translation-related machinery at the ER (Fig. 4.1.C). This supports the notion that these candidates are involved in steroidogenesis.

While the ablation of each candidate decreased steroid production (Fig. 4.2.A,B), in the initial experiment this effect was most consistent for BLOC1S6, the loss of which affected all important steroids in the pathways and most strongly decreased glucocorticoids such as cortisol. Deletion of EMC10 and SSR3 caused defects in most steroids except for the most important final product, cortisol. On the other hand, effects on intermediate steroids like pregnenolone and progesterone were most drastic by SSR3 deletion. It is unclear how defects of intermediate steroid production could be compensated in downstream glucocorticoid production. One possible explanation is that increased turnover of intermediates led to a decrease in their steady-state levels, yet how SSR3KO could cause such an effect is equally unknown. This could be explored further by supplementing these cells with intermediate steroids and evaluating their turnover compared to wild-type. Taken together, BLOC1S6 emerged as the strongest candidate for a novel regulator of steroidogenesis. This was confirmed by detection of similar defects in shorter induction of steroidogenesis and its rescue by re-expression of BLOC1S6 in cells lacking BLOC1S6 (Fig. 4.2.E,F,H). Therefore, the involvement of BLOC1S6 was investigated further.

5.2.3 BLOC1S6-containing structures are frequently in proximity to mitochondria

I attempted to validate the detection of BLOC1S6 in mitochondria isolated by IP via immunoblot. However, I did not detect BLOC1S6 in immunopurified mitochondrial fractions (Fig. 4.3.G). It is possible that only a small fraction of the total BLOC1S6 in the cell is localizing to mitochondria. Additionally, BLOC1S6 may have multiple subcellular localizations, transiently associating with membrane-bound organelles in a dynamic manner. Low abundance of BLOC1S6 or transient association of it with mitochondria could explain why it is difficult to detect using biochemical methods. The antibody against BLOC1S6 used here has low sensitivity and specificity, resulting in low signal to background ratio and additional non-specific bands in immunoblot (Fig. 4.3.A). This could explain why in these experiments, proteomics might have been more sensitive to low levels of BLOC1S6 than immunoblot. To determine whether this explains the discrepancy, a cell line labeling mitochondria and BLOC1S6 by different tags could be generated. With such a cell line the mitoIP immunoblot analysis could be repeated to see if detection by an epitope-tag reveals low levels of BLOC1S6 at mitochondria. BLOC1S6 was also not co-enriched in lysosomes purified by IP of TMEM142, however this method does not capture all types of endolysosomes and likely does not coenrich LROs.

The subcellular localization of BLOC1S6 was also assessed by biochemical separation of membrane-bound fractions and cytosol. BLOC1S6 was present in both the cytosolic and membrane-bound fraction (Fig. 4.3.A). This suggests multiple subcellular localizations exist for BLOC1S6. Alternatively, it could be only transiently associated with membrane-bound organelles, but this is unlikely based on previous research on BLOC1S6 and BLOC1 which is established to direct lysosome differentiation to LROs (Jani et al., 2022).

In order to characterize the organelle(s) that BLOC1S6 localizes to it was immunopurified, to see if interactors from other organelles are co-purified. Two mitochondrial proteins were coenriched with BLOC1 subunits (Fig. 4.3.B). That GrpEL1, which is associated with mitochondrial protein import machinery, was found co-enriched with BLOC1S6 is intriguing. Its behavior upon SG stimulation, and whether deletion of GrpEL1 mirrors the SG defects of BLOC1S6 deletion would elucidate whether an interaction between these proteins is required for steroidogenesis. Remarkably, no LRO proteins other than BLOC1 components were copurified with BLOC1S6. This suggests that the association of BLOC1 with LROs may be labile, furthermore if interaction of this complex with LROs is with low affinity this may also be the case for its interaction with other organelles.

Characterization of BLOC1S6 localization by confocal microscopy shows localizes to foci, consistent with how LRO vesicles have been described. However, BLOC1S6-positive foci were distinct from other organelles, including mitochondria, ER, Golgi, lysosomes, early endosomes

and lipid droplets (Fig. 4.3.C-F). These results are consistent with LROs being distinct from other organelles, including endosomes and Golgi, from which they are generated, and lysosomes, which contain proteins also found in LROs (Ge et al., 2025). Interestingly, BLOC1S6-positive structures preferentially associated with mitochondria and lysosomes, when compared to other organelles. This may suggest contacts between these organelles exist and could play a role in steroidogenesis. Further research in this direction is needed. In the future, it would be interesting to tag BLOC1S6 to different organelle compartments in cells lacking endogenous BLOC1S6 and evaluate how this affects steroidogenesis. This could reveal whether a certain subcellular localization of BLOC1S6 is stimulative for SG.

5.2.4 BLOC1S6 may affect cholesterol that is needed for steroidogenesis

When BLOC1S6 KO was treated with 22R, cortisol levels were rescued, similar to the case in StAR KO cells (Fig. 4.4.B). Since StAR regulates import of cholesterol into mitochondria for steroidogenesis, it would stand to reason that BLOC1S6 function impacts cholesterol homeostasis. However, whether cholesterol import, storage, or supply into mitochondria is affected cannot be discerned by these results. It is unlikely that cholesterol synthesis is affected based upon the minor contribution it has to cholesterol used in steroidogenesis during the first 24 h of induction.

That levels of pregnenolone (and other intermediate steroids) is unaffected by BLOC1S6 KO in most experiments contradicts the notion that BLOC1S6 supports cholesterol supply, as it is directly synthesized from cholesterol (Fig. 4.2.E; Fig. 4.4.A). Only the first steroidogenesis experiment performed on these cells showed decreased pregnenolone, which may be due to inter-experiment variation. On the other hand, glucocorticoid synthesis from intermediate steroids could be regulated by sensing of cholesterol levels at the - not yet characterized point where BLOC1S6 affects cholesterol. Such cholesterol sensing could explain the apparent contradiction between BLOC1S6 KO not affecting pregnenolone synthesis and its effects being rescued by 22R. It would be prudent to investigate if the well characterized cellular cholesterol sensing mechanism through SREBP2 is affected by BLOC1S6 KO. It has been shown that Insig-2 binds hydroxycholesterol and that this binding mimics the effects of cholesterol binding to SREBP2 (Radhakrishnan et al., 2007), therefore a mechanism where hydroxycholesterol can activate cholesterol sensing already exists. If cholesterol sensing by SREBP2 is connected to SG, this could be explored further by analyzing transcription and translation as well as posttranslational modification of SG enzymes dependent on SREBP2 activation. If glucocorticoid production is dependent on cholesterol sensing, this would be a novel mechanism of SG regulation. The concept is plausible, because in other metabolic pathways, such as in the

synthesis of cholesterol, downstream synthesis steps have been shown to be regulated by the availability of precursors (Garcia et al., 2024).

5.3 Conclusion and future directions

Steroidogenesis is a complex metabolic pathway requiring a high level of coordination between many cellular organelles and their functions. There appears to be a high degree of flexibility with multiple sources of cholesterol contributing and a variety of mechanisms for its transport. The existence of StAR-independent steroidogenesis in placenta and brain shows even StAR is not entirely essential. Thus, the search for factors contributing to steroidogenesis is likely impeded by compensatory mechanisms for most disruptions and it remains poorly understood.

I found indications that many of the mechanisms contributing to steroidogenesis are incompletely understood, as lysosomes seem to contribute more than being involved in cholesterol import and stress from impaired translation at the ER was linked to steroidogenesis. Compounding this finding, translation-related complexes at the ER appear to be required for steroidogenesis. More detailed investigation of these organellar functions and the candidates I found could advance our understanding of steroidogenesis.

I identified BLOC1S6 as a novel contributor to steroidogenesis, particularly glucocorticoids. However, the mechanism by which BLOC1S6 regulates steroidogenesis and its immediate function remains unknown. Cholesterol sensing by SREBP2 is a likely candidate mechanism that needs to be investigated. Whether other BLOC1 subunits are similarly important for steroidogenesis would indicate either that BLOC1 – as a complex alone or associated to LROs and their function – or that BLOC1S6 as an individual factor affects steroidogenesis. This can be evaluated by the effects of knock-out of other BLOC1 subunits on SG. Interestingly, BLOC1S1 has been described to support recycling of LDLR from endosomes to the plasma membrane (Zhang et al., 2020). Taken together with the finding of LDLR being trafficked to mitochondria during SG (Zhou et al., 2023), downregulation of BLOC1S1 and upregulation of BLOC1S6 could be a mechanism to increase LDLR delivery to mitochondria. Overexpression and knock-out of BLOC1S1 could be used to test this hypothesis. Furthermore, to better understand the localization or localizations of BLOC1S6 and the functional implications, one could selectively manipulate BLOC1S6 localization to explore whether its effects are localization dependent. Discovery of transient interactors of BLOC1S6 or BLOC1 may be achieved by cross-linking IP proteomics and could reveal factors by which BLOC1S6 exerts its

effects on steroidogenesis, which would be especially interesting if those factors are localized to steroidogenic organelles.

Mutations in BLOC1S6 and other BLOC1 components cause a wide variety of skin and hair pigmentation phenotypes in humans – called Hermansky-Pudlack syndrome – and rodents (Huizing et al., 2008). So far, deficiency in SG has not been described in this disease. This could be due to redundancy in the mechanisms contributing to SG. It would be interesting to study changes in steroid levels and in protein expression of SG organs of the mouse models of this disease to characterize the physiological role of BLOC1S6 in SG.

6 Materials and Methods

Cell lines, culture methods and treatments

The cell lines used in this thesis are listed in Table 1. NCI-H295R cells were cultured in DMEM/F12 supplemented with ITS-X and 5% NuSerum®, or DMEM/F12 supplemented with ITS-X and 1% FBS, as well as 1x penicillin/streptomycin. The cell lines 769-P and UMCR-2 were cultured in RPMI1640 with 10% FBS and 1x penicillin/streptomycin. HEK293T cells were cultured in DMEM with 10% FBS. Culture conditions were 37°C and 5% CO2. The cells were regularly tested for mycoplasma contamination by PCR. For experiments, cells were seeded 24 h prior beginning of treatments. During steroidogenic stimulation, cells were cultured in the respective base media without supplements and treated by the indicated compounds from stock solutions in DMSO, or in the case of 22(R)-hydroxycholesterol dissolved in ethanol, at the indicated final concentrations.

Table 1. In vitro cell lines used in this thesis.

Cell line	Source
NCI-H295R	Katrin Köhler (Universitätsklinikum Dresden, Dresden, Germany) and Katia Helfenberger (Universidad de Buenos Aires, Ciudad de Buenos Aires, Argentina)
796-P	ATCC CRL-1933
UM-RC-2	ECACC 08090511
HEK293T	ATCC CRL-1573

Molecular cloning of vectors and delivery by viral transduction

The plasmids used for this thesis were pMXs (Addgene #xx) and pCHMWS (Addgene #xx) for overexpression and pLentiCRISPRv2 (Addgene #5296) for knock-outs. Overexpression vectors were generated using NEBuilder® HiFi DNA Assembly Master Mix according to the manufacturer's instructions. The primers used are listed in Table 2. To produce knock-out pLentiCRISPRv2 vectors, sgRNA sequences were inserted as double-strand DNA oligos using golden-gate cloning according to the protocol developed by the lab that produced this vector. The sequences of DNA oligos encoding the sgRNAs are listed in Table 3.

To achieve stable expression, plasmid vectors were transduced using pseudotyped lentiviral particles. These were produced in HEK293T cells transfected using Xtremegene9 according to the manufacturer's instructions. To produce the viral particles the delivered vectors were cotransfected with the following vectors for viral particle generation: for packing of overexpression vectors pUMVC (addgene #14887); for packaging of CRISPR/Cas9-KO vectors pSPAX2 (addgene #12260); both combined with the envelope vector pCMV-VSVG (Addgene 8454). At

24 h after transfection the culture medium was renewed. On the next day, culture media was collected from the transfected HEK293T cells and passed through a 0.45 μ M PES syringe filter. This viral suspension was added with 6 μ g/mL polybrene to the target cells. After 24 h, fresh media was added to the cells. After another 24 h, cells were selected with 13 μ g/mL puromycin or 1.3 μ g/mL blasticidin, depending on the antibiotic selection resistance gene encoded on the transduced vector.

Table 2. Primers used in this thesis.

HA-BLOC1S6_IRES_GFP_fwd	atgctggagggtccgcgggaatgagtgtccctgggccg	Fwd
HA-BLOC1S6_IRES_GFP_rev	atttacgtagcggccgctcatcacatccttttggctggtctg	Rev
HA-BLOC1S1_IRES_GFP_fwd	atgctggaggtccgcgggaatggccccggggagccga	Fwd
HA-BLOC1S1_IRES_GFP_rev	atttacgtagcggccgctcactaggaaggggcagactgcagctg	Rev

Table 3. ssDNA oligos used for dsDNA oligo annealing into pLentiCRISPRv2.

sgBLOC1S6_1 Fwd	CACCG TAAACACTATCATGCCAAGT	Fwd
sgBLOC1S6_1 Rev	AAAC ACTTGGCATGATAGTGTTTA C	Rev
sgBLOC1S6_2 Fwd	CACCG TAACTGCCAGACCAGCCAAA	Fwd
sgBLOC1S6_2 Rev	AAAC TTTGGCTGGTCTGGCAGTTA C	Rev
sgSSR3_1 Fwd	CACCG AAGCAACAATGACCACGACC	Fwd
sgSSR3_1 Rev	AAAC GGTCGTGGTCATTGTTGCTT C	Rev
sgStAR_1 Fwd	CACC GGAGCGCATGGAAGCAATGG	Fwd
sgStAR_1 Rev	AAAC CCATTGCTTCCATGCGCTCC	Rev
sgStAR_2 Fwd	CACCG CCTCTAAGACCAAACTTACG	Fwd
sgStAR_2 Rev	AAAC CGTAAGTTTGGTCTTAGAGG C	Rev
sgEMC10_1 Fwd	CACCG TCGGTGGTGACGCACCCCGG	Fwd
sgEMC10_1 Rev	AAAC CCGGGGTGCGTCACCACCGA C	Rev
sgEMC10_2 Fwd	CACC GTCACAGCGGCAGCTCAGCG	Fwd
sgEMC10_2 Rev	AAAC CGCTGAGCTGCCGCTGTGAC	Rev

Immunoblotting

Cells were harvested by dissociation in accutase solution for 5 min at 37° C, then centrifuged at $1000 \times g$ for 2 min. The supernatant was removed and the cells resuspended in $50-100~\mu L$ lysis buffer (50mM Hepes-KOH pH 7.4, 40mM NaCl, 2mM EDTA, 1.5mM NaVO4, 50mM NaF, 10mM NaPyrophosphate (tetrabasic), 10mM, NaBetaGlycerophosphate (disodium salt pentahydrate) and 1% Triton X-100) containing protease and phosphatase inhibitor tablets at 4° C.

Protein concentration in lysates was quantified using Pierce™ BCA Protein Assay Kit and to equal amounts of protein per sample SDS-PAGE sample loading buffer was added to a final concentration of 1X SDS. In IP or fractionation experiments, protein concentration

determination was omitted. Samples were then applied to 12% Tris-Glycine gels and separated by SDS-PAGE for 90 min at 120V. Separated proteins were then transferred to PVDF membranes by blotting for 95 min at 440 mAmp. The membranes were blocked with trisbuffered saline (TBS) containing 0.1% Tween20 (TBS-T) and 5% bovine serum albumin (BSA) for 30-60 min at room temperature (RT). Next, membranes were incubated in TBS-T containing 1% BSA and the primary antibody (1:1000) overnight. The next day, membranes were washed three times in TBS-T and then incubated with horseradish peroxidase (HRP)-conjugated to anti-mouse IgG (CST #7076) or anti-rabbit IgG (CST #7074) at a 1:10000 dilution for 4 hours at RT and chemiluminescence during HRP substrate application was detected using a camera chamber imager (ChemoStar Imager). The antibodies used are listed in Table 4.

Immunofluorescence Assay

For immunofluorescence (IF) analysis 1×10⁴ cells were plated in a 24-well glass-bottom plate (Greiner Bio-One). 24 h after plating the experimental treatment was initiated. At the end of the experiment, cells were fixed in 4% formaldehyde in DMEM/F12 for 10 min at 37°C, then permeabilized for 20 min with 0.1% triton X100 in PBS at RT, and subsequently blocked in 3% BSA in PBS for 60 min. Next, the samples were incubated with primary antibodies as indicated at 1:500 in 3% BSA and 0.01% triton X100 overnight. On the next day, the samples were rinsed 3 times in PBS, and incubated with secondary antibodies anti-rabbit Alexa Fluor Plus 594 (Life Technologies, #A32740) and anti-rat Alexa Fluor Plus 647 (xxx) at a concentration of 1:2000 for 1 h. After further three rinses in PBS for 5 minutes each, images were taken using an confocal Olympus IXplore SpinSR spinning disk microscope https://www.olympuslifescience.com/en/microscopes/inverted/ixplore-spinsr/). images were taken with a 100X/1.35 silicon oil objective and excitation with 561 nm and 640 nm lasers using cellSens software (https://www.olympus-lifescience.com/pt/software/cellsens/).

Mitochondrial Network Analysis

Confocal images were analyzed by MiNA using Fiji following the method described in the original publication (Valente et al., 2017).

Analysis of confocal microscopy

Confocal images were analyzed using Fiji. The cell delimitation was performed by gaussian blur. Organelles were defined by the area surrounding maximal intensity of fluorescence, their

size determined by an appropriate threshold. Thus defined organelles were compared and the overlap with other organelles was quantified.

Table 4. Antibodies used in this thesis.

Target antigen name	Supplier	Catalog Number
ACTIN	Proteintech	66009-1-IG
ATF4	Cell Signaling Technology	11815S
BLOC1S6	Sigma Aldrich	HPA039928
CALNEXIN	GeneTex	GTX109669
CALRETICULIN	Cell Signaling Technology	12238S
CYP11A1	Cell Signaling Technology	14217
EMC10	Sigma Aldrich	HPA053905-25UL
HA	Cell Signaling Technology	3724S
LDLR	Novus Biologicals	NBP1-06709
SDHA	Cell Signaling Technology	11998S
SSR3	Sigma Aldrich	HPA014906-25UL
TUBULIN	Proteintech	66031-1-IG
VDAC1/2	Proteintech	0866-1-AP

Immunoprecipitation

Cells were scraped from confluent 10-cm dishes, resuspended in ice cold PBS and broken by trituration. Nuclei were spun out and the supernatant applied to magnetic beads. After incubation for 3 min, samples were washed 3x with PBS and resuspended in a buffer appropriate for the respective analysis.

Metabolomics of steroids and cholesterol and proteomics

All metabolomics and proteomics samples that I generated were analyzed by the metabolomics and proteomics core facilities of the MPI for Biology of Ageing. The methods used are described below.

GC-MS analysis of small molecules after derivatisation with methoxyamine and MSTFA

The analysis of polar metabolites was carried out using GC-MS (Gas Chromatography coupled to a Q-Exactive-Orbitrap mass spectrometer, Thermo Fisher Scientific). For this purpose, metabolites were derivatized using a two-step procedure starting with an methoxyamination (methoxyamine hydrochlorid, Sigma) followed by a trimethyl-silylation using N-Methyl-N-trimethylsilyl-trifluoracetamid (MSTFA, Macherey-Nagel). Analysis was performed as described previously (Dethloff et al., 2014)with slight modifications.

In brief: Dried samples were methoxyaminated by re-suspending them in 10 µL of a freshly prepared (40 mg/mL) solution of methoxyamine in pyridine (Sigma). The samples were incubated for 45 min at 40°C on an orbital shaker (VWR) at 1500 rpm. In the second step 90 μL of MSTFA spiked with 0.18 μl of C8 - C40 Alkane standard (40147-U, Sigma Aldrich) was added and the samples were incubated for additional 45 min at 40°C and 1500 rpm. At the end of the derivatisation the samples were centrifuged for 2 min at 21100x g and the clear supernatant was transferred to fresh auto sampler vials with conical glass inserts (Chromatographie Zubehoer Trott). For the GC-MS analysis 0.5 µL of each sample was injected using a TriPlus RSH autosampler system (Thermo Fisher Scientifc) using a Split/SplitLess (SSL) injector at 250°C in splitless mode. The carrier gas flow (helium) was set to 1ml/min using a 30m MEGA-5 MS capillary column (0.250 mm diameter and 0.25 µm film thickness, MEGA). The GC temperature program was: 1 min at 70°C, followed by a 9°C per min ramp to 350°C. At the end of the gradient the temperature is held for additional 5 min at 350°C. The transfer line and source temperature are both set to 280°C. The filament, which was operating at 70 V, was switched on 4.5 min after the sample was injected. During the whole gradient period the MS was operated in full scan mode covering a mass range m/z 70 and 700 with a scan speed of 20 Hertz and a resolution of 60000.

The GC-MS data analysis was performed using for compound annotation in combination with the quan module of Trace Finder (Version 5.1, Thermo Fisher Scientific).

The identity of each compound was validated by authentic reference compounds, which were measured at the beginning or at the end of the sequence; further by matching of the EI spectra and the retention index (RI).

For data analysis the peak areas of extracted ion chromatograms from selected fragment ions were determined with Trace Finder. The corresponding peak areas from mass peaks of every required compound were extracted and integrated using the underlying algorithm within Trace Finder, only in rare cases mass peaks were manually re-integrated. Extracted ion chromatograms were generated with a mass accuracy of <5 ppm and a retention time (RT) tolerance of <0.05 min as compared to the independently measured reference compounds. These areas were then normalized to the internal standards, which were added to the extraction buffer.

Sample derivatisation with Amplefex Keto

Derivatisation: Amplifex Keto Reagent (AB Sciex, 4465962)

Dried samples were derivatized with Amplifex Keto reagent according to the provided protocol. In brief, 50ul freshly mixed reagent is added to the dried sample and incubated at room temperature for 60 min. Subsequently, 10 ul of H2O were added, mixed and centrifuged for 5 min at 16000 g before transferring to a 1.5ml glass vial with a 300 ul glass insert.

LC-MS analysis of Keto-derivatized steroids

For the LC-HRMS analysis, 2 µl of the derivatized sample was injected onto a 100 x 2.1 mm HSS T3 UPLC column (Waters). The flow rate was set to 400 µl/min using a binary buffer system consisting of buffer A (10 mM ammonium formate (Sigma), 0.15% [v/v] formic acid (Sigma) in water (ULC-MS grade, Biosolve, Valkenswaard, Netherlands). Buffer B consisted of acetonitrile (ULC-MS grade, Biosolve, Valkenswaard, Netherlands). The column temperature was set to 40°C, while the LC gradient was: 0% B at 0 min, 0-15% B 0- 4.1min; 15-17% B 4.1 – 4.5 min; 17-55% B 4.5-11 min; 55-70% B 11 – 11.5 min, 70-100% B 11.5 - 13 min; B 100% 13 - 14 min; 100-0% B 14 -14.1 min; 0% B 14.1-19 min; 0% B. The mass spectrometer (Q-Exactive Plus, Thermo Fisher Scientific) was operating in positive ionization mode recording the mass range m/z 100-1000. The heated ESI source settings of the mass spectrometer were: Spray voltage 3.5 kV, capillary temperature 300°C, sheath gas flow 60 AU, aux gas flow 20 AU at 330°C and the sweep gas was set to 2 AU. The RF-lens was set to a value of 60.

Semi-targeted data analysis for the samples was performed using the TraceFinder software (Version 5.1, Thermo Fisher Scientific). The identity of each compound was validated by authentic reference compounds, which were run before and after every sequence and by internal standards added to the sample upon extraction. Peak areas of [M + H]+ ions were extracted using a mass accuracy (<3 ppm) and a retention time tolerance of <0.05 min.

For absolute quantification of metabolites in positive and negative ESI MRM (multi reaction monitoring) mode a Acquitiy UPLCTM I-class System / XevoTM TQ-S (WatersTM) with MassLynxTM (WatersTM) were used. With settings for capillary 2.0 kV, desolvation temp. 500°C, desolvation gas flow 800L/Hr, Cone 150L/Hr, Collision Gas Flow 0.08ml/min. Chromatographic method was addaped from(Matysik & Liebisch, 2017). A phenomenex KinetexTM 2.6µm Biphenyl 100Å, 2.1 x 50mm Column was used at 30°C. Solvent A was ULC-MS-grade water (Biosolve, Valkenswaard, Netherlands) containing 5mM Ammonium Acetate (Biosolve) + 0.1% Formic Acid (Biosolve) and B ULC-MS-grade Methanol (Biosolve) + 5mM Ammonium Acetate(Biosolve) + 0.1% Formic Acid (Biosolve). A gradient from 75% A to 0% in 6.1min at a flow rate of 0.5ml/min and an equilibration step from 8.1min to 11min was used. The MRMs used for quantification are shown in Table1. All compounds were dissolved in MeOH (100µg/ml). A mix standard was prepared of all the compounds (Mix 1; 10000ng/ml)

except of 17a-hydroxypregnenolone and DHEAS (Mix 2; 25000ng/ml) in MeOH. For all compounds a calibration curve was measured. Using concentrations from 0.61-5000 ng/ml for Mix 1 and from 97.66-25000 ng/mL Mix 2. 10µl of the internal standard (MassChromTM Steroids Chromsystem Oder No. 72044) was spiked in.

The U(H)PLC-MS data analysis was performed using the open-source software El Maven (Agrawal et al., 2019)(Version 0.12.0). For this purpose, Waters raw mass spectra files were converted to mzML format using MSConvert (Chambers et al., 2012)(Version 3.0.22060, Proteowizard). The identity of each compound was validated by authentic reference compounds, which were measured at the beginning or at the end of the sequence; further by matching of the El spectra. For data analysis the peak areas of extracted ion chromatograms from selected fragment ions were determined with El Maven. The absolute quantification of all compounds were analysed by R.

Tabelle 5. LC/MS charachteristics of steroids used.

	Parent	Daughter	Cone	Collision	
Compound	(m/z)	(m/z)	(V)	(V)	Polarity
Androstenedion	287.2	79.06	54	40	+
Androstenedion-13C3	290.35	81.2	32	42	+
DHEA	289	213	80	20	+
DHEAS	367.22	226.95	2	44	-
DHEAS-d6	375.33	100.02	16	32	-
Testosterone	289.09	97.1	82	12	+
Testosterone-d3	292.29	97.1	64	20	+
Progesterone	315.21	97.16	50	18	+
Pregnenolone	317.21	281.24	2	16	+
11-Deoxycorticosterone	331.15	97.1	2	20	+
11-Deoxycorticosterone-					
d8	339.29	100.04	36	22	+
17-Hydroxyprogesterone	331.29	97.1	18	20	+
17a-					
Hydroxypregnenolone	333.28	279.22	28	16	+
Corticosterone	347.29	121.11	72	30	+
Corticosterone-d8	355.29	125.08	70	26	+
11-Deoxycortisol	347.29	121.04	26	26	+
11-Deoxycortisol-d5	352.27	128.15	24	36	+
Cortison	361.22	163.16	56	30	+
Cortison-d8	369.29	168.11	58	26	+
Cortisol	363.09	121.13	84	22	+
Cortisol-d4	367.29	121.12	70	22	+
Aldosterone	359.35	271.29	24	20	-
Aldosterone-d4	363.29	335.3	24	16	-

Proteomics sample preparation for mitolP

TMTPro Labeling

Tryptic peptides were eluted from STAGE tips with 40% acetonitrile (ACN) /0.1% formic acid (FA). Four micrograms of the eluted peptides were dried out and reconstituted in 9 μ L of 0.1M TEAB. Tandem mass tag (TMTpro, Thermo Fisher Scientific cat. No A44522) labeling was carried out according to manufacturer's instruction with the following changes: 0.5 mg of TMTPro reagent was re-suspended with 33 μ L of anhydrous ACN. Seven microliters of TMTPro reagent in ACN was added to 9 μ L of clean peptide in 0.1M TEAB. The final ACN concentration was 43.75% and the ratio of peptides to TMTPro reagent was 1:20. After 60 min of incubation the reaction was quenched with 2 μ L of 5% hydroxylamine. Labelled peptides were pooled, dried, re-suspended in 200 μ L of 0.1% formic acid (FA), split into two equal parts, and desalted using home-made STAGE tips (Li et al., 2021).

Fractionation of TMTPro-labeled peptide mixture

One of the two parts was fractionated on a 1 mm x 150 mm ACQUITY column, packed with 130 Å, 1.7 μ m C18 particles (Waters cat. no SKU: 186006935), using an Ultimate 3000 UHPLC (Thermo Fisher Scientific). Peptides were separated at a flow of 30 μ L/min with a 88 min segmented gradient from 1% to 50% buffer B for 85 min and from 50% to 95% buffer B for 3 min; buffer A was 5% ACN, 10mM ammonium bicarbonate (ABC), buffer B was 80% ACN, 10mM ABC. Fractions were collected every three minutes, and fractions were pooled in two passes (1 + 17, 2 + 18 ... etc.) and dried in a vacuum centrifuge (Eppendorf).

LC-MS/MS analysis

Dried fractions were re-suspended in 0.1% formic acid (FA) and separated on a 50 cm, 75 µm Acclaim PepMap column (Thermo Fisher Scientific, Product No. 164942) and analysed on a Orbitrap Lumos Tribrid mass spectrometer (Thermo Fisher Scientific) equipped with a FAIMS device (Thermo Fisher Scientific). The FAIMS device was operated in two compensation voltages, -50 V and -70 V. Synchronous precursor selection based MS3 was used for the acquisition of the TMTPro reporter ion signals. Peptide separations were performed on an EASY-nLC1200 using a 90 min linear gradient from 6% to 31% buffer; buffer A was 0.1% FA, buffer B was 0.1% FA, 80% ACN. The analytical column was operated at 50°C. Raw files were split based on the FAIMS compensation voltage using FreeStyle (Thermo Fisher Scientific)

Data analysis

Proteomics data was analyzed using MaxQuant, version 1.6.17.0, (J. Cox & M. Mann, 2008) using the default parameters against the one-protein-per-gene reference proteome for Homo sapiens, UP000005640, downloaded August, 2022. Methionine oxidation and protein N-

terminal acetylation were set as variable modifications; cysteine carbamidomethylation was set as fixed modification. The digestion parameters were set to "specific" and "Trypsin/P," with two missed cleavages permitted. The isotope purity correction factors, provided by the manufacturer, were included in the analysis. Differential expression analysis was performed using limma, version 3.34.9, (M. E. Ritchie et al., 2015) in R, version 3.4.3.

Proteomics sample preparation for HA-BLOC1S6 IP

TMTPro Labeling

Tryptic peptides were eluted from STAGE tips with 40% acetonitrile (ACN) /0.1% formic acid (FA). Four micrograms of the eluted peptides were dried out and reconstituted in 9 μ L of 0.1M TEAB. Tandem mass tag (TMTpro, Thermo Fisher Scientific cat. No A44522) labeling was carried out according to manufacturer's instruction with the following changes: 0.5 mg of TMTPro reagent was re-suspended with 33 μ L of anhydrous ACN. Seven microliters of TMTPro reagent in ACN was added to 9 μ L of clean peptide in 0.1M TEAB. The final ACN concentration was 43.75% and the ratio of peptides to TMTPro reagent was 1:20. After 60 min of incubation the reaction was quenched with 2 μ L of 5% hydroxylamine. Labelled peptides were pooled, dried, re-suspended in 200 μ L of 0.1% formic acid (FA), split into two equal parts, and desalted using home-made STAGE tips (Li et al., 2021).

Fractionation of TMTPro-labeled peptide mixture

One of the two parts was fractionated on a 1 mm x 150 mm ACQUITY column, packed with 130 Å, 1.7 μ m C18 particles (Waters cat. no SKU: 186006935), using an Ultimate 3000 UHPLC (Thermo Fisher Scientific). Peptides were separated at a flow of 30 μ L/min with a 88 min segmented gradient from 1% to 50% buffer B for 85 min and from 50% to 95% buffer B for 3 min; buffer A was 5% ACN, 10mM ammonium bicarbonate (ABC), buffer B was 80% ACN, 10mM ABC. Fractions were collected every three minutes, and fractions were pooled in two passes (1 + 17, 2 + 18 ... etc.) and dried in a vacuum centrifuge (Eppendorf).

LC-MS/MS analysis

Dried fractions were re-suspended in 0.1% formic acid (FA) and separated on a 50 cm, 75 µm Acclaim PepMap column (Thermo Fisher Scientific, Product No. 164942) and analysed on a Orbitrap Lumos Tribrid mass spectrometer (Thermo Fisher Scientific) equipped with a FAIMS device (Thermo Fisher Scientific). The FAIMS device was operated in two compensation voltages, -50 V and -70 V. Synchronous precursor selection based MS3 was used for the acquisition of the TMTPro reporter ion signals. Peptide separations were performed on an EASY-nLC1200 using a 90 min linear gradient from 6% to 31% buffer; buffer A was 0.1% FA,

buffer B was 0.1% FA, 80% ACN. The analytical column was operated at 50°C. Raw files were split based on the FAIMS compensation voltage using FreeStyle (Thermo Fisher Scientific).

Data analysis

Proteomics data was analyzed using MaxQuant, version 1.6.17.0, (J. Cox & M. Mann, 2008; Jürgen Cox & Matthias Mann, 2008) using the default parameters against the one-protein-pergene reference proteome for Homo sapiens, UP000005640, downloaded August, 2022. Methionine oxidation and protein N-terminal acetylation were set as variable modifications; cysteine carbamidomethylation was set as fixed modification. The digestion parameters were set to "specific" and "Trypsin/P," with two missed cleavages permitted. The isotope purity correction factors, provided by the manufacturer, were included in the analysis. Differential expression analysis was performed using limma, version 3.34.9, (Matthew E. Ritchie et al., 2015; M. E. Ritchie et al., 2015) in R, version 3.4.3.

Statistical analyses and data visualization

One-way ANOVA or two-way ANOVA as indicated were performed in GraphPad Prism 9 or 10 software (https://www.graphpad.com/features).

All plots were generated with GraphPad Prism software version 9 or 10.

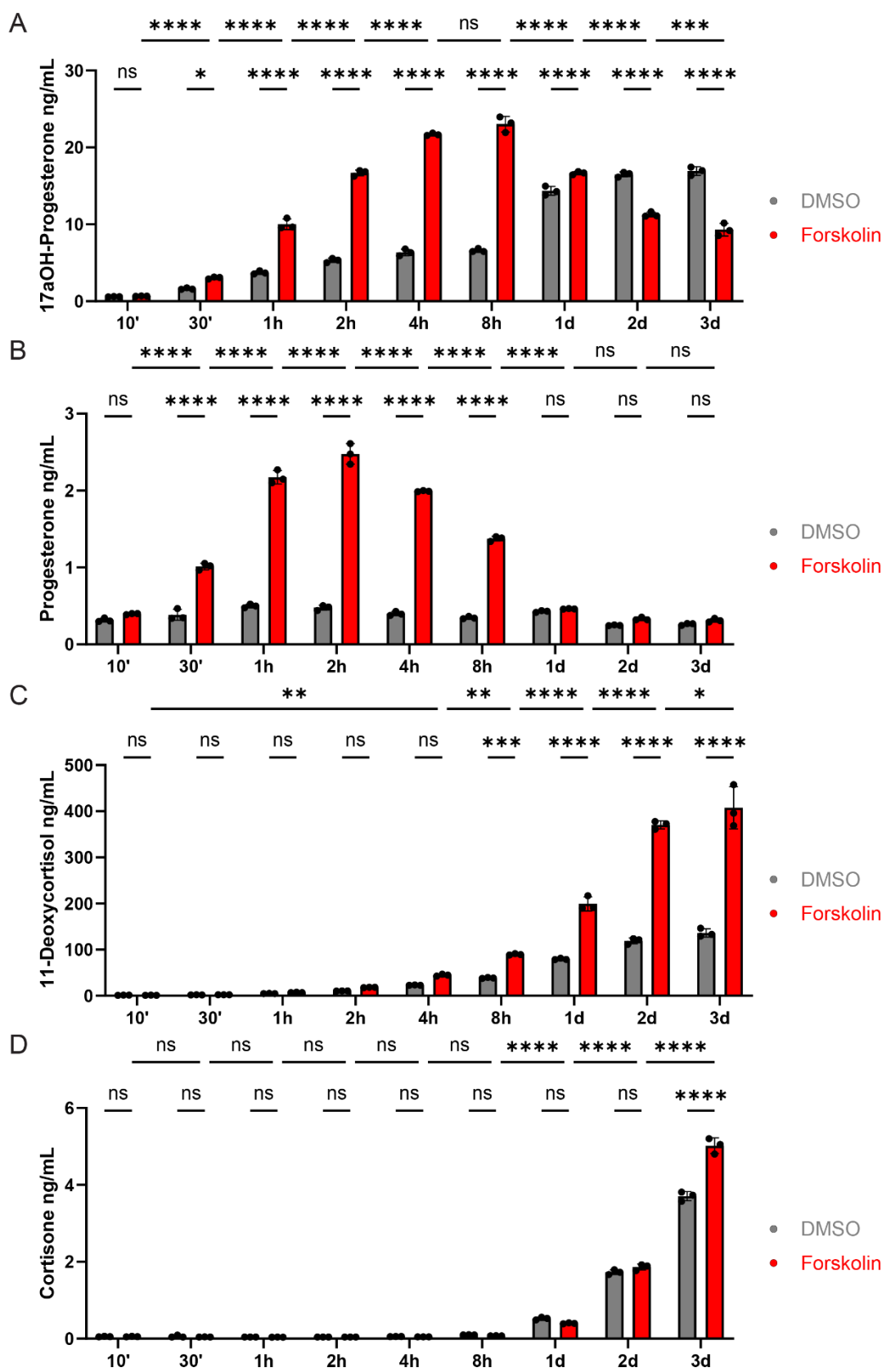
Cartoons were made with Biorender (https://www.biorender.com/).

Figures were assembled in Adobe Illustrator 2023

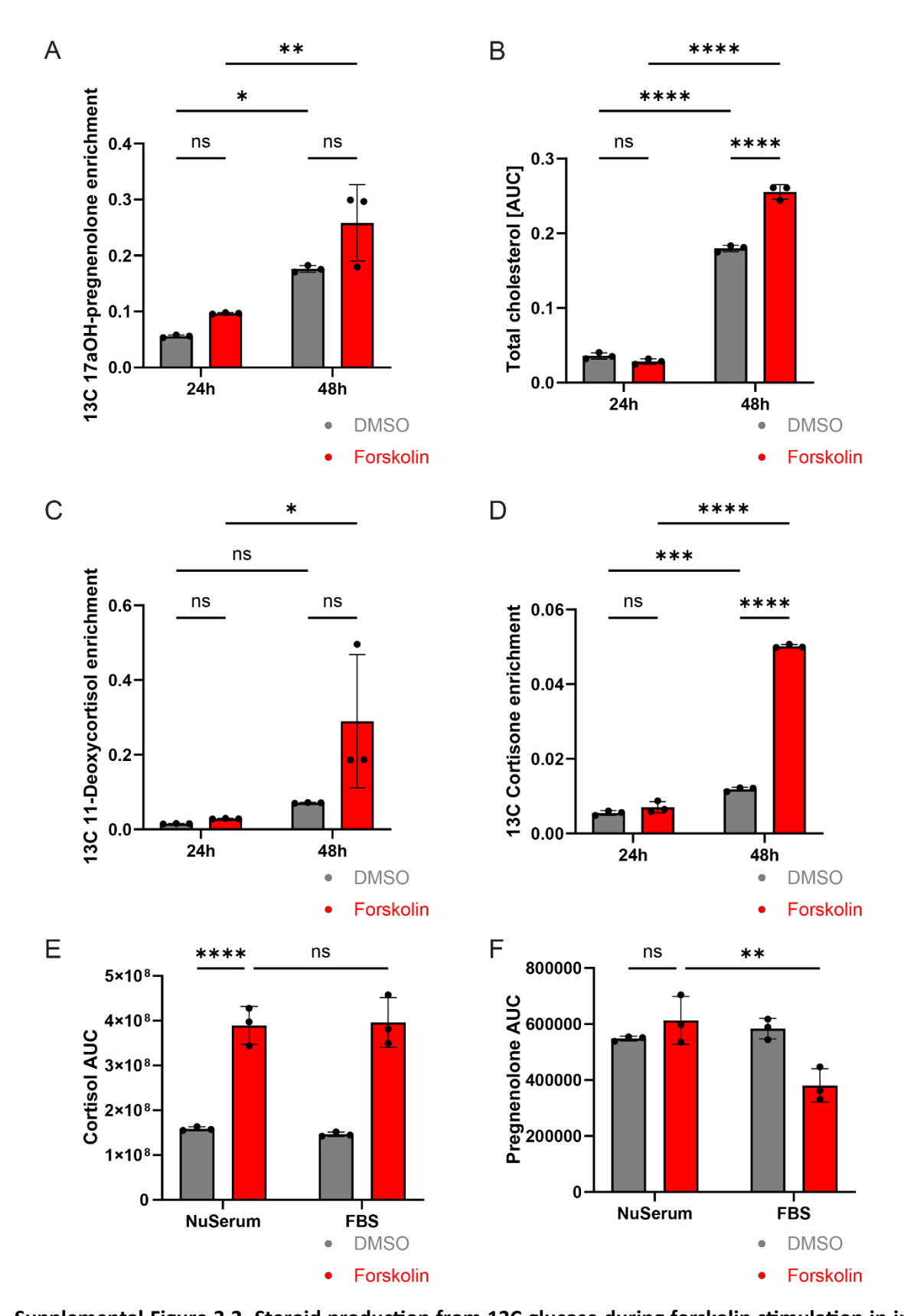
(https://www.adobe.com/products/illustrator.html).

For microscopy image analysis Fiji (https://imagej.net/software/fiji/downloads) was used.

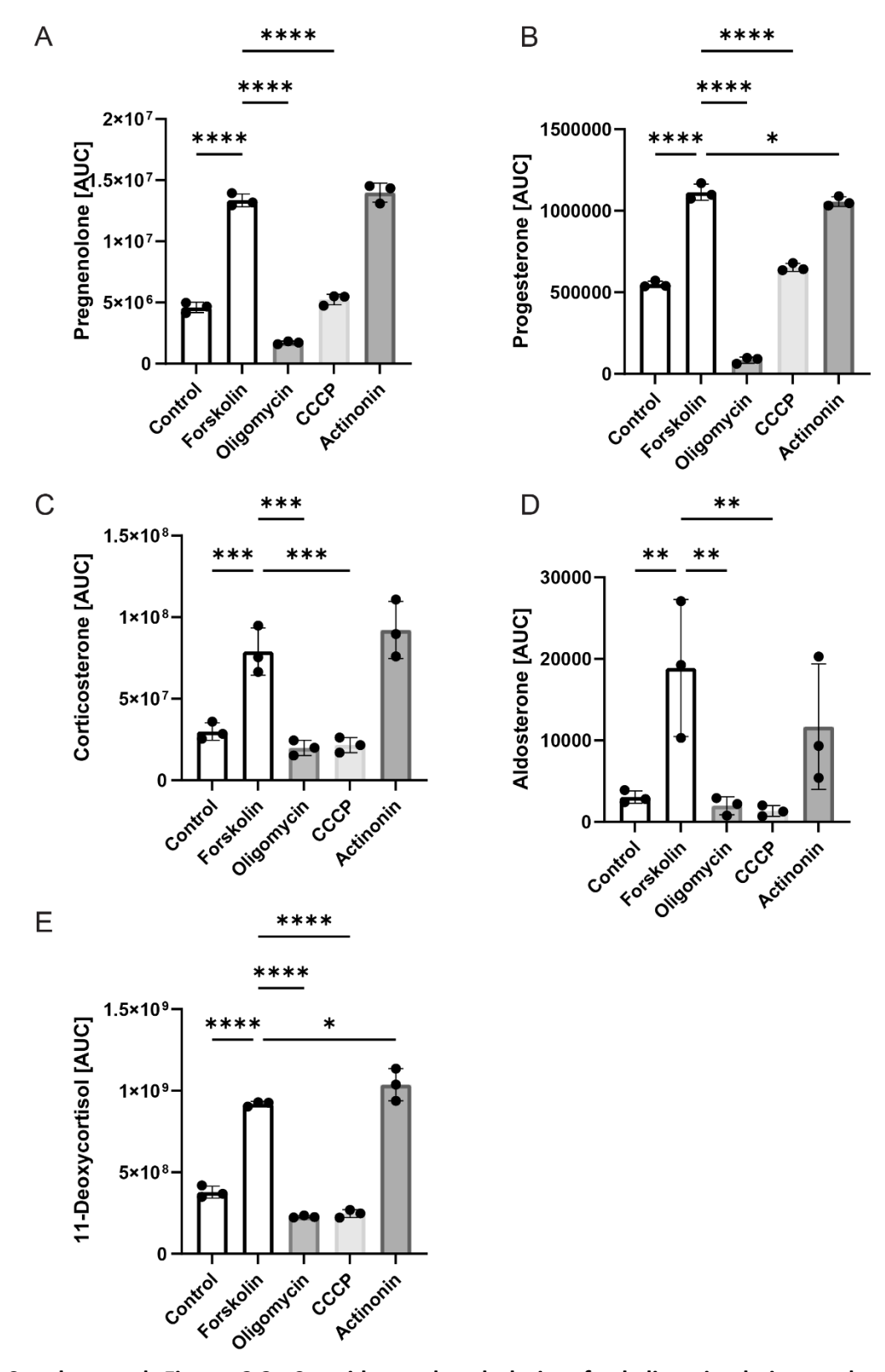
7 Supplemental Figures



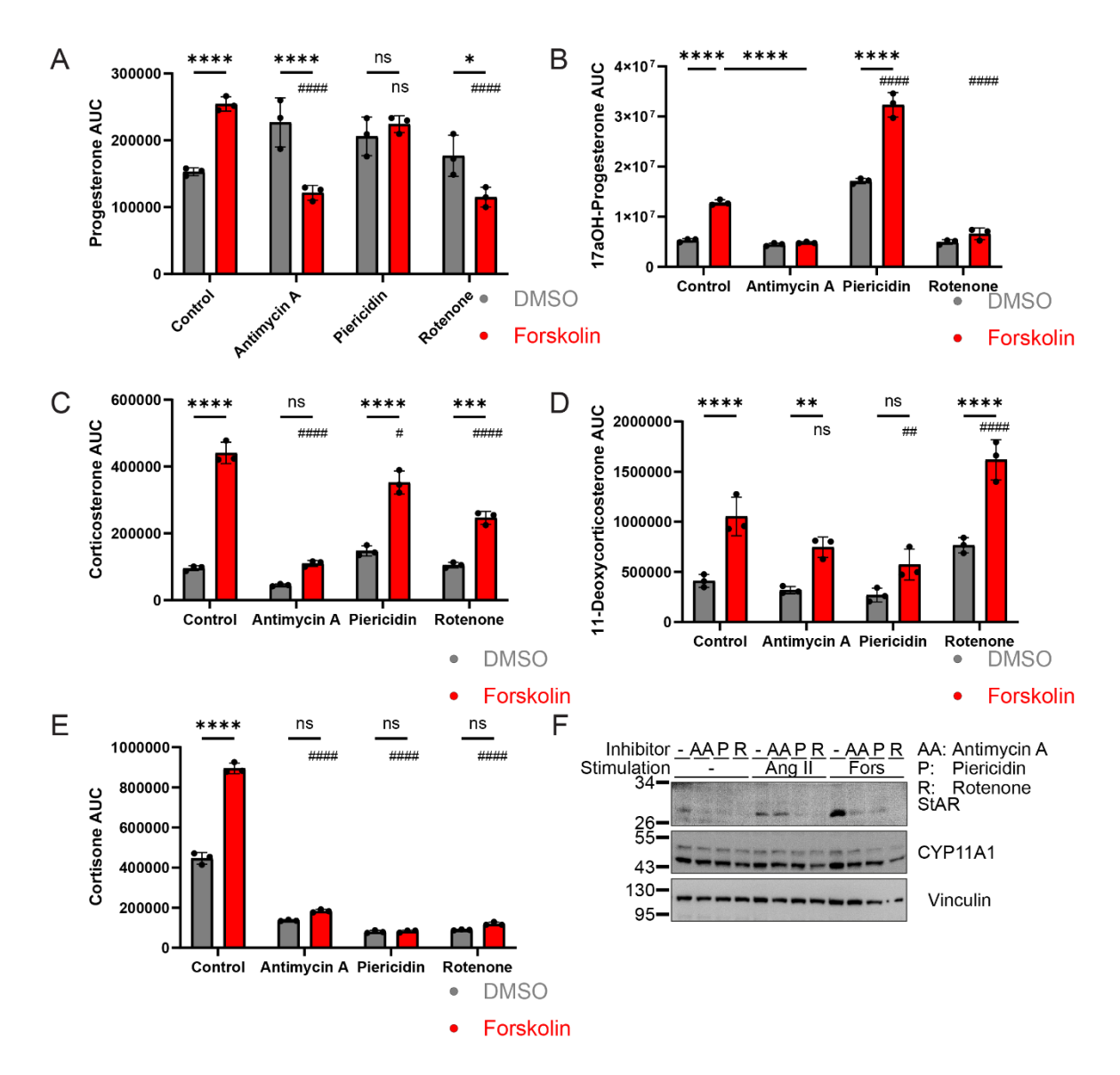
Supplemental Figure 3.1. Steroid production over time of forskolin stimulation in in NCI-H295R. A) 17OH-Pregnenolone, B) progesterone, C) 11-Deoxycortisol, or D) cortisone secreted by wt NCI-H295R into the cultured media for the indicated time analyzed by LC/MS. LC/-MS data are mean \pm s.d. of n=3 replicates. '= minutes, h = hours, d = days, grey = vehicle DMSO, red = 10 μ M forskolin, 65 nd = not detected, ns = not significant, ** = p<0.01, *** = p<0.001, **** = p<0.0001 (two-way ANOVA).



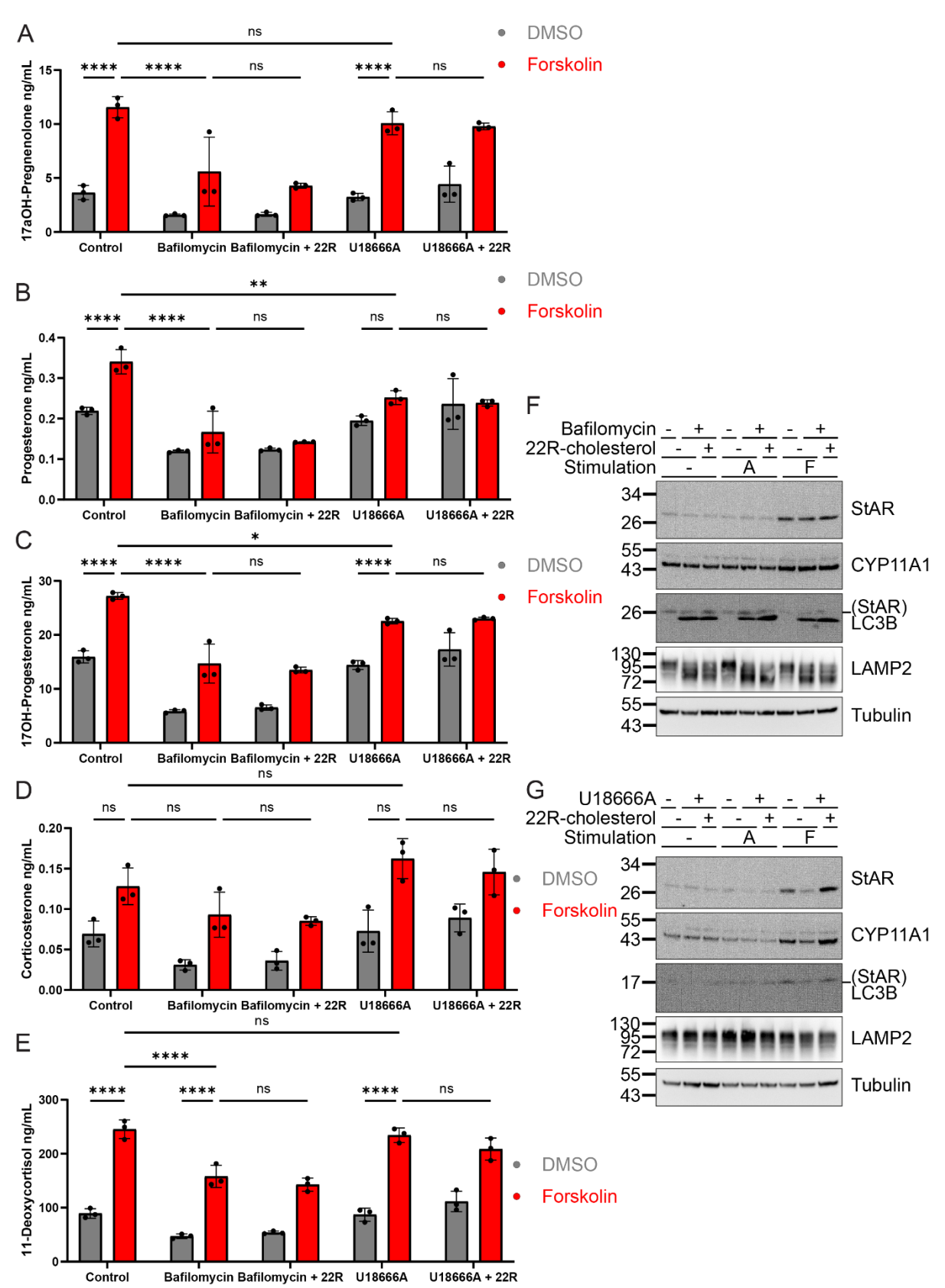
Supplemental Figure 3.2. Steroid production from 13C glucose during forskolin stimulation in in NCI-H295R. A) 17OH-Pregnenolone, B) total cholesterol C) 11-Deoxycortisol D) cortisone secreted by wt NCI-H295R into the cultured media for the indicated time analyzed by LC/MS. E) Cortisol and F) pregnenolone secreted during culture with different media analyzed by LC/MS. LC/-MS data are mean \pm s.d. of n=3 replicates. '= minutes, h = hours, d = days, grey = vehicle DMSO, red = 10 μ M forskolin, nd = not detected, ns = not significant, ** = p<0.01, *** = p<0.001, **** = p<0.0001 (two-



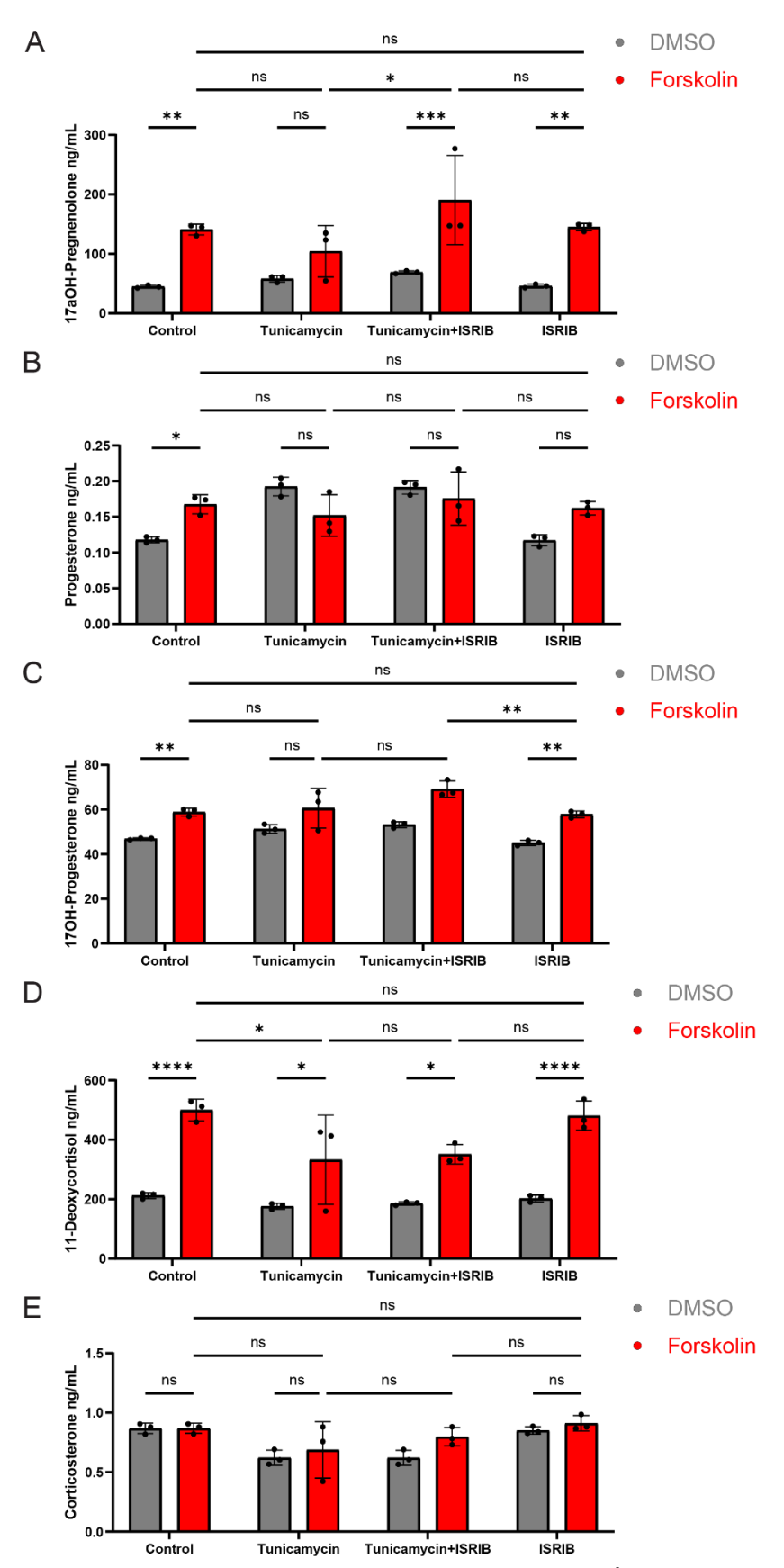
Supplemental Figure 3.3. Steroids produced during forskolin stimulation and mitochondrial inhibition. A) Pregnenolone B), progesterone, C) corticosterone D) aldosterone, E) deoxycortisol secreted by WT NCI-H295R during 24 h treatment with 10 μ M forskolin, 2 μ M antimycin A, 3.7 μ M piericidin or 5 μ M rotenone as indicated, analyzed by LC/MS. Data are mean \pm s.d. of n=3 replicates. AUC = area under curve. Grey = vehicle DMSO, red = 10 μ M forskolin, * = p<0.05, ** = p<0.01, **** = p<0.001, **** = p<0.0001 (one-way ANOVA).



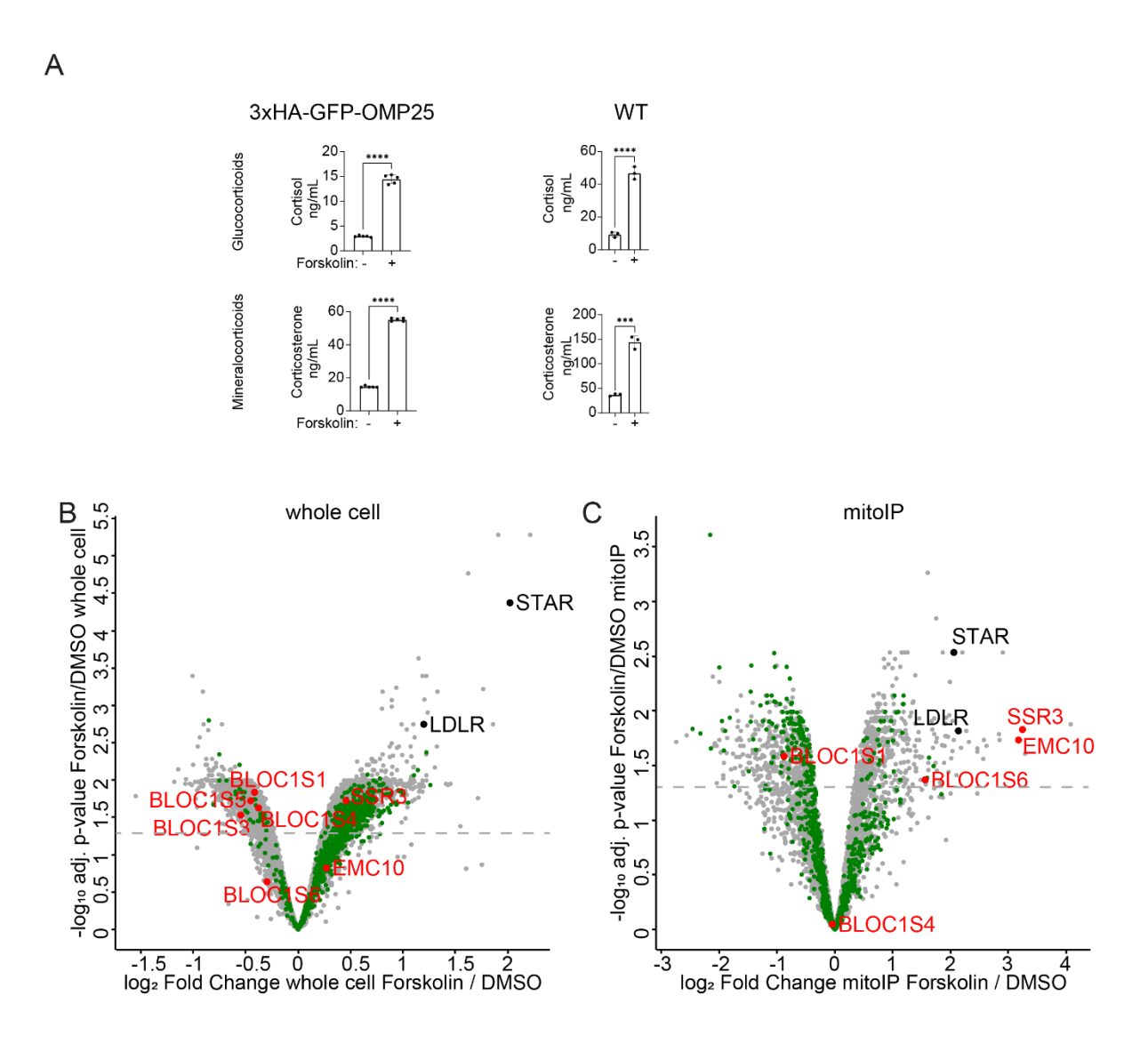
Supplemental Figure 3.4. Steroids produced during forskolin stimulation and mitochondrial inhibition. A) Progesterone, B), 170H-progesterone, C) corticosterone, D) 11-deoxycorticosterone E) cortisone secreted by WT NCI-H295R during 24 h treatment with 10 μ M forskolin, 2 μ M antimycin A, 3.7 μ M piericidin or 5 μ M rotenone as indicated, analyzed by LC/MS. Data are mean \pm s.d. of n=3 replicates. AUC = area under curve. Grey = vehicle DMSO, red = 10 μ M forskolin, */#=p<0.05, **/##=p<0.01, ***/###=p<0.001, ***/###=p<0.001; asterisks refer to comparison indicated by line, hashtags compare to control (two-way ANOVA).



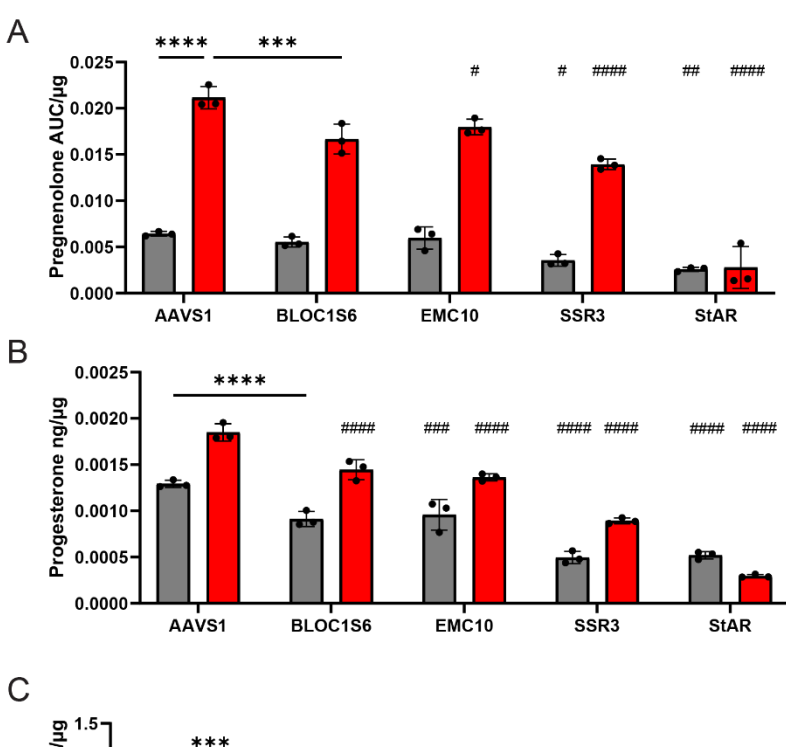
Supplemental Figure 3.5. Lysosomal acidification is required for steroidogenesis independent of cholesterol homeostasis. A) Pregnenolone, B) cortisol, C) 17OH-progesterone, D) corticosterone, E) 11-deoxycortisol secreted by wt NCI-H295R during 24 h treatment with 10 μ M forskolin, 100 nM bafilomycin, 10 μ M μ M 22R-hydroxycholesterol or 100 nM u1666A as indicated, analyzed by LC-MS. F) Immunoblot detection of StAR, CYP11A1, LC3B, LAMP2 and GAPDH for bafilomycin and untreated samples. G) Immunoblot detection of StAR, CYP11A1, LC3B, LAMP2 and GAPDH for U1666A and untreated samples. Full blots are shown here, as angiotensin II (A) stimulation is not discussed in this 69 thesis. Data are mean \pm s.d. of n=3 replicates. Grey = vehicle DMSO, red = 10 μ M forskolin, ns = not significant, * = p<0.05, ** = p<0.01, *** = p<0.001, **** = p<0.0001 (two-way ANOVA).

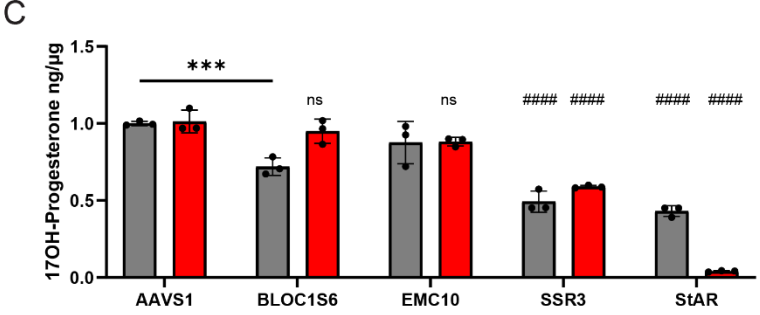


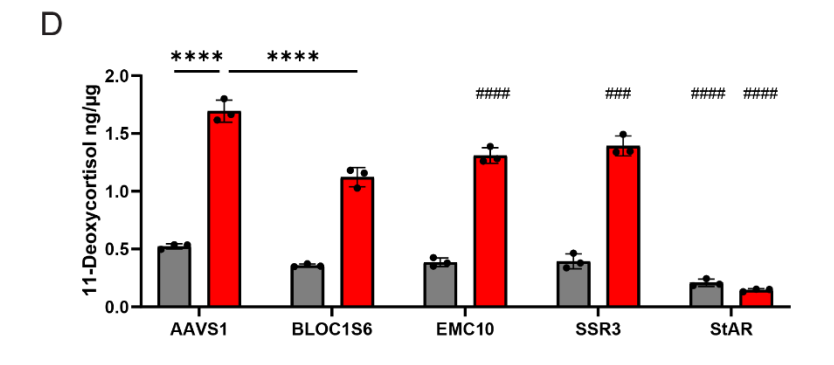
Supplemental Figure 3.6. ER stress impairs steroidogenesis. A) 17aOH-Pregnenolone, and B) pregnenolone, C) 17OH-Progesterone, D) 11-deoxycortisol, and E) corticosterone secreted by wt NCI-H295R during 24 h treatment with 10 μ M forskolin, and 10 μ M tunicamycin, or 1 μ M ISRIB as indicated, analyzed by LC/MS. Data are mean \pm s.d. of n=3 replicates. Grey = vehicle DMSO, red = 10 μ M forskolin, * = p<0.05, ** = p<0.01, *** = p<0.001, **** = p<0.0001 (two-way ANOVA).



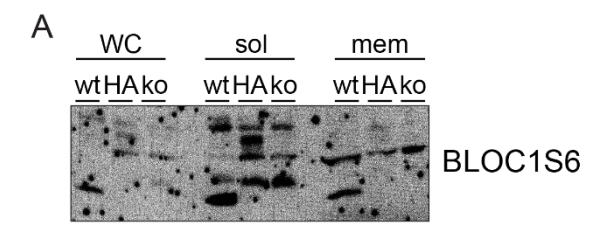
Supplemental Figure 4.1. Specific factors of LROs and ER increase at mitochondria during steroidogenesis induction. A) Steroids from NCI-H295R WT or expressing 3xHA-GFP-OMP25 treated with 10 μ M forskolin or vehicle DMSO for 24 h analyzed by LC/MS. B) Proteomic changes in the mitochondrial and the whole cell proteome, induced by forskolin, detected by LC/MS. Green: mitochondrial proteins as attributed by MitoCarta3.0.







Supplemental Figure 4.2. Biogenesis of lysosome-related organelles complex 1 subunit 6 is required for steroidogenesis. A) Pregnenolone, B) progesterone, C) 17OH-Pregnenolone, D) 11-Deoxycortisol secreted by NCI-H295R CRISPR/Cas9 knockouts with sgRNAs against indicated proteins after 24 h of 10 μ M forskolin analyzed by LC-MS. Data are mean \pm s.d. of n=3 replicates. Grey = vehicle DMSO, red=10 μ M forskolin, ns=not significant, */#=p<0.05, **/##=p<0.01, ***/###=p<0.001, ***/###=p<0.0001 asterisks refer to comparison indicated by line, hashtags compare to AAVS1 (two-way ANOVA).



Supplemental Figure 4.3. BLOC1S6 is found in the cytosolic fraction and with membrane-bound organelles. A) Immunoblot of whole cells (WC), cytosolic/low density (sol), and membrane-bound organelle (mem) fractions from organellar suspension of NCI-H295R AAVS1, BLOC1S6 KO, and BLOC1S6 KO expressing HA-BLOC1S6. Analyzed for BLOC1S6, full membrane for Fig. 4.3.

8 References

- Agarwal, A. K., & Auchus, R. J. (2005). Minireview: Cellular Redox State Regulates Hydroxysteroid Dehydrogenase Activity and Intracellular Hormone Potency. *Endocrinology*, *146*(6), 2531-2538. https://doi.org/10.1210/en.2005-0061
- Agrawal, S., Kumar, S., Sehgal, R., George, S., Gupta, R., Poddar, S., Jha, A., & Pathak, S. (2019). El-MAVEN: A Fast, Robust, and User-Friendly Mass Spectrometry Data Processing Engine for Metabolomics. *Methods Mol Biol*, *1978*, 301-321. https://doi.org/10.1007/978-1-4939-9236-2
- Allen, J. A., Shankara, T., Janus, P., Buck, S., Diemer, T., Held Hales, K., & Hales, D. B. (2006).

 Energized, Polarized, and Actively Respiring Mitochondria Are Required for Acute Leydig Cell Steroidogenesis. *Endocrinology*, 147(8), 3924-3935. https://doi.org/10.1210/en.2005-1204
- Anand, A. A., & Walter, P. (2020). Structural insights into ISRIB, a memory-enhancing inhibitor of the integrated stress response. *The FEBS Journal*, *287*(2), 239-245. https://doi.org/https://doi.org/10.1111/febs.15073
- Arakane, F., King, S. R., Du, Y., Kallen, C. B., Walsh, L. P., Watari, H., Stocco, D. M., & Strauss, J. F. (1997). Phosphorylation of Steroidogenic Acute Regulatory Protein (StAR) Modulates Its Steroidogenic Activity*. *Journal of Biological Chemistry*, *272*(51), 32656-32662. https://doi.org/https://doi.org/10.1074/jbc.272.51.32656
- Arakane, F., Sugawara, T., Nishino, H., Liu, Z., Holt, J. A., Pain, D., Stocco, D. M., Miller, W. L., & Strauss, J. F. (1996). Steroidogenic acute regulatory protein (StAR) retains activity in the absence of its mitochondrial import sequence: Implications for the mechanism of StAR action. *Proceedings of the National Academy of Sciences*, 93(24), 13731-13736. https://doi.org/doi:10.1073/pnas.93.24.13731
- Artemenko, I., Zhao, D., & Hales, D. (2001). Mitochondrial processing of newly synthesized steroidogenic acute regulatory protein (StAR), but not total StAR, mediates cholesterol transfer to cytochrome P450 side chain cleavage enzyme in adrenal cells. *J Biol Chem*, *276*, 46583-46596.
- Auchus, R. J., Lee, T. C., & Miller, W. L. (1998). Cytochrome b 5 Augments the 17,20-Lyase Activity of Human P450c17 without Direct Electron Transfer*. *Journal of Biological Chemistry*, 273(6), 3158-3165. https://doi.org/https://doi.org/10.1074/jbc.273.6.3158
- Auchus, R. J., & Rainey, W. E. (2004). Adrenarche physiology, biochemistry and human disease. *Clinical Endocrinology*, *60*(3), 288-296. https://doi.org/https://doi.org/10.1046/j.1365-2265.2003.01858.x
- Banushi, B., & Simpson, F. (2022). Overlapping Machinery in Lysosome-Related Organelle Trafficking: A Lesson from Rare Multisystem Disorders. *Cells*, *11*(22), 3702. https://www.mdpi.com/2073-4409/11/22/3702
- Bloch, K. (1965). The Biological Synthesis of Cholesterol. *Science*, *150*(3692), 19-28. https://doi.org/doi:10.1126/science.150.3692.19
- Bose, H., Bose, M., & Whittal, R. (2023). Tom40 in cholesterol transport. iScience, 26.
- Bose, H. S., Lingappat, V. R., & Miller, W. L. (2002). Rapid regulation of steroidogenesis by mitochondrial protein import [Article]. *Nature*, *417*(6884), 87-91. https://doi.org/10.1038/417087a
- Bowman, E. J., Siebers, A., & Altendorf, K. (1988). Bafilomycins: a class of inhibitors of membrane ATPases from microorganisms, animal cells, and plant cells. *Proceedings of the National Academy of Sciences*, 85(21), 7972-7976. https://doi.org/doi:10.1073/pnas.85.21.7972
- Brewer, J. W., Cleveland, J. L., & Hendershot, L. M. (1997). A pathway distinct from the mammalian unfolded protein response regulates expression of endoplasmic reticulum chaperones in non-stressed cells. *The EMBO Journal*, *16*(23), 7207-7216. https://doi.org/https://doi.org/10.1093/emboj/16.23.7207

- Brown, A. J., Coates, H. W., & Sharpe, L. J. (2021). Chapter 10 Cholesterol synthesis. In N. D. Ridgway & R. S. McLeod (Eds.), *Biochemistry of Lipids, Lipoproteins and Membranes (Seventh Edition)* (pp. 317-355). Elsevier. https://doi.org/https://doi.org/10.1016/B978-0-12-824048-9.00005-5
- Brown, M. S., & Goldstein, J. L. (1980). Multivalent feedback regulation of HMG CoA reductase, a control mechanism coordinating isoprenoid synthesis and cell growth. *Journal of Lipid Research*, 21(5), 505-517. https://doi.org/https://doi.org/10.1016/S0022-2275(20)42221-7
- Bruchovsky, N., & Wilson, J. D. (1968). The Intranuclear Binding of Testosterone and 5α -Androstan-17 β -ol-3-one by Rat Prostate. *Journal of Biological Chemistry*, 243(22), 5953-5960. https://doi.org/https://doi.org/10.1016/S0021-9258(18)94513-8
- Bull, V. H., & Thiede, B. (2012). Proteome analysis of tunicamycin-induced ER stress. *ELECTROPHORESIS*, 33(12), 1814-1823. https://doi.org/https://doi.org/10.1002/elps.201100565
- Chambers, M. C., Maclean, B., Burke, R., Amodei, D., Ruderman, D. L., Neumann, S., Gatto, L., Fischer, B., Pratt, B., Egertson, J., Hoff, K., Kessner, D., Tasman, N., Shulman, N., Frewen, B., Baker, T. A., Brusniak, M. Y., Paulse, C., Creasy, D.,...Mallick, P. (2012). A cross-platform toolkit for mass spectrometry and proteomics. *Nat Biotechnol*, *30*(10), 918-920. https://doi.org/10.1038/nbt.2377
- Chaplin, D. D., Galbraith, L. J., Seidman, J. G., White, P. C., & Parker, K. L. (1986). Nucleotide sequence analysis of murine 21-hydroxylase genes: mutations affecting gene expression. *Proceedings of the National Academy of Sciences*, 83(24), 9601-9605. https://doi.org/doi:10.1073/pnas.83.24.9601
- Chen, W. W., Freinkman, E., Wang, T., Birsoy, K., & Sabatini, D. M. (2016). Absolute Quantification of Matrix Metabolites Reveals the Dynamics of Mitochondrial Metabolism. *Cell*, *166*(5), 1324-1337 e1311. https://doi.org/10.1016/j.cell.2016.07.040
- Clifford, B. L., Jarrett, K. E., Cheng, J., Cheng, A., Seldin, M., Morand, P., Lee, R., Chen, M., Baldan, A., de Aguiar Vallim, T. Q., & Tarling, E. J. (2023). RNF130 Regulates LDLR Availability and Plasma LDL Cholesterol Levels. *Circulation Research*, *132*(7), 849-863. https://doi.org/doi:10.1161/CIRCRESAHA.122.321938
- Condon, J. C., Pezzi, V., Drummond, B. M., Yin, S., & Rainey, W. E. (2002). Calmodulin-Dependent Kinase I Regulates Adrenal Cell Expression of Aldosterone Synthase. *Endocrinology*, *143*(9), 3651-3657. https://doi.org/10.1210/en.2001-211359
- Cox, J., & Mann, M. (2008). MaxQuant enables high peptide identification rates, individualized p.p.b.-range mass accuracies and proteome-wide protein quantification. *Nat Biotechnol*, 26(12), 1367-1372. https://doi.org/10.1038/nbt.1511
- Cox, J., & Mann, M. (2008). MaxQuant enables high peptide identification rates, individualized p.p.b.-range mass accuracies and proteome-wide protein quantification. *Nature Biotechnology*, 26(12), 1367-1372. https://doi.org/10.1038/nbt.1511
- Davis, C. G., Elhammer, A., Russell, D. W., Schneider, W. J., Kornfeld, S., Brown, M. S., & Goldstein, J. L. (1986). Deletion of clustered O-linked carbohydrates does not impair function of low density lipoprotein receptor in transfected fibroblasts. *Journal of Biological Chemistry*, 261(6), 2828-2838. https://doi.org/https://doi.org/10.1016/S0021-9258(17)35862-3
- De Kloet, E. R. (2004). Hormones and the stressed brain. *Annals of the New York Academy of Sciences*, 1018(1), 1-15.
- Dethloff, F., Erban, A., Orf, I., Alpers, J., Fehrle, I., Beine-Golovchuk, O., Schmidt, S., Schwachtje, J., & Kopka, J. (2014). Profiling methods to identify cold-regulated primary metabolites using gas chromatography coupled to mass spectrometry. *Methods Mol Biol*, *1166*, 171-197. https://doi.org/10.1007/978-1-4939-0844-8 14
- Dietschy, J. M. (1984). Regulation of cholesterol metabolism in man and in other species. *Klinische Wochenschrift*, 62(8), 338-345. https://doi.org/10.1007/BF01716251
- Do-Rego, J.-L., Seong, J. Y., Burel, D., LEPRINCE, J., Vaudry, D., Luu-The, V., Tonon, M.-C., Tsutsui, K., Pelletier, G., & Vaudry, H. (2012). Regulation of Neurosteroid Biosynthesis by

- Neurotransmitters and Neuropeptides [Review]. *Frontiers in Endocrinology, 3*. https://doi.org/10.3389/fendo.2012.00004
- Duarte, A., Castillo, A. F., Castilla, R., Maloberti, P., Paz, C., Podestá, E. J., & Cornejo Maciel, F. (2007). An arachidonic acid generation/export system involved in the regulation of cholesterol transport in mitochondria of steroidogenic cells. *FEBS Letters*, *581*(21), 4023-4028. https://doi.org/https://doi.org/10.1016/j.febslet.2007.07.040
- Fardella, C. E., & Miller, W. L. (1996). Molecular Biology of Mineralocorticoid Metabolism. *Annual Review of Nutrition*, *16*(Volume 16, 1996), 443-470. https://doi.org/https://doi.org/10.1146/annurev.nu.16.070196.002303
- Fischer, T. D., Wang, C., Padman, B. S., Lazarou, M., & Youle, R. J. (2020). STING induces LC3B lipidation onto single-membrane vesicles via the V-ATPase and ATG16L1-WD40 domain. *Journal of Cell Biology*, 219(12). https://doi.org/10.1083/jcb.202009128
- Friedlander, R., Jarosch, E., Urban, J., Volkwein, C., & Sommer, T. (2000). A regulatory link between ER-associated protein degradation and the unfolded-protein response. *Nature cell biology*, 2(7), 379-384.
- Fujimoto, M., Hayashi, T., & Su, T.-P. (2012). The role of cholesterol in the association of endoplasmic reticulum membranes with mitochondria. *Biochemical and Biophysical Research Communications*, *417*(1), 635-639. https://doi.org/https://doi.org/10.1016/j.bbrc.2011.12.022
- Garcia, B. M., Melchinger, P., Medeiros, T., Hendrix, S., Prabhu, K., Corrado, M., Kingma, J., Gorbatenko, A., Deshwal, S., Veronese, M., Scorrano, L., Pearce, E., Giavalisco, P., Zelcer, N., & Pernas, L. (2024). Glutamine sensing licenses cholesterol synthesis. *The EMBO Journal*, 43(23), 5837-5856. https://doi.org/https://doi.org/10.1038/s44318-024-00269-0
- Gaudet, P., Livstone, M. S., Lewis, S. E., & Thomas, P. D. (2011). Phylogenetic-based propagation of functional annotations within the Gene Ontology consortium. *Briefings in Bioinformatics*, 12(5), 449-462. https://doi.org/10.1093/bib/bbr042
- Gazdar, A. F., Oie, H. K., Shackleton, C. H., Chen, T. R., Triche, T. J., Myers, C. E., Chrousos, G. P., Brennan, M. F., Stein, C. A., & La Rocca, R. V. (1990). Establishment and Characterization of a Human Adrenocortical Carcinoma Cell Line That Expresses Multiple Pathways of Steroid Biosynthesis1. *Cancer Research*, *50*(17), 5488-5496.
- Ge, X., Ren, J., Gu, K., Gong, W., Shen, K., & Feng, W. (2025). The structure and assembly of the hetero-octameric BLOC-one-related complex. *Structure*, *33*(2), 234-246.e236. https://doi.org/10.1016/j.str.2024.12.001
- Gemmer, M., & Förster, F. (2020). A clearer picture of the ER translocon complex. *Journal of Cell Science*, 133(3). https://doi.org/10.1242/jcs.231340
- Gill, S., Stevenson, J., Kristiana, I., & Brown, Andrew J. (2011). Cholesterol-Dependent Degradation of Squalene Monooxygenase, a Control Point in Cholesterol Synthesis beyond HMG-CoA Reductase. *Cell Metabolism*, 13(3), 260-273. https://doi.org/10.1016/j.cmet.2011.01.015
- Go, G. W., & Mani, A. (2012). Low-density lipoprotein receptor (LDLR) family orchestrates cholesterol homeostasis. *Yale J Biol Med*, *85*(1), 19-28.
- Goul, C., Peruzzo, R., & Zoncu, R. (2023). The molecular basis of nutrient sensing and signalling by mTORC1 in metabolism regulation and disease. *Nature Reviews Molecular Cell Biology*, 24(12), 857-875. https://doi.org/10.1038/s41580-023-00641-8
- Guna, A., Volkmar, N., Christianson, J. C., & Hegde, R. S. (2018). The ER membrane protein complex is a transmembrane domain insertase. *Science*, *359*(6374), 470-473. https://doi.org/doi:10.1126/science.aao3099
- Gyles, S. L., Burns, C. J., Whitehouse, B. J., Sugden, D., Marsh, P. J., Persaud, S. J., & Jones, P. M. (2001). ERKs Regulate Cyclic AMP-induced Steroid Synthesis through Transcription of the Steroidogenic Acute Regulatory (StAR) Gene*. *Journal of Biological Chemistry*, 276(37), 34888-34895. https://doi.org/10.1074/jbc.M102063200

- Hattangady, N. G., Olala, L. O., Bollag, W. B., & Rainey, W. E. (2012). Acute and chronic regulation of aldosterone production. *Molecular and Cellular Endocrinology*, 350(2), 151-162. https://doi.org/https://doi.org/10.1016/j.mce.2011.07.034
- Helfenberger, K. E., Castillo, A. F., Mele, P. G., Fiore, A., Herrera, L., Finocchietto, P., Podestá, E. J., & Poderoso, C. (2019). Angiotensin II stimulation promotes mitochondrial fusion as a novel mechanism involved in protein kinase compartmentalization and cholesterol transport in human adrenocortical cells. *The Journal of Steroid Biochemistry and Molecular Biology*, 192, 105413. https://doi.org/https://doi.org/10.1016/j.jsbmb.2019.105413
- Huizing, M., Helip-Wooley, A., Westbroek, W., Gunay-Aygun, M., & Gahl, W. A. (2008). Disorders of lysosome-related organelle biogenesis: clinical and molecular genetics. *Annu Rev Genomics Hum Genet*, *9*, 359-386. https://doi.org/10.1146/annurev.genom.9.081307.164303
- Infante, R. E., Wang, M. L., Radhakrishnan, A., Kwon, H. J., Brown, M. S., & Goldstein, J. L. (2008). NPC2 facilitates bidirectional transfer of cholesterol between NPC1 and lipid bilayers, a step in cholesterol egress from lysosomes. *Proceedings of the National Academy of Sciences*, 105(40), 15287-15292. https://doi.org/doi:10.1073/pnas.0807328105
- Itzhak, D. N., Davies, C., Tyanova, S., Mishra, A., Williamson, J., Antrobus, R., Cox, J., Weekes, M. P., & Borner, G. H. H. (2017). A Mass Spectrometry-Based Approach for Mapping Protein Subcellular Localization Reveals the Spatial Proteome of Mouse Primary Neurons. *Cell Reports*, 20(11), 2706-2718. https://doi.org/https://doi.org/10.1016/j.celrep.2017.08.063
- Jani, R. A., Di Cicco, A., Keren-Kaplan, T., Vale-Costa, S., Hamaoui, D., Hurbain, I., Tsai, F.-C., Di Marco, M., Macé, A.-S., Zhu, Y., Amorim, M. J., Bassereau, P., Bonifacino, J. S., Subtil, A., Marks, M. S., Lévy, D., Raposo, G., & Delevoye, C. (2022). PI4P and BLOC-1 remodel endosomal membranes into tubules. *Journal of Cell Biology*, 221(11). https://doi.org/10.1083/jcb.202110132
- Jeon, H., & Blacklow, S. C. (2005). Structure and physiologic function of the low-density lipoprotein receptor. *Annu Rev Biochem*, 74, 535-562. https://doi.org/10.1146/annurev.biochem.74.082803.133354
- Jo, Y., King, S. R., Khan, S. A., & Stocco, D. M. (2005). Involvement of Protein Kinase C and Cyclic Adenosine 3',5'-Monophosphate-Dependent Kinase in Steroidogenic Acute Regulatory Protein Expression and Steroid Biosynthesis in Leydig Cells1. *Biology of Reproduction*, 73(2), 244-255. https://doi.org/10.1095/biolreprod.104.037721
- Kanehisa, M., Furumichi, M., Tanabe, M., Sato, Y., & Morishima, K. (2016). KEGG: new perspectives on genomes, pathways, diseases and drugs. *Nucleic Acids Research*, *45*(D1), D353-D361. https://doi.org/10.1093/nar/gkw1092
- Kurlbaum, M., Sbiera, S., Kendl, S., Martin Fassnacht, M., & Kroiss, M. (2020). Steroidogenesis in the NCI-H295 Cell Line Model is Strongly Affected By Culture Conditions and Substrain. *Exp Clin Endocrinol Diabetes*, 128(10), 672-680. https://doi.org/10.1055/a-1105-6332
- Kuwada, M., Kitajima, R., Suzuki, H., & Horie, S. (1991). Purification and properties of cytochrome P-450 (SCC) from pig testis mitochondria. *Biochemical and Biophysical Research Communications*, 176(3), 1501-1508. https://doi.org/https://doi.org/10.1016/0006-291X(91)90457-l
- Labrie, F., Luu-The, V., Lin, S.-X., Claude, L., Simard, J., Breton, R., & Bélanger, A. (1997). The key role of 17β-hydroxysteroid dehydrogenases in sex steroid biology. *Steroids*, *62*(1), 148-158. https://doi.org/https://doi.org/10.1016/S0039-128X(96)00174-2
- Lange, Y., Ye, J., Rigney, M., & Steck, T. (2000). Cholesterol Movement in Niemann-Pick Type C Cells and in Cells Treated with Amphiphiles*. *Journal of Biological Chemistry*, *275*(23), 17468-17475. https://doi.org/https://doi.org/10.1074/jbc.M000875200
- Lee, H. H., Nemecek, D., Schindler, C., Smith, W. J., Ghirlando, R., Steven, A. C., Bonifacino, J. S., & Hurley, J. H. (2012). Assembly and Architecture of Biogenesis of Lysosome-related Organelles Complex-1 (BLOC-1)*. *Journal of Biological Chemistry*, 287(8), 5882-5890. https://doi.org/https://doi.org/10.1074/jbc.M111.325746

- Li, X., Franz, T., Atanassov, I., & Colby, T. (2021). Step-by-Step Sample Preparation of Proteins for Mass Spectrometric Analysis. *Methods Mol Biol, 2261*, 13-23. https://doi.org/10.1007/978-1-0716-1186-9 2
- Lin, D., Sugawara, T., Strauss, J. F., Clark, B. J., Stocco, D. M., Saenger, P., Rogol, A., & Miller, W. L. (1995). Role of Steroidogenic Acute Regulatory Protein in Adrenal and Gonadal Steroidogenesis. *Science*, *267*(5205), 1828-1831. https://doi.org/doi:10.1126/science.7892608
- Lorence, M. C., Murry, B. A., Trant, J. M., & Mason, J. I. (1990). Human 3β-Hydroxysteroid Dehydrogenase/ δ5→4lsomerase from Placenta: Expression in Nonsteroidogenic Cells of a Protein that Catalyzes the Dehydrogenation/Isomerization of C21 and C19 Steroids*. *Endocrinology*, 126(5), 2493-2498. https://doi.org/10.1210/endo-126-5-2493
- Lu, H., Cassis, L. A., Kooi, C. W. V., & Daugherty, A. (2016). Structure and functions of angiotensinogen. *Hypertension Research*, *39*(7), 492-500. https://doi.org/10.1038/hr.2016.17
- Luo, J., Yang, H., & Song, B.-L. (2020). Mechanisms and regulation of cholesterol homeostasis. *Nature Reviews Molecular Cell Biology*, *21*(4), 225-245. https://doi.org/10.1038/s41580-019-0190-7
- Marriott, K., Prasad, M., & Thapliyal, V. (2012). σ -1 receptor at the mitochondrial-associated endoplasmic reticulum membrane is responsible for mitochondrial metabolic regulation. *J Pharmacol Exp Ther*, 343, 578-586.
- Matysik, S., & Liebisch, G. (2017). Quantification of steroid hormones in human serum by liquid chromatography-high resolution tandem mass spectrometry. *Journal of Chromatography A*, 1526, 112-118. https://doi.org/https://doi.org/https://doi.org/10.1016/j.chroma.2017.10.042
- Medar, M. L. J., Marinkovic, D. Z., Kojic, Z., Becin, A. P., Starovlah, I. M., Kravic-Stevovic, T., Andric, S. A., & Kostic, T. S. (2021). Dependence of Leydig Cell's Mitochondrial Physiology on Luteinizing Hormone Signaling. *Life*, 11(1), 19. https://www.mdpi.com/2075-1729/11/1/19
- Mele, P. G., Duarte, A., Paz, C., Capponi, A., & Podestá, E. J. (2012). Role of Intramitochondrial Arachidonic Acid and Acyl-CoA Synthetase 4 in Angiotensin II-Regulated Aldosterone Synthesis in NCI-H295R Adrenocortical Cell Line. *Endocrinology*, *153*(7), 3284-3294. https://doi.org/10.1210/en.2011-2108
- Miller, W. L. (2005). Minireview: Regulation of Steroidogenesis by Electron Transfer. *Endocrinology*, 146(6), 2544-2550. https://doi.org/10.1210/en.2005-0096
- Miller, W. L. (2013). Steroid hormone synthesis in mitochondria. *Mol Cell Endocrinol*, *379*(1-2), 62-73. https://doi.org/10.1016/j.mce.2013.04.014
- Miller, W. L. (2025). Thirty years of StAR gazing. Expanding the universe of the steroidogenic acute regulatory protein. *Journal of Endocrinology*, *264*(3), e240310. https://doi.org/10.1530/joe-24-0310
- Miller, W. L., & Auchus, R. J. (2011). The Molecular Biology, Biochemistry, and Physiology of Human Steroidogenesis and Its Disorders. *Endocrine Reviews*, *32*(1), 81-151. https://doi.org/10.1210/er.2010-0013
- Morizono, M. A., McGuire, K. L., Birouty, N. I., & Herzik, M. A. (2024). Structural insights into GrpEL1-mediated nucleotide and substrate release of human mitochondrial Hsp70. *Nature Communications*, *15*(1), 10815. https://doi.org/10.1038/s41467-024-54499-1
- Mountjoy, K. G., Bird, I. M., Rainey, W. E., & Cone, R. D. (1994). ACTH induces up-regulation of ACTH receptor mRNA in mouse and human adrenocortical cell lines. *Molecular and Cellular Endocrinology*, 99(1), R17-R20. https://doi.org/https://doi.org/10.1016/0303-7207(94)90160-0
- Mulatero, P., Curnow, K. M., Aupetit-Faisant, B., Foekling, M., Gomez-Sanchez, C., Veglio, F., Jeunemaitre, X., Corvol, P., & Pascoe, L. (1998). Recombinant CYP11B Genes Encode Enzymes that Can Catalyze Conversion of 11-Deoxycortisol to Cortisol, 18-Hydroxycortisol, and 18-Oxocortisol1. *The Journal of Clinical Endocrinology & Metabolism*, 83(11), 3996-4001. https://doi.org/10.1210/jcem.83.11.5237
- Nakajin, S., Shinoda, M., Haniu, M., Shively, J. E., & Hall, P. F. (1984). C21 steroid side chain cleavage enzyme from porcine adrenal microsomes. Purification and characterization of the 17 alpha-

- hydroxylase/C17,20-lyase cytochrome P-450. *Journal of Biological Chemistry*, 259(6), 3971-3976. https://doi.org/https://doi.org/10.1016/S0021-9258(17)43191-7
- Osman, A., & Clayton, R. (2017). Adrenocortical hormones. *Anaesthesia & Intensive Care Medicine*, 18(10), 519-521. https://doi.org/10.1016/j.mpaic.2017.06.014
- Pakos-Zebrucka, K., Koryga, I., Mnich, K., Ljujic, M., Samali, A., & Gorman, A. M. (2016). The integrated stress response. *EMBO Rep*, *17*(10), 1374-1395. https://doi.org/10.15252/embr.201642195
- Papadopoulos, A. S., & Cleare, A. J. (2012). Hypothalamic–pituitary–adrenal axis dysfunction in chronic fatigue syndrome. *Nature Reviews Endocrinology*, 8(1), 22-32. https://doi.org/10.1038/nrendo.2011.153
- Parker, K. L., Chaplin, D. D., Wong, M., Seidman, J. G., Smith, J. A., & Schimmer, B. P. (1985). Expression of murine 21-hydroxylase in mouse adrenal glands and in transfected Y1 adrenocortical tumor cells. *Proceedings of the National Academy of Sciences*, 82(23), 7860-7864. https://doi.org/doi:10.1073/pnas.82.23.7860
- Peñaranda-Fajardo, N. M., Meijer, C., Liang, Y., Dijkstra, B. M., Aguirre-Gamboa, R., den Dunnen, W. F. A., & Kruyt, F. A. E. (2019). ER stress and UPR activation in glioblastoma: identification of a noncanonical PERK mechanism regulating GBM stem cells through SOX2 modulation. *Cell Death & Disease*, 10(10), 690. https://doi.org/10.1038/s41419-019-1934-1
- Phoomak, C., Cui, W., Hayman, T. J., Yu, S.-H., Zhao, P., Wells, L., Steet, R., & Contessa, J. N. (2021). The translocon-associated protein (TRAP) complex regulates quality control of N-linked glycosylation during ER stress. *Science Advances*, 7(3), eabc6364. https://doi.org/doi:10.1126/sciadv.abc6364
- Prasad, M., Pawlak, K., & Burak, W. (2017). Mitochondrial metabolic regulation by GRP78. *Sci Adv, 3*. Rabouw, H. H., Langereis, M. A., Anand, A. A., Visser, L. J., de Groot, R. J., Walter, P., & van Kuppeveld, F. J. M. (2019). Small molecule ISRIB suppresses the integrated stress response within a defined window of activation. *Proceedings of the National Academy of Sciences,* 116(6), 2097-2102. https://doi.org/doi:10.1073/pnas.1815767116
- Radhakrishnan, A., Ikeda, Y., Kwon, H. J., Brown, M. S., & Goldstein, J. L. (2007). Sterol-regulated transport of SREBPs from endoplasmic reticulum to Golgi: Oxysterols block transport by binding to Insig. *Proceedings of the National Academy of Sciences*, 104(16), 6511-6518. https://doi.org/doi:10.1073/pnas.0700899104
- Radhakrishnan, A., Sun, L.-P., Espenshade, P. J., Goldstein, J. L., & Brown, M. S. (2010). Chapter 298 The SREBP Pathway: Gene Regulation through Sterol Sensing and Gated Protein Trafficking. In R. A. Bradshaw & E. A. Dennis (Eds.), *Handbook of Cell Signaling (Second Edition)* (pp. 2505-2510). Academic Press. https://doi.org/https://doi.org/10.1016/B978-0-12-374145-5.00298-9
- Rainey, W. E., Bird, I. M., & Mason, J. I. (1994). The NCI-H295 cell line: a pluripotent model for human adrenocortical studies. *Molecular and Cellular Endocrinology*, 100(1), 45-50. https://doi.org/https://doi.org/10.1016/0303-7207(94)90277-1
- Rath, S., Sharma, R., Gupta, R., Ast, T., Chan, C., Durham, T. J., Goodman, R. P., Grabarek, Z., Haas, M. E., Hung, W. H. W., Joshi, P. R., Jourdain, A. A., Kim, S. H., Kotrys, A. V., Lam, S. S., McCoy, J. G., Meisel, J. D., Miranda, M., Panda, A.,...Mootha, V. K. (2020). MitoCarta3.0: an updated mitochondrial proteome now with sub-organelle localization and pathway annotations. *Nucleic Acids Research*, 49(D1), D1541-D1547. https://doi.org/10.1093/nar/gkaa1011
- Reddy, D. S. (2010). Chapter 8 Neurosteroids: Endogenous role in the human brain and therapeutic potentials. In I. Savic (Ed.), *Progress in Brain Research* (Vol. 186, pp. 113-137). Elsevier. https://doi.org/https://doi.org/10.1016/B978-0-444-53630-3.00008-7
- Ritchie, M. E., Phipson, B., Wu, D., Hu, Y., Law, C. W., Shi, W., & Smyth, G. K. (2015). limma powers differential expression analyses for RNA-sequencing and microarray studies. *Nucleic Acids Research*, 43(7), e47-e47. https://doi.org/10.1093/nar/gkv007

- Ritchie, M. E., Phipson, B., Wu, D., Hu, Y., Law, C. W., Shi, W., & Smyth, G. K. (2015). limma powers differential expression analyses for RNA-sequencing and microarray studies. *Nucleic Acids Res*, 43(7), e47. https://doi.org/10.1093/nar/gkv007
- Sakai, J., Duncan, E. A., Rawson, R. B., Hua, X., Brown, M. S., & Goldstein, J. L. (1996). Sterol-Regulated Release of SREBP-2 from Cell Membranes Requires Two Sequential Cleavages, One Within a Transmembrane Segment. *Cell*, *85*(7), 1037-1046. https://doi.org/10.1016/S0092-8674(00)81304-5
- Sidrauski, C., Acosta-Alvear, D., Khoutorsky, A., Vedantham, P., Hearn, B. R., Li, H., Gamache, K., Gallagher, C. M., Ang, K. K. H., Wilson, C., Okreglak, V., Ashkenazi, A., Hann, B., Nader, K., Arkin, M. R., Renslo, A. R., Sonenberg, N., & Walter, P. (2013). Pharmacological brake-release of mRNA translation enhances cognitive memory. *eLife*, *2*, e00498. https://doi.org/10.7554/eLife.00498
- Simpson, E. R., Clyne, C., Rubin, G., Boon, W. C., Robertson, K., Britt, K., Speed, C., & Jones, M. (2002). Aromatase—A Brief Overview. *Annual Review of Physiology*, *64*(Volume 64, 2002), 93-127. https://doi.org/10.1146/annurev.physiol.64.081601.142703
- Spady, D. K., & Dietschy, J. M. (1983). Sterol synthesis in vivo in 18 tissues of the squirrel monkey, guinea pig, rabbit, hamster, and rat. *Journal of Lipid Research*, *24*(3), 303-315. https://doi.org/https://doi.org/10.1016/S0022-2275(20)37999-2
- Spiga, F., & Lightman, S. L. (2015). Dynamics of adrenal glucocorticoid steroidogenesis in health and disease. *Molecular and Cellular Endocrinology*, 408, 227-234. https://doi.org/https://doi.org/10.1016/j.mce.2015.02.005
- Steiger, M., & Reichstein, T. (1937). Desoxy-cortico-steron (21-Oxy-progesteron) aus Δ5-3-Oxy-ätio-cholensäure. *Helvetica Chimica Acta*, 20(1), 1164-1179. https://doi.org/https://doi.org/10.1002/hlca.193702001158
- Sugawara, T., Sakuragi, N., & Minakami, H. (2006). CREM confers cAMP responsiveness in human steroidogenic acute regulatory protein expression in NCI-H295R cells rather than SF-1/Ad4BP. *Journal of Endocrinology*, 191(1), 327-337. https://doi.org/10.1677/joe.1.06601
- Suzuki, T., Sasano, H., Takeyama, J., Kaneko, C., Freije, W. A., Carr, B. R., & Rainey, W. E. (2000). Developmental changes in steroidogenic enzymes in human postnatal adrenal cortex: immunohistochemical studies. *Clinical Endocrinology*, *53*(6), 739-747. https://doi.org/https://doi.org/10.1046/j.1365-2265.2000.01144.x
- Thomas, J. L., Myers, R. P., & Strickler, R. C. (1989). Human placental 3β-hydroxy-5-ene-steroid dehydrogenase and steroid 5→ 4-ene-isomerase: Purification from mitochondria and kinetic profiles, biophysical characterization of the purified mitochondrial and microsomal enzymes. *Journal of Steroid Biochemistry*, 33(2), 209-217.

 https://doi.org/https://doi.org/10.1016/0022-4731(89)90296-3
- Toaff, M. E., SCHLEYER, H., & STRAUSS, J. F., III. (1982). Metabolism of 25-Hydroxycholesterol by Rat Luteal Mitochondria and Dispersed Cells*. *Endocrinology*, *111*(6), 1785-1790. https://doi.org/10.1210/endo-111-6-1785
- Tsujishita, Y., & Hurley, J. (2000). Structure and lipid transport mechanism of a StAR-related domain. *Nat Struct Biol*, *7*, 408-414.
- Tuckey, R. C., & Cameron, K. J. (1993a). Catalytic properties of cytochrome P-450scc purified from the human placenta: comparison to bovine cytochrome P-450scc. *Biochimica et Biophysica Acta (BBA) Protein Structure and Molecular Enzymology, 1163*(2), 185-194. https://doi.org/https://doi.org/10.1016/0167-4838(93)90180-Y
- Tuckey, R. C., & Cameron, K. J. (1993b). Human placenta cholesterol side-chain cleavage: enzymatic synthesis of (22R)- 20α,22-dihysroxycholesterol. *Steroids*, *58*(5), 230-233. https://doi.org/https://doi.org/10.1016/0039-128X(93)90024-H
- Tugaeva, K. V., & Sluchanko, N. N. (2019). Steroidogenic Acute Regulatory Protein: Structure, Functioning, and Regulation. *Biochemistry (Mosc)*, *84*(Suppl 1), S233-s253. https://doi.org/10.1134/s0006297919140141

- Tunganuntarat, J., Kanjanasirirat, P., Khumpanied, T., Benjaskulluecha, S., Wongprom, B., Palaga, T., Siregar, T. A. P., Borwornpinyo, S., Chaiprasert, A., Palittapongarnpim, P., & Ponpuak, M. (2023). BORC complex specific components and Kinesin-1 mediate autophagy evasion by the autophagy-resistant Mycobacterium tuberculosis Beijing strain. *Sci Rep*, *13*(1), 1663. https://doi.org/10.1038/s41598-023-28983-5
- Vagnerová, K., Jágr, M., Mekadim, C., Ergang, P., Sechovcová, H., Vodička, M., Olša Fliegerová, K., Dvořáček, V., Mrázek, J., & Pácha, J. (2023). Profiling of adrenal corticosteroids in blood and local tissues of mice during chronic stress. *Scientific Reports*, *13*(1), 7278. https://doi.org/10.1038/s41598-023-34395-2
- Valente, A. J., Maddalena, L. A., Robb, E. L., Moradi, F., & Stuart, J. A. (2017). A simple ImageJ macro tool for analyzing mitochondrial network morphology in mammalian cell culture. *Acta Histochem*, 119(3), 315-326. https://doi.org/10.1016/j.acthis.2017.03.001
- van Meer, G., Voelker, D. R., & Feigenson, G. W. (2008). Membrane lipids: where they are and how they behave. *Nature Reviews Molecular Cell Biology*, *9*(2), 112-124. https://doi.org/10.1038/nrm2330
- Watari, H., Blanchette-Mackie, E. J., Dwyer, N. K., Sun, G., Glick, J. M., Patel, S., Neufeld, E. B., Pentchev, P. G., & Strauss, J. F. (2000). NPC1-Containing Compartment of Human Granulosa-Lutein Cells: A Role in the Intracellular Trafficking of Cholesterol Supporting Steroidogenesis. *Experimental Cell Research*, 255(1), 56-66. https://doi.org/https://doi.org/10.1006/excr.1999.4774
- White, P. C., Curnow, K. M., & Pascoe, L. (1994). Disorders of Steroid 11β-Hydroxylase Isozymes*. *Endocrine Reviews*, 15(4), 421-438. https://doi.org/10.1210/edrv-15-4-421
- Wong, M., & Tuan, R. S. (1993). NuSerum, a synthetic serum replacement, supports chondrogenesis of embryonic chick limb bud mesenchymal cells in micromass culture. *In Vitro Cellular & Developmental Biology Animal*, 29(12), 917-922. https://doi.org/10.1007/BF02634229
- Zanoni, P., Khetarpal, S. A., Larach, D. B., Hancock-Cerutti, W. F., Millar, J. S., Cuchel, M., DerOhannessian, S., Kontush, A., Surendran, P., Saleheen, D., Trompet, S., Jukema, J. W., De Craen, A., Deloukas, P., Sattar, N., Ford, I., Packard, C., Majumder, A. a. S., Alam, D. S.,...Zalloua, P. A. (2016). Rare variant in scavenger receptor BI raises HDL cholesterol and increases risk of coronary heart disease. *Science*, *351*(6278), 1166-1171. https://doi.org/doi:10.1126/science.aad3517
- Zhang, C., Hao, C., Shui, G., & Li, W. (2020). BLOS1 mediates kinesin switch during endosomal recycling of LDL receptor. *eLife*, *9*, e58069. https://doi.org/10.7554/eLife.58069
- Zhou, Y. X., Wei, J., Deng, G., Hu, A., Sun, P. Y., Zhao, X., Song, B. L., & Luo, J. (2023). Delivery of low-density lipoprotein from endocytic carriers to mitochondria supports steroidogenesis. *Nat Cell Biol*, 25(7), 937-949. https://doi.org/10.1038/s41556-023-01160-6
- Zuber, M. X., Simpson, E. R., & Waterman, M. R. (1986). Expression of Bovine 17α-Hydroxylase Cytochrome P-450 cDNA in Nonsteroidogenic (COS 1) Cells. *Science*, *234*(4781), 1258-1261. https://doi.org/doi:10.1126/science.3535074

9 Acknowledgements

I thank Dr. Lena Pernas for the opportunity to pursue my PhD in her lab. I thank all the Pernas lab members, especially those in Germany for the amazing collegial atmosphere. I thank Dr. Ina Hupperz, Dr. Katrin Köhler and Prof. Dr. Jan Riemer for their advice. I am also grateful to Katrin and Dr. Katia Helfenberger for sharing the cells used here.

The core facilities of the MPI for Biology of Ageing – metabolomics, proteomics and FACS and imaging – have my sincere gratitude for their support. Specifically, Yvonne, Frederik, Patrick, Xinping, Tom, Ilian, and Marcel thank you – without you this project would not have been possible.

Lena, Ina, Tania, and Patrick have my thanks for providing feedback on the Thesis.

Special thanks to Julian for lending a hand with the mitoIP for proteomics. Also thank you, Kavan, for helping with microscopy. Bruna, thank you for helping me find my way around the lab when I was new and showing me how stuff works.

Dr. Maarouf Baghdadi I thank for endeavoring on a collaboration with me, even though we did not discover anything of interest.

I was honored to be part of the RTG2550 reloc, funded by the DFG. It provided a useful and lively program framework for my project. I especially am grateful to my fellow RTG members for being such a great community.

My deepest gratitude goes to my family and the friends I made during the time of my thesis for their unwavering support.